Analysis of friction development at microtunneling case study

Microtunneling under the river IJ – Amsterdam

Author: N. Machado Borges
Date: 21/02/2025

TU Delft

Analysis of friction development at microtunneling case study

Microtunneling under the river IJ – Amsterdam

By

N. Machado Borges

In partial fulfilment of the requirements for the degree of:

Master of Science
in Geo Engineering

at the Delft University of Technology,
to be defended publicly on Thursday February 27, 2025 at 04:00 PM.

Supervisor:	Dr. ir. W. Broere	
Thesis committee:	Dr. Ir. D.J.M. Ngan-Tillard,	TU Delft
	Dr. G. Rongier	TU Delft

Table of Contents

Table of Figures

List of symbols

A	Area
D	Diameter
F	Force
L	Length
σ_{total}	Total Stress
σ'	Effective Stress
K_a	Active earth-pressure coefficient
$\emptyset$	Internal friction angle
γ_w	Water specific gravity
γ_g	Soil specific gravity
h	height
I_r	Penetration resistance
f	Friction coefficient
φ	Soil Internal friction angle

Abstract

In 2005, a pipeline construction was undertaken under the river IJ in Amsterdam. The microtunneling method was used and it consisted of a closed front TBM of 1800mm diameter over a length of 785m in Pleistocene Sand and extremely soft Holocene sediments and anthropogenic sediments. This construction was accompanied by instrumentation that registered the drilling process with force measurements in the main jacks and intermediate jacking stations, strain in the concrete, joint width, tilt of the element and displacement measurements.

All this data was analysed with the focus on the friction development over the entire boring length. The first part of data analysis was to plot and describe the findings of the available parameters, along the total route, that could have an influence on the friction. Next, the microtunnel route was divided into six sections based on changes in soil conditions and in alignment so the analysed parameters (horizontal and vertical deviations, tilt, main jacking force , front force and friction) could be correlated. In order to better understand the results, a Pearson's correlation analysis was created to identify any statistically relevant correlation between the available parameters. The final analysis was performed to estimate the impact that subsequent pipe segment installations have on the friction over time at a specific location.

The friction development over the entire length at the boring under the river IJ (less than 2kPa, with the exception of the start) was compared with the friction coefficient value described in the NEN 3650 when overcut and lubrication are used for concrete pipes (f =7.5 kPa). The friction coefficient is overestimated during design phase and can be optimized. Also for all six sections, after a standstill, an increase in friction is observed. At locations where correlation between alignment and forces are apparently present, the horizontal deviation is observed as the influencing parameter. This is also confirmed by the Pearson's correlation analysis results. Regarding the impact that subsequent pipe segment installations have on the friction, the results of this analysis clearly shows a tendency for a decrease in friction when considering soil type and changes in alignment.

Overall, this work indicates the need of a more thorough friction prediction calculation to be included in the design standards. One that includes more influencing parameters other than overcut and lubricant. Such understanding would enable more accurate predictions in future projects, reducing both risks and costs.

Acknowledgments

I would like to express my gratitude to all my friends that supported me throughout the years. Each participated at a different stage and I am extremely grateful for them. Thank you Anchal, Tess, Babu and Marina. Special thanks to Nadia and Fernando who gave me the push when I needed it and also for allowing me to borrow their brains for a while at times when I felt stuck. A big thanks to Angela for being my emotional support from the start and a more than special appreciation to my wife, Gi, who always believed in me and was always by my side, I could not have done without you and Bigs.

I extend my gratitude to Wout who had the patience to guide me through this period even with all the pauses I needed.

1. Introduction

The underground space in the Netherlands has become extremely complex specially in the past decades. Small traditional infrastructure used to contain sewers, water mains, gas mains, electricity mains and telephone cables. Nowadays, network for cable TV, internet, district heating and separate sewage system for drainage and wastewater have been added to the equation. Given the increased need for underground infrastructure and the decreasing acceptance of disturbance of open-cut, trenchless technologies have become more and more popular, since these limit the disturbance at surface as much as possible and can be used to install new infrastructure below these first few meters of chaos on the ground. They can be classified into 5 techniques such as: open-front technology, air-percussion boring techniques, closed front techniques, horizontal directional drilling (HDD) and methods for repairs and replacement (Broere & van der Woude, 2012).

Microtunneling is a non-disruptive closed front boring method of installing utility pipes usually with internal diameters from 0.25m up to 3.5m (Milligan & Norris, 1999) (Broere & van der Woude, 2012). It is a combination of tunnel boring machine (TBM) and pipejacking. At the starting shaft, hydraulic jacks are placed on a jacking frame. They will push the TBM through the shaft wall and once it is far enough into the soil a prefabricated segment pipe will be placed behind the machine and the whole line is jacked forward into the ground. This process of coupling a new prefabricated segment pipe and jacking is repeated until the line reaches the receiving shaft. This is the main difference to large diameter tunnels, where the TBM pushes itself into the ground and the wall is built from inside the machine usually with reinforced concrete segments.

In that process, frictional forces are developed over the pipeline surface as it advances through the soil (Reilly & Orr, 2017). Therefore, the length of a microtunneling is restricted to the maximum allowable jacking force which needs to be larger than the frictional resistance on the pipe string and on the face of the shield, combined (Marshall, 1998). It is possible to add intermediate jacking stations (IJS) to construct longer tunnels, which will increase the possible drilling lengths. An IJS consists of hydraulic jacks placed in a steel ring which is inserted into the pipe string. This allows the tunnel to be divided in sections that can be pushed separately distributing the frictional forces to the respective jacking elements behind. However, this technique can only be used in diameters accessible to workers (Broere & van der Woude, 2012).

In 2005, a pipeline construction was undertaken under the river IJ in Amsterdam. The microtunneling method was used and it consisted of a closed front TBM of 1800mm diameter over a length of 785m. This construction was accompanied by instrumentation that registered the drilling process with force measurements in the main jacks and IJS, strain in the concrete, joint width, tilt of the element and displacement measurements. This monitoring was part of the Delft Cluster work package DC 01-01 Controlled Drilling in Urban Areas under the guidance and request of the research association Gemeenschappelijk Basisonderzoek Boren (GBB). Their goal was to determine the force distribution in the pipes during penetration for different soil types and design profiles. Only part of this data set was analysed mostly focusing on the element joints. The data set can also be used to analyse the soil-structure interaction regarding friction, which is the focus of this thesis.

The final report from the Delft Cluster project already indicated that the total friction averaged over the entire length of the pipe was more than the predicted value even with reduced friction due to lubrication. Also, the friction over the front parts of the tunnel tubes has been determined using the IJS pressure and results in a much higher value than the average friction. Therefore, there is clearly room for improvement in the friction prediction process at the design phase.

Another important observation was that at some sections, there were constant or even decrease in the total jacking forces which is against what is expected (linear increase with distance). The mismatch on the frictional forces and the decrease in jacking forces were not further investigated and supports the need of this research.

The main goal of this thesis is to analyse the frictional forces development over length and time of the boring under the IJ river and to understand the reason why the predicted values differ from the measurements. The analysis includes the orientation of the TBM and the orientation of two instrumented pipe segments (located approximately 60 m behind the TBM), the lubricant influence specially in sandy soils and the calculation methods of friction resistance factors which is used for the friction determination.

1.1. Problem Statement

According to (Ye et al., 2019), the friction resistance is often overestimated or underestimated by the existing prediction models when lubricant is used in the microtunneling method. The models do not fully take into consideration all the following factors combined: pipe diameter, soil properties, overcut, lubricant efficiency, pipe misalignments and stoppages. This is an issue, because an inaccurate prediction of the frictional resistance can directly impact the structural safety and the construction cost of the microtunneling (Ye et al., 2019).

As described in the previous section, such inconsistencies between predicted and executed frictional values were found in the boring under the IJ. It is of great importance that these differences are better understood so they can be avoided or at least have their affects diminished and controlled in future projects.

Analysing the reported frictional forces development over length and time of the boring under the river IJ, and understanding the reason why the predicted values differ from the measurements, should contribute to the existing knowledge of microtunneling studies.

1.2. Aim and Objective

This master thesis aims to investigate the difference between the predicted friction values during design phase and the actual friction during the construction phase of the boring under the IJ. To do that, causality will be investigated considering relations within local circumstances, such as site conditions and operational parameters like steering corrections and other local deviations from a straight alignment. In order to better understand the local influence of the soil-structure interaction in the friction resistance parameters, the analysis must also contain an assessment of travelled distance of pipe segments over time. For every, the friction resistance calculation method will be assessed.

Because the frictional resistance is the main component of the jacking forces (Ye et al., 2019), the non-expected constant or decreasing jacking force values at certain sections during the project should also be analysed. The tunnel orientation, local soil conditions and steering corrections are going to be the main focus of the first stage of this investigation. A second stage of the study will be considered in case more causal parameters should be included to explain the non-expected jacking force values.

1.3. Extent and Limitation

The dataset considered and analysed for this project is limited to the Delft Cluster (DC) data set and any hypothesis will be tested against this data set only.

1.4. Research Questions

1. What are the parameters that influence friction and jacking forces during Microtunneling. Which factors are considered in the friction design calculations?
2. What additional factors can be identified by a new analysis of the Gemeenschappelijk Basisonderzoek Boren (GBB) microtunneling intervention? Specifically
    - 2.1. What is the impact of the orientation history of the TBM at the time of excavation on the recorded friction for the subsequently installed pipeline?
    - 2.2. What is the impact of the amount of pipe segments that travelled past at a specific location over time on the recorded friction at that location?

2. Research background or Literature review

2.1. Definition

Microtunneling is a trenchless closed front boring method of installing utility pipes usually with diameters between 0.15 and 3.50 m (Broere & van der Woude, 2012). It is a combination of a tunnel boring machine (TBM) and pipejacking. At the starting shaft, hydraulic jacks are placed on a jacking frame. They will push the TBM through the shaft wall and once it is far enough into the soil a next prefabricated segment pipe will be coupled behind the machine and the whole line is jacked forward into the ground. This process of coupling a new prefabricated segment pipe and jacking is repeated until the line reaches the receiving shaft.

2.2. Types of shields

According to International Tunnelling and Underground Space Association (n.d.-a)a shield is : “A movable steel tube, framework, or canopy shaped to fit the excavation line of a tunnel and used to provide immediate support for the tunnel and protect the men excavating and providing the long-term support. May be fitted with a cutting device for excavating the tunnel lining. […] The general principle of the shield is based on a cylindrical steel assembly pushed forward on the axis of the tunnel while at the same time excavating the soil.”

Many different types of boring shields are available for microtunneling, but the selection of the correct type of shield is dependent on the geological and hydro-geological conditions. Since in the Netherlands a high water table is encountered throughout the entire country, only borings with closed front shields are possible (Broere & van der Woude, 2012). Therefore, the types of shields available following this criteria are: Slurry shields, Earth Pressure Balance (EPB), Mix shields and Mechanical pressure balance. Their functioning are further explained below.

2.2.1. EPB shield

In an Earth Pressure Balance shield, the excavated soil fills in the bore chamber and this is used to stabilize the tunnel front. This means that the soil pressure outside the excavation chamber needs to be in equilibrium or has to be smaller than the soil mixture inside it (Figure 1). This is controlled by the rate of excavation, by the hydraulic jacks that press the machine forward, and excavated soil that is extracted from the excavation chamber through a screw conveyor to the rear of the shield.

This type of shield can be used in soils with high cohesion and low permeability, such clay . In sand this type is also possible to use with the use of additives.

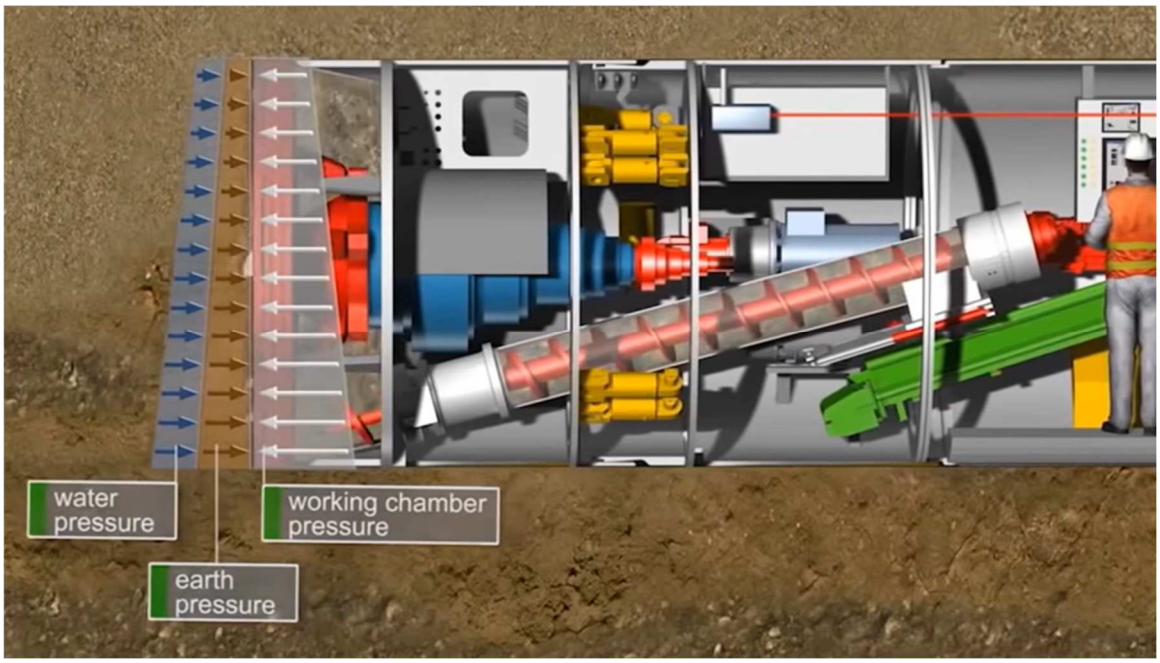

Figure 1 - EPB M-TBM shield illustration [ref. https://www.youtube.com/watch?v=z5QUz0sfeug taken on 17/11/2024]

2.2.2. Slurry shield

The slurry shield is used in soils that have both low and high permeability like sand. A bentonite suspension is used to support the soil body in front of the shield by maintaining an overpressure in the mixing chamber and Due to this pressure difference, the bentonite penetrates a few centimetres into the ground and creates an impermeable layer. Figure 2 illustrates the main components of a slurry shield machine.

The excavated material which is a mix of soil and slurry is transported to the surface through pipes where it will reach a separation plant so the slurry can be recirculated and reused.

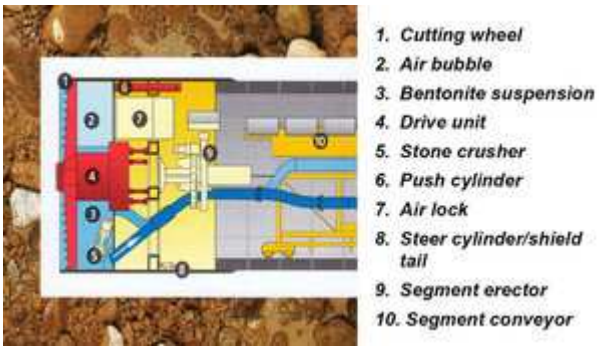

Figure 2 - Slurry shield illustration (International Tunnelling and Underground Space Association, n.d.-b)

2.2.3. Mechanical pressure balance shield

With the mechanical pressure balance shield, the bore front is supported almost entirely by the cutter-wheel. The soil is removed through gaps, whose opening width is variable, located in the cutter-wheel and the stability of the bore can be controlled by the amount of soil that enters the working chamber. The material is removed via conveyor belts, scraper chains or by hydraulic means. (International Tunnelling and Underground Space Association, n.d.-c, p. 25)

2.3. Microtunneling elements

2.3.1. Shafts

The common practice in microtunneling is to have a watertight starting shaft and reception shaft. They can vary with respect to depth (close to surface or deeper), shape (round, rectangular, oval), dimension and construction material (sheet piled, caisson constructed, etc) since they are related to different parameters as type of machine being used, ground conditions and has to be financially viable.

In the microtunneling project under the IJ, the starting shaft was approximately 22m deep with sheet pile walls, watertight seal and 3 levels of struts (Figure 3).

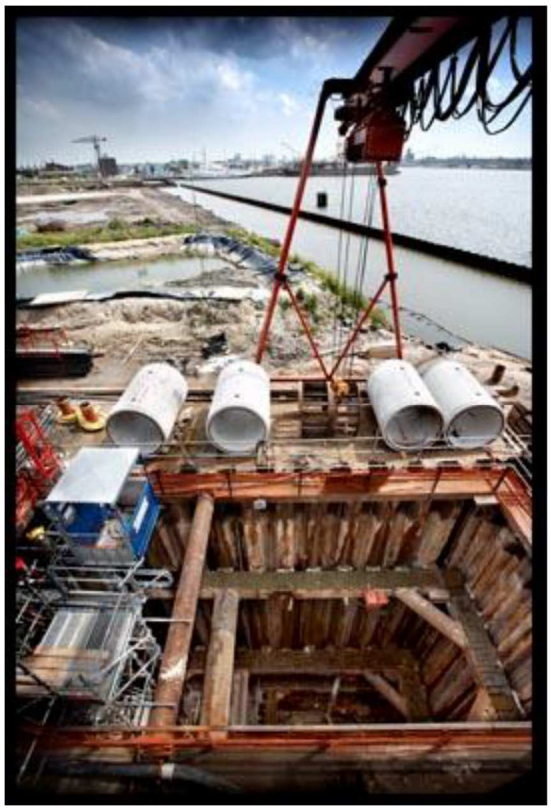

Figure 3 - Starting shaft of microtunneling project under the river IJ (Delft Cluster, 2007)

Since the pipe-jacking technique requires a surface to be pushed against in order to have a reaction force, a trust wall or a reinforced slab needs to the constructed in the starting pit. This needs to ensure the integrity of the shaft structure and surroundings while the jacking frame is used in its maximum capacity. Part of this involves the design of a softer part in the wall that allows the boring machine to enter the reception shaft from the ground. Also, design effort needs to be done when working below the water levels to keep the starting shaft dry when starting the boring. A rubber sealing ring can be installed in the wall and it has different variations dependent on the material of which the wall was built, for instance for diaphragm walls or sheet pile walls (Broere & van der Woude, 2012).

2.3.2. Pipe elements

According to Pipe Jacking Association (2017, p.6), at the jacking frame, a thrust ring is mounted ensuring that the jacking forces are equally distributed around the circumference of a pipe being jacked (Figure 4) and the jacks are interconnected hydraulically. Also, in between two pipes, a pressure distribution ring (wooden packer ring) is placed to maintain this constant force progression along all the pipes installed and to avoid cracks in case of uneven pressure independent of the material. A great variety of materials are available for microtunneling including concrete (reinforced and unreinforced), steel, clay, and others but their choice are dependent on project requirements.

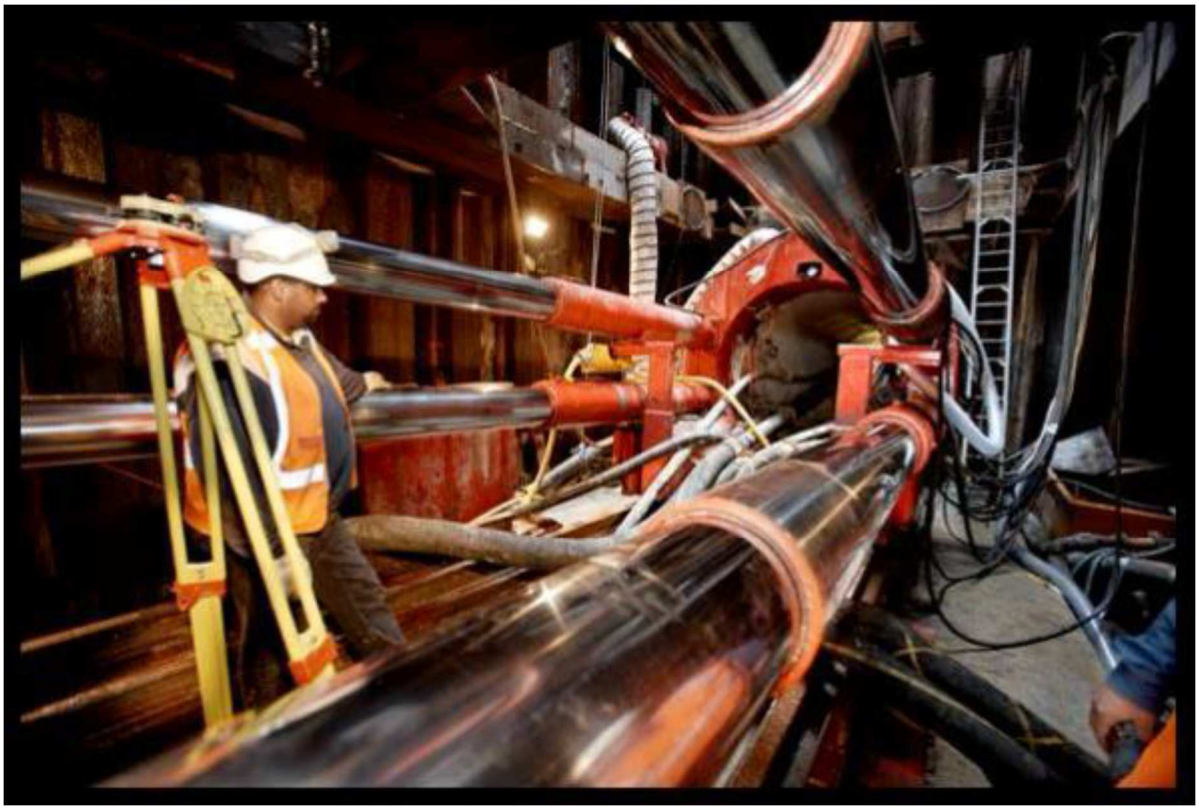

Figure 4 - Main jack installation at the project under the IJ (Delft Cluster, 2007)

2.3.3. Intermediate jacking stations

The length of a microtunneling is restricted to the maximum allowable jacking force which needs to be larger than the frictional resistance on the pipe string and on the face of the shield, combined (Marshall, 1998). It is possible to add intermediate jacking stations (IJS) to construct longer tunnels, which will increase the possible drilling lengths. An IJS consists of hydraulic jacks placed in a steel ring which is inserted into the pipe string (Figure 5). This allows the tunnel to be divided in sections that can be pushed separately distributing the frictional forces to the respective jacking elements behind (Broere & van der Woude, 2012).

Figure 5 - Intermediate Jacking Station (IJS) at the project under the IJ (Delft Cluster, 2007)

2.4. Pipe -soil interaction

In this section, the loads and resultant forces that are included in the microtunneling design and analysis are discussed, followed by an analysis on the assumed values for design purposes that can be found in the literature and finally an overview of the influencing factors that should be taken into consideration during design phase of a microtunneling.

2.4.1. Loads and Resistance forces

The current design practice, focusing on pipe-soil interaction analysis for a microtunneling design, describes that the force needed to push the TBM and the pipes into the soil is the jacking force coming from the jacking frame. This force needs to overcome the soil resistance that comes from the head of the shield and from the friction along the outside of the tunnel elements (Figure 6). Therefore:

(1) $F_{jack} \geq F_{head} + F_{friction}$

F jack	jacking force	kN
F head	pressure on the head	kN
F friction	Friction force	kN

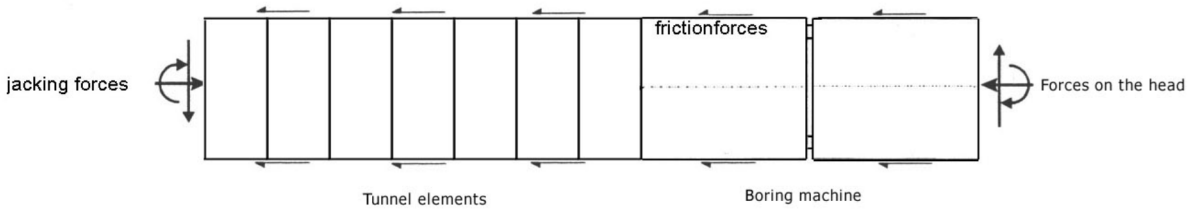

Figure 6 - Microtunneling acting forces (Broere & van der Woude, 2012)

2.4.1.1. Head of shield resistance

In (1), F head depends on the penetration force of the cutting wheel (F wheel) and the soils and water pressures (F ground). Normally conservative and simplified (2D) face stability calculation is used in microtunneling design. A full 3D analysis is not needed in this case since, different from large diameters TBM's, the overburden are very large compared to the tunnel diameter, therefore the tunnel is already stable, in not abnormal soil conditions.

Where,

(2) $F_{ground} = \sigma_{total} * A_{head}$

F ground	soils and water pressures	kN
σ total	Total horizontal stress	kN/m²
A head	Area from front of the shield	m²

(3) $A_{head} = \frac{\pi * D^2}{4}$

D	Outer diameter of the shield	m

The horizontal effective stress that acts on the face needs to be calculated. That requires the earth pressure coefficient K to be determined. Since the soil will collapse in front of the machine if no support is given, the active earth-pressure coefficient will be used in the simplified 2D approaches:

(4) $K_a = \frac{1-sin\phi}{1+sin\phi}$

K_a	Active earth-pressure coefficient	-
$\emptyset$	Internal friction angle	degrees

The horizontal effective stress (assumes soil surface and water table to be the same) is then calculated using formula (4) followed by the calculation of the total horizontal stress:

(5) $\sigma'_{h,soil} = (\gamma_g - \gamma_w) * K_a * h$

$\sigma'_{h,soil}$	Horizontal effective stress of soil	kPa

(6) $\sigma_{h,soil} = (\gamma_g - \gamma_w) * K_a * h + \gamma_w * h$

$\sigma_{h,soil}$	Total horizontal stress of soil	kPa

To summarize, F_{ground} (2) is described as formula (7).

(7) $F_{ground} = [(\gamma_g - \gamma_w) * K_a * h + \gamma_w * h] * \frac{\pi * D^2}{4}$

As mentioned above, the penetration force of the cutting wheel also contains the soil resistance that comes from the head of the shield (contact of the cutting wheel directly with the soil).

(8) $F_{wheel} = A_{head} * I_r$

F_{wheel}	Shield penetration force into the ground	kN
A_{head}	Area from front of the shield	m²
I_r	Penetration resistance	kN/m²

The penetration resistance is a value that is assumed and usually for homogenous soils it is set to be Ir=50kN/m² (Broere & van der Woude, 2012). The total contribution to the jacking force by a precise determination of the mechanical contact force between cutter head and soil is limited therefore this is commonly used.

2.4.1.2. Friction force

Friction forces are created along the outside of the tunnel elements when they are being pushed through the soil. According to Thomson (1993), the equations used to describe friction resistance are using the assumption of a straight drive with a uniform external pipe surface or no impact from local steering corrections. Therefore it increases linearly with the length of the boring. This study's goal is to see to what extent this assumption is reasonable. See formulas below:

(9) $F_{friction} = f * A_{tunnel}$

$F_{friction}$	Friction force	kN
A_{tunnel}	Area of tunnel outside surface	m²
f	Friction coefficient	kN/m²

Where,

(10) $A_{tunnel} = \pi * D * L_{total}$

D	External diameter of pipe	m
L_{total}	Total boring length	m

(11) $f = \sigma'_n * tan\varphi$

σ'_n	Effective stress on the contact surface between the soil and the pipe	kPa
φ	Soil internal friction angle	degree

In reality, the contact surface between pipe and soil is variable. Figure 7 presents conceptual models for pipe and soil interaction with an increase in normal stress resulting in an increase in local contact area (Milligan & Norris, 1999). An increase in contact area can lead to an increase in friction along the drive.

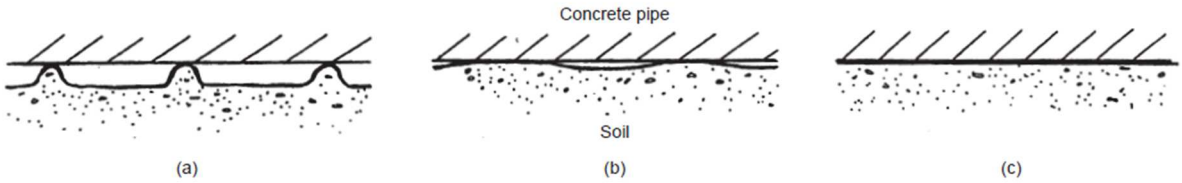

Figure 7 - Conceptual models for pipe/soil interaction showing: (a) localized `asperities'; (b) limited contact areas; and (c) full area. (Milligan & Norris, 1999)

Ye et al. (2019) proposes a new friction resistance prediction approach on slurry pipe jacking that different from the model described above and considers the effect of lubrication, soi properties and design parameters. The new approach of this paper introduces an effective friction coefficient to replace the original pipe-soil friction coefficient.

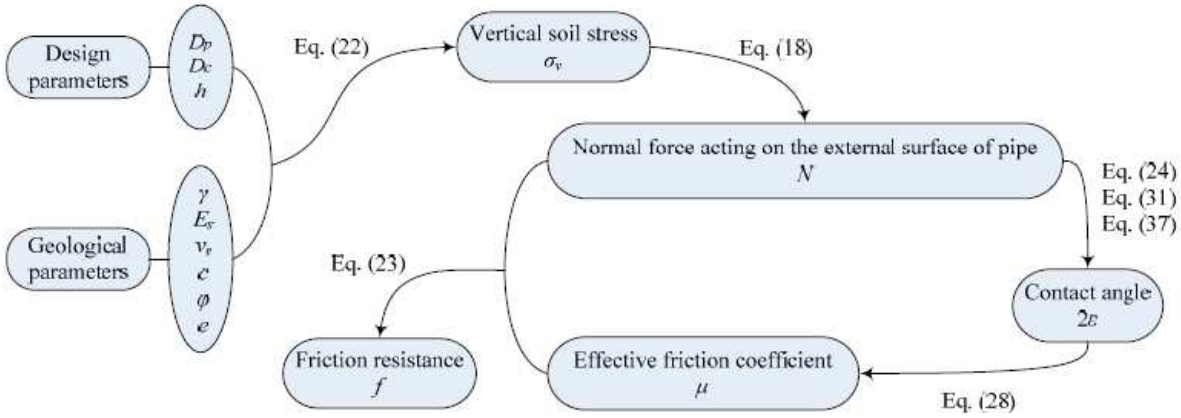

Figure 8 - Flow chart of friction resistance prediction Ye et al. (2019)

2.4.2. Influencing factors

Many factors influence the jacking forces and, as a result, also influence the frictional forces. According to Thomson (1993) ,Milligan and Norris (1993), (1996), Marshall (1998), Pellet-Beaucour, & Kastner, (2002), Verburg (2006) and Broere and van der Woude (2012) the following are the construction-related factors that influence them:

- Misalignment and steering corrections;
- Overcut;
- Lubrication;
- Steps at joints and/or joint deformation;
- Jacking around curves;
- The use of intermediate jacking stations;
- The rate of advancement of the pipeline;
- The frequency and duration of stops;

Some of the factors that are directly relevant to the goal of this thesis investigation as Misalignment and steering corrections, Overcut, Lubrication, and the frequency and duration of stops, will be discussed in more detail in the following sections. Joint deformation goes beyond the scope of this thesis and intermediate jacking stations were previously briefly explained.

2.4.2.1. Misalignment and steering corrections

According to Milligan and Norris (1993) misalignment is the angular deviation (β) between the central axes of successive pipes (Figure 9). When present, they can certainly induce contact stress between pipe and soil increasing the friction resistance and consequently increasing the jacking force needed for the drive. Instrumented field research done by Norris and Milligan (1992) indicated a clear correlation between angular deviation and increase in radial total stress indicating locations where misalignment are present (Figure 10). Also, the misalignment can be dependent on the soil type in which the boring is being installed (Ni & Cheng, 2012).

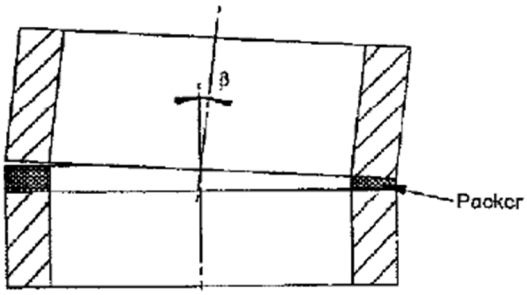

Figure 9 - Misalignment angle,β (Marshall, 1998)

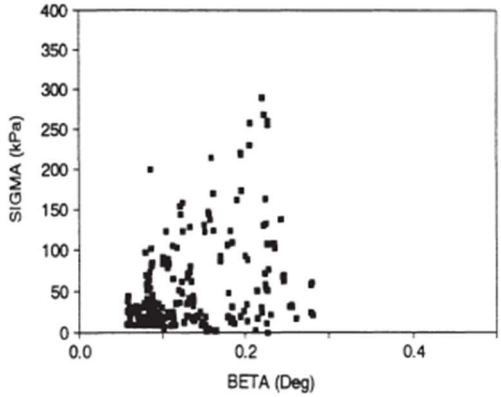

Figure 10 - Pipe angular misalignment against total radial stress (Norris & Milligan, 1992)

In Figure 11, it is possible to see the theoretical forces acting on the pipe when the boring is deviating from a straight line. In the design phase, limits can be specified to the allowable errors at any point along the tunnel which is typically in line 75mm and level 50mm (Milligan & Norris, 1999).

The prediction of misalignment forces is very difficult since it can be misled by all other influencing factors along the boring. According to published jacking records, it is possible to assume that greater force increases are a result of vertical misalignments rather than horizontal ones, no exact values were presented for further comparison (Thomson, 1993). Since the TBM uses the reaction force in the ground to make a curvature, in stiffer soils the TBM reacts faster leading to a sharper corner than compared to softer soils where a slower reaction leads to a more gentle alignment (Verburg, 2006).

In order to avoid or diminish a misalignment, steering corrections are made with the main jacks to maintain the line and level as close as possible to the one designed. However, Milligan and Norris (1993) observed in their research, using successive surveys, that once a local curvature is established it remains throughout the drive since “There is no apparent tendency of the line to straighten with the passing of successive pipes.” (Milligan & Norris, 1999, p. 30).

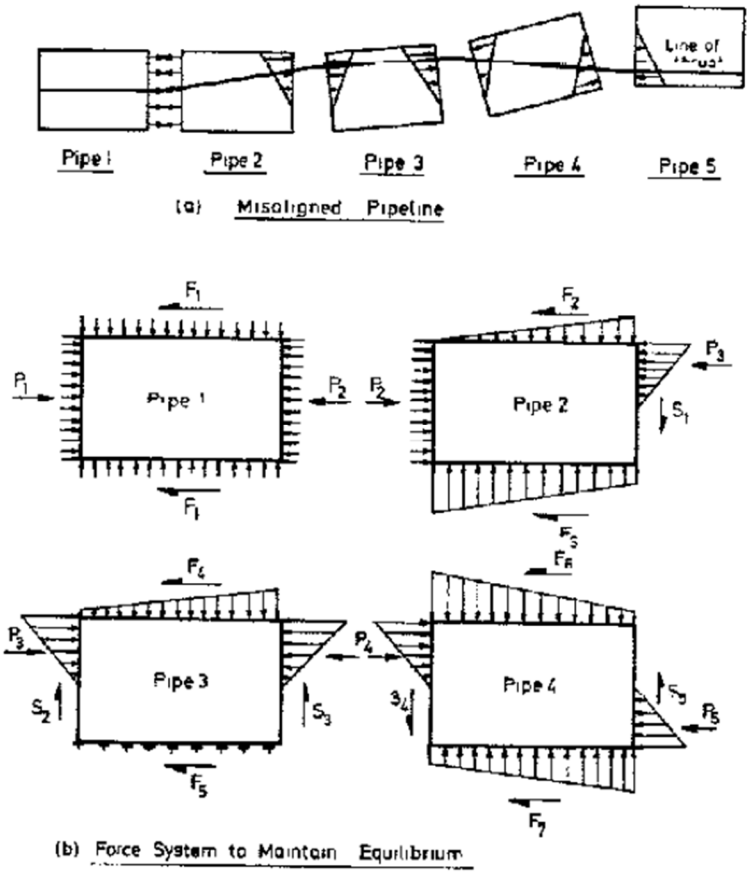

Figure 11 - Theoretical misalignment forces (after Norris 1992b) (Marshall, 1998)

2.4.2.2. Overcut

In microtunneling, the shield has a slight larger external diameter than the pipes being installed, this creates a space which is called the overcut (Figure 13). According to Milligan and Norris (1993) and (1996), the overcut should remain open while the boring is in place so the pipes can slide along the base of an open bore, reducing the pipe-soil friction. Then the total jacking forces will be minimised. Thomson (1993) mentions that typical values for overcut on radius are 10 to 12 mm, although values as large as 75 to 150 mm on radius have already been used. In the latter case, the void has to be backfilled by grouting once the boring is complete to avoid future settlements.

It is possible to see the effect of an increase in frictional stress after the reduction of the overcut in Sand and gravel soils (Figure 12). In this case, after 16m of drive length, the diameter of the installed pipes were increased by 20mm which decreased the overcut from 32mm to 12mm (Pellet-Beaucour & Kastner, 2002).

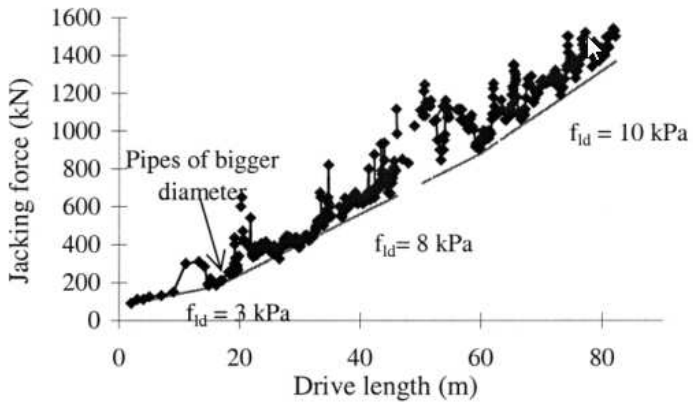

Figure 12 - Evolution of the total jacking force in Neuilly 2, showing the influence of overbreak on frictional stress (Pellet-Beaucour, A. L., & Kastner, R., 2002).

Verburg (2006) mentions the internal friction angle as one important indicator of the stability of the overcut in non-cohesive soils where the higher the internal friction angle, the coarser the grains are. For the stability, having irregular shaped and sized grains are ideal.

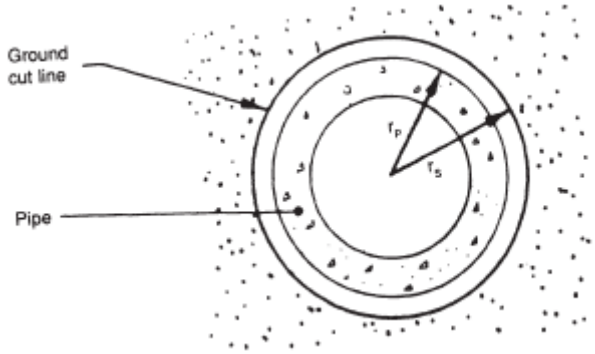

Figure 13 - Overcut representation (Thomson, 1993)

2.4.2.3. Lubrication

There are many types of lubricants, but for microtunneling mostly bentonite slurry is used. Bentonite is a range of natural clay minerals such as potassium, calcium and sodium montmorillonites. As an alternative, polymer based slurries can be used. In the tunnelling industry, natural polymers (e.g. sugars, celluloses, protein) and man-made polymers are used (Milligan, 2000).

Lubrication is used to fill the overcut void (Figure 13). In a theoretical ideal scenario, the overcut is completely filled with lubrication and there is no contact between pipe and soil, but between pipe and lubricant and the pipes will become buoyant. This would decrease the friction resistance significantly, and by consequence the jacking force needed (Milligan, 2000).An example of this decrease is illustrated in Figure 14. According to Thomson (1993), “It has been calculated that in such a condition it would be possible to push a length up to 1000 times greater than without the fluid for the same load” (p.189).

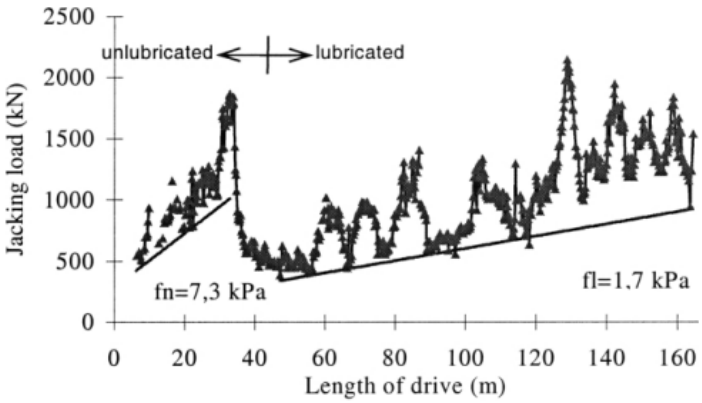

Figure 14 - Evolution of jacking force - jacking force related to drive length (Pellet-Beaucour & Kastner, 2002)

In reality, in non-cohesive sediments, the bentonite will penetrate into the pores in between the soil particles and be lost unless a 'filter cake' is created which is essentially a mixture of soil and lubricant that will fill the soil pores forming a low permeability membrane in the ground, see Figure 15 (Milligan, 2000). According to Reilly & Orr (2017), this layer presents a lower angle of friction than the soil as well.

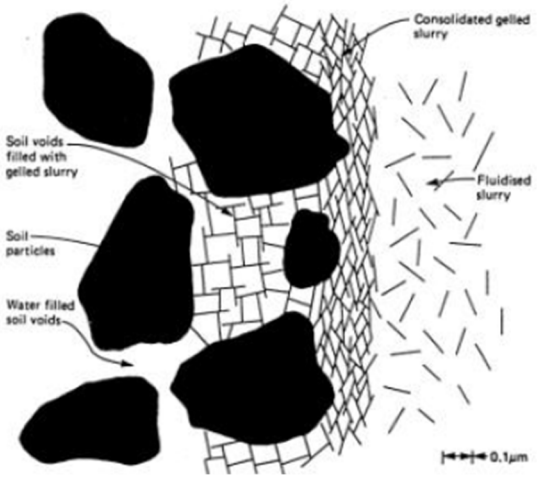

Figure 15 - Formation of filter cake

Marshall (1998) could measure the reduction in friction after the use of lubricant in 6 different types of instrumented borings. In Figure 16, their results are depicted and it is possible to notice a significant reduction on friction in cohesive and granular soils reaching up to 93% in dense silty sand.

Scheme No	Pipe ID (mm)	Soil Type	Cover (m)	Mean frictional resistance (kN/m)		Reduction in friction (%)
				Unlubricated	Lubricated	
4	1200	Dense silty sand	7-10	23	9	59
5	1200	Sand and gravel	4-7	100	10	90
6	1500	London clay	6-8	-	13	-
7	1000	Dense silty sand	5-8	- - -	9 42 (break) 3	- 79 (increase) 93
8	1800	Stiff glacial clay	6	48	15	69
9	1500	Very soft clay	5.5-6	25	14	44

Figure 16 - Reduction in frictional resistance (Marshall, 1998)

Ye et al. (2019) presents a strong increase in lubricant efficiency from 64% to 91% when the overcut increases from 0 to 15mm (Figure 17). This confirms the importance of a sufficiently wide overcut filled with lubricant so the elastic unloading of the ground does not lead to a complete closure of the annular gap.

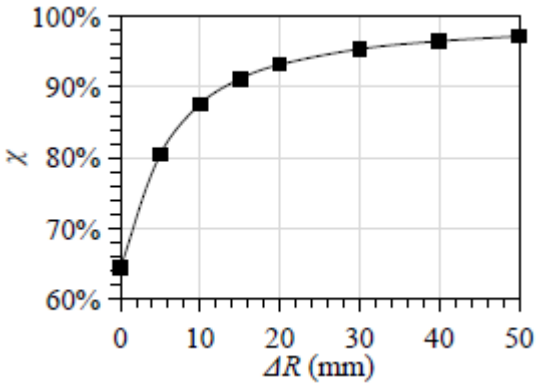

Figure 17 - The influence of overcut (ΔR) on the lubricant efficiency (x) Ye et al. (2019)

Orr (2017) used direct shear and triaxial tests to analyse the effects of pressurized and unpressurized lubricant on the interface shearing resistance. The presence of an unpressurized bentonite-based lubricant layer against a concrete surface gave only a small reduction in shear resistance. The most beneficial solution was to shear against a smooth interface, for example a Perspex sheet, in which case the angle of shearing resistance was reduced by one third. In the presence of pressurized lubricant, the slurry blocks the pores in the soil and the fluid pressure is then transferred to the soil skeleton. With this method a more substantial reduction of shearing resistance was shown. In summary, “pipe jacking lubricants should be applied under conditions of controlled pressure rather than controlled volume to gain the maximum beneficial reduction in skin friction resistance in coarse-grained soils.” (Reilly & Orr, 2017)

2.4.2.4. The frequency and duration of stops

There are many reasons to stop the boring in the middle of a pipe installation such as bringing in the next pipe section (Reilly & Orr, 2017, p. 9). When this happens, a higher jacking force is needed to restart the movement of the pipe into the soil compared to the force before the stoppage. There is a static and a dynamic friction coefficient where after a standstill the static friction occurs and during movement the dynamic friction occurs (Van Seters et al., 1999 as cited in Verburg, 2006). The dynamic friction is generally lower than the static one. Table 1 presents values for concrete in sand and clay to illustrate this difference, showing a smaller friction when the pipe is already moving.

Table 1 - Static and dynamic friction coefficients (Van Seters et al., 1999 as cited in Verburg, 2006)

Material x Soil type	tan(δ) static friction	tan(δ) dynamic friction
Concrete in sand	0.5 – 0.6	0.3 – 0.4
Concrete in clay	0.3 – 0.4	0.2 – 0.3

According to Pellet-Beaucour & Kastner (2002) and Milligan and Norris (1993) and (1996), in cohesive soils, an even higher jacking force is needed due to pore pressure dissipation. “When total radial stresses decrease but effective stresses increase Norris (1992b) suggested that shearing had generated excess pore pressures which then dissipated during the stoppages more rapidly than the decrease in total stress resulting in increased effective stresses and larger loads.” (Marshall, 1998, p. 6.45). Therefore, the jacking force increase is related to the total amount of time in which the boring was interrupted, see Figure 18 as an example. This is mostly apparent for cohesive soils, whereas time effects are negligible in cohesionless soil (Milligan & Norris, 1999).

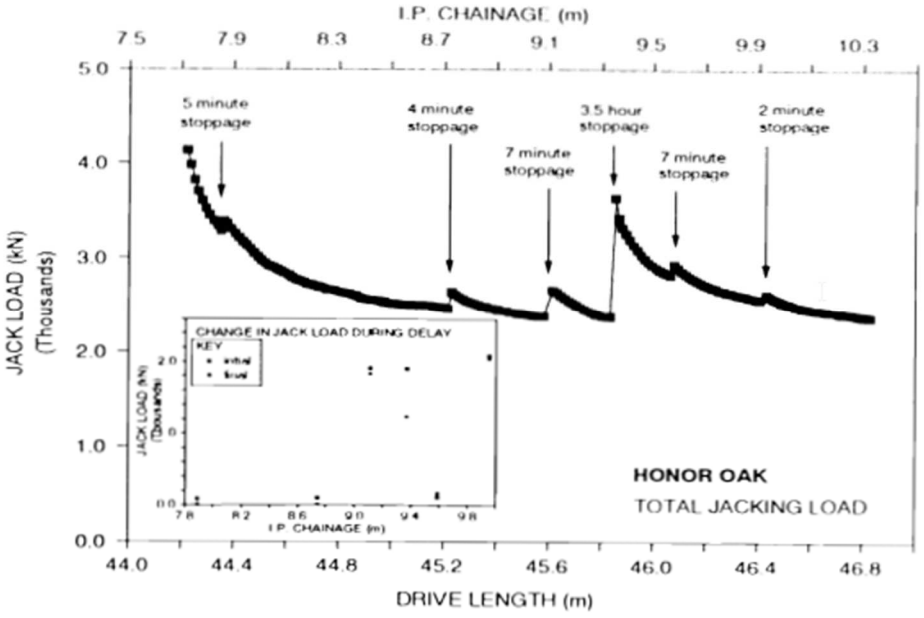

Figure 18 - Change in jacking load during stoppages after Milligan and Norris (1993)

2.4.3. Assumed values for design purposes

After having an overview of basic parameters needed for a microtunneling design, in this section some common used values in the industry are going to be discussed.

To start, the friction coefficient f used in actual project design is often an estimate based on experience and some common values used in practice are given in the Dutch norm NEN 3650. These values can vary depending on the soil type, the use of lubricants and the presence of overcut along the boring. When overcut is present, in the Netherlands, f =10 kN/m² is often used for concrete pipes and when lubricant is also used the value usually used is f =7.5 kN/m². When overcut is not present, the values of f can vary from <10kN/m² in mud, silty soils to > 30 kN/m² in hard clay.

Tomson (1993) gathered values of friction coefficients used in different countries and it represents their variation as soil type dependent. According to Marshall (1998), these values are presented in terms of mean shear stress which assumes uniform contact around the pipeline, whilst it is already known this contact is non-uniform.

Part of this study is to understand the variations in the numbers presented in Table 2. Within a specific soil type the friction coefficient varies in a considerably large range and it can be due to different factors that will be discussed in the next Section.

Table 2 - Friction coefficient of pipes in different soils. Source Tomson J. (1993)

Soil type	**France** ***f*** **[kN/m²]**	**UK** ***f*** **[kN/m²]**	**Australia** ***f*** **[kN/m²]**	**Germany** ***f*** **[kN/m²]**
Rock		2 to 3	1	
Boulder Clay		5 to 18		2.8 to 18.4
Firm clay	8 to 10	5 to 20	5 to 7.5	5.3 to 9.3
Wet sand		10 to 15	13	2.2 to 16.1
Silt	17	2 to 20		4.9 to 8.5
Dry dense sand				1.1 to 6.7
Dry loose sand	20 to 30	24 to 45		

As already mentioned in the previous section, the penetration resistance is also an assumed value. Broere and van der Woude (2012) indicates that for homogenous soils the common value used is 50kN/m². However, in Thomson (1993), it is recommended to use values ranging from 300 to 600 kN/m³ depending on the soil type. The contact forces between soil and cutting tools represented by I_r (and consequently the exact value of I_r) can be neglected when assessing the total jack force for a given project since the friction along the pipe is the dominant factor.

2.4.4. Monitoring

Previous research with the purpose of collecting data on jacking loads and stresses at the pipe-soil interface to improve future microtunneling designs were performed and this single setup was recorded by Milligan and Norris (1993), Milligan and Norris (1996) and Marshall (1998). The complete instrumentation used for their research work are the following (Milligan & Norris, 1996, p. 6):

- “Four contact stress cells, to measure both total radial and shear stresses on the surface of the pipe: their active face was flush with the pipe surface and provided with a similar surface to the pipe;
- Four pore pressure cells adjacent to the contact stress cells, measuring the local pore water pressure and hence allowing determination of the effective radial stress;
- Three joint movement indicators at each end of the pipe, to measure the three-dimensional angular misalignment of the joint gap;
- Up to twelve pressure cells built into the packer in the joint at either end of the pipe, to measure the magnitude and distribution of the stresses transferred across the joints;
- Up to six extensometers fitted to the internal surface of the pipe and equally spaced around it to measure the compression of the pipe under load. ”

Figure 19 presents the instruments arrangement described above in the main instrumented concrete pipe. These information together with the location and jacking forces are able to be correlated with tunnel alignment, lubrication operations, site activities and understand the soil response to the tunnelling process.

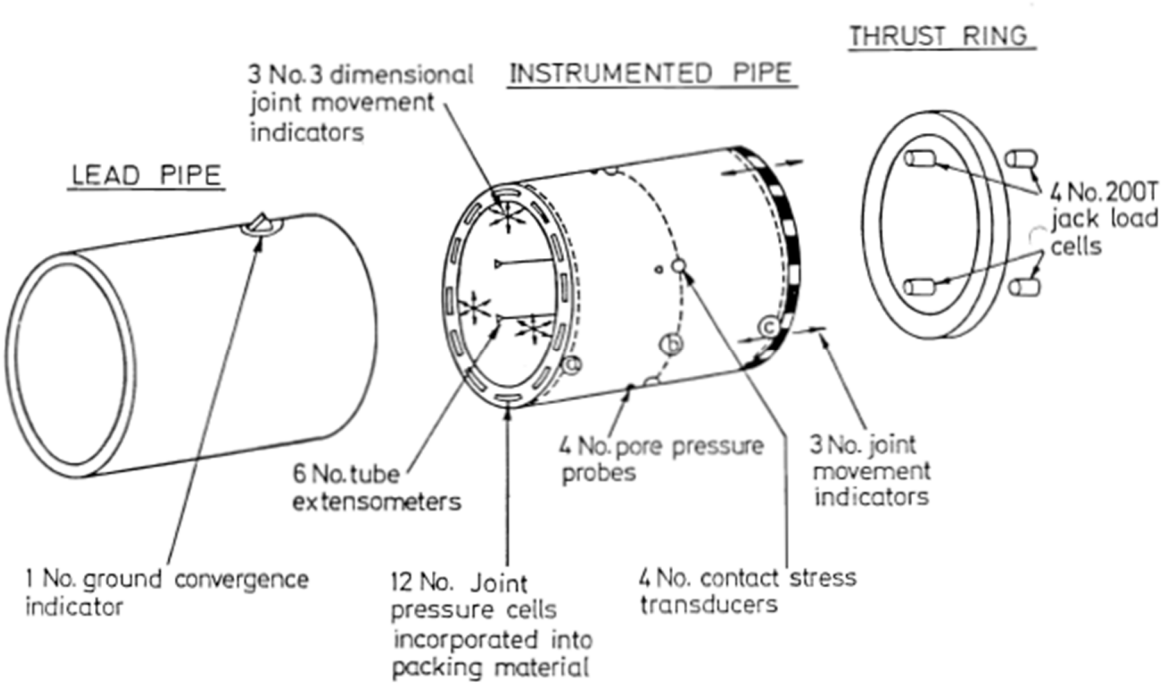

Figure 19 - Schematic of instrument arrangement (Milligan & Norris, 1993)

Important to be highlighted is:

> "The contact stress cells built into the side wall of the instrumented pipe have provided two main types of information. The magnitudes extent to which pipe and ground are in contact, while their ratio gives a direct measure of the interface friction between pipe and ground. The two combine to give the total frictional resistance to jacking." Milligan and Norris (1999, p. 31)

A more recent monitored project was the Castlerigg tunnel drive presented in Phillips (2023). The purpose of this project was to measure and record overcut conditions and pipe behaviour by means of instrumented pipe sections (Figure 20), with the focus in exploring the mechanics of the soil-lubricant-structure, which contained:

- Four load cells to monitor external soil contact stresses (local normal and shear contact stresses).
- An Omega PX309-200GV electrical pressure transducer was installed beside each load cell to monitor the pore water pressure in the tunnel overcut.
- 16 Soil Instruments ST4 vibrating wire strain gauges (VWS) into the pipe wall (Figure 21)
    - At four locations (N, W, S, E) the strain gauges were placed in rosette formation to measure axial, hoop, and 45° in-plane strain.
    - An additional four strain gauges were deployed to measure hoop strains only, one each at locations NW, SW, SE, and NE

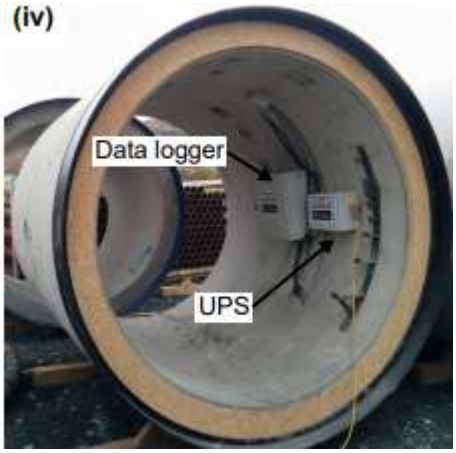

Figure 20 - Instrumented pipe on site (Phillips, B., 2023)

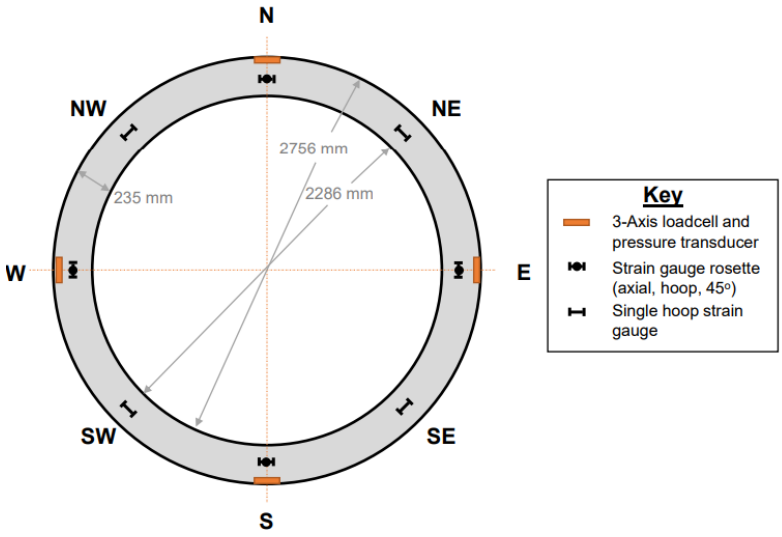

Figure 21 - Schematic of the sensors installed into the Castlerigg instrumented pipe (Phillips, 2023)

According to Norris & Milligan (1992), when plotting shear against radial stresses, a linear relationship is observed that is a clear indication that the response is mainly from pipe-soil friction (Figure 22). If the plot is scattered then other parameters might be influencing the friction, for instance lubrication (Figure 23). As can be seen in the examples provided by Norris and Milligan (1992) in cohesionless soils, the skin friction angle can be derived from this type of plot.

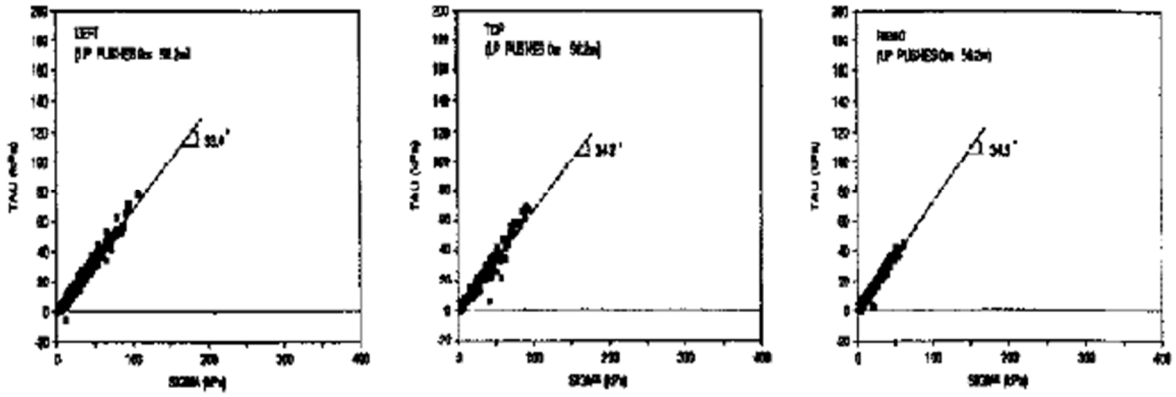

Figure 22 - Shear stress/total radial stress relationships during Scheme 4 prior to lubrication (Norris & Milligan, 1992)

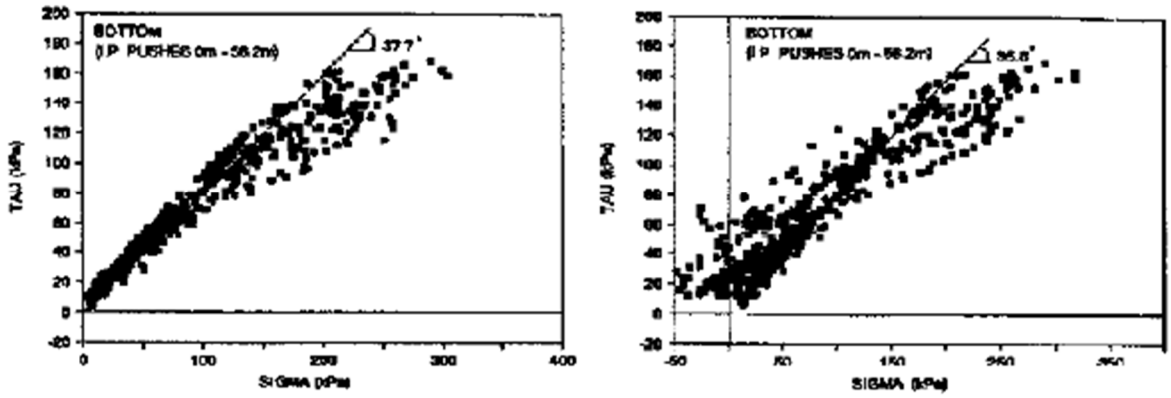

Figure 23 - Shear stress/total radial stress relationships on the pipe bottom during Scheme 4 prior to lubrication (Norris & Milligan, 1992)

According to Marshall (1998), it is ideal if the interface stress could be measured at two different locations along the boring with a reasonable distance in between instruments so the changes in stress can be recorded due to repeated shearing and stoppages.

2.5. Conclusion

In the works cited above Norris and Milligan (1994) and Milligan (2000) had the friction measured by instrumentation and did a thorough comparison against the jacking forces and the influencing factors focusing on pipe joints. In Verburg (2006), the friction forces are calculated and then compared with jacking forces and influencing factors with a focus on misalignment and lubrication. In Ye et al. (2019) , a new friction resistance prediction model is proposed to help improve future designs including more influencing factors.

In Orr (2017) it is recommended that lubricants should be applied under controlled pressure rather than controlled volume with the aim of maximizing skin friction reduction.

The penetration resistance component of the total jacking loads has not yet been explicitly measured as part of the projects cited above. On jacking records, a constant face resistance is assumed whereas in practice the resistance would probably vary throughout the drive (Marshall, 1998).

The literature reviewed in this chapter gives an overview of how interesting and challenging it is to take into account all the influencing factors in a drive for design purposes and also for future improvement. This thesis will follow a similar approach as the studies above with the difference that a case study is available where no instrumentation was used for measuring the friction directly and limited information was recorded regarding stoppages and working times, therefore some influencing factors cannot be assessed.

3. Case study

3.1. Introduction

In 2005, the municipality of Amsterdam and the Amstel, Gooi en Vecht water board (AGV) collaborated in a project called A-4 (AGV's Wastewater Other in Amsterdam). The plan was to demolish two existing sewage treatment plants (WWTPs) in the city, build a new one and properly adapt Amsterdam's sewage system. Therefore, approximately 42 km of new pressure pipes with between 600 and 1800 mm diameter were needed. Also, a section would have to cross the river IJ and it concerns a 785 m drilling length with a closed front microtunneling of 1800 mm diameter.

This drilling was monitored in the period May-July 2005 at the 785 m long IJ junction by WL | Delft Hydraulics in collaboration with GeoDelft, DWR, Betonson and Smet Tunnelling, under request of Waternet with the purpose of preventing damage to the pipes and reducing risk of jamming. The aim was to follow the drilling execution and to map the forces on the tunnel tubes based on the jacking forces of the hydraulic cylinders, friction of the ground due to drilling fluid lubrication and the ground reactions both in straight sections and in bends. In previous projects, problems had arisen and a lack of knowledge was clear with regard to the force effects and the interplay between TBM and pipe orientation and resulting soil friction. Involved parties.

The research association GBB (Gezamenlijk Basisonderzoek Boortechnologie - Joint Basic Research Drilling Technology), founded in 2001, in which WL | Delft Hydraulics, GeoDelft and TU Delft participate with contractors, engineering firms and suppliers working in the sector had the aim to research and develop the field of underground drilling methods for the construction of tunnels and pipelines. In 2005, the research association emphasis was placed on microtunneling. In 2006, the GBB participants were presented with the results of the implemented microtunneling project (crossing the IJ) and the Action Plan for the elaboration and analysis of the measurements was discussed. It has been agreed to further elaborate the measurement results obtained in the context of the Delft Cluster work package DC 01-01 Controlled Drilling in Urban Areas in 2006 in collaboration with TU Delft and GeoDelft with the aim of better prediction and control of the force effect on the tunnel tubes in implementation. WL | Delft Hydraulics, in this research framework, would focus on the processes of drilling fluid flow, interaction with the soil and tunnel tube, rheology and sand-sludge mixtures.

The GBB research for 2006 has been integrated into the work carried out by WL | Delft Hydraulics and GeoDelft submitted Delft Cluster Work Package WP 01.16.11 "Process Control Construction Underground Infrastructure OGI - GBB" part of the Delft Cluster Project 01 10 Controlled use of the Subsurface (Z3876.40). The goal was to determine the force distribution in the pipes during penetration (microtunneling) for different soil types and design profiles. These should result in a calculation or design guideline with which the participants can generate a better design and a safer implementation.

3.1.1. Site and soil conditions

3.1.1.1. Microtunnel location

The microtunnel was drilled under the river IJ in Amsterdam, Netherlands. This area is located at the northwest side of the country (Figure 24). The river IJ crosses the city dividing Amsterdam-Noord from the old touristic town (Figure 25). The drilling is located north from the Westpark and it started at the Amsterdam North side and ended at Danzigerkade (Figure 26).

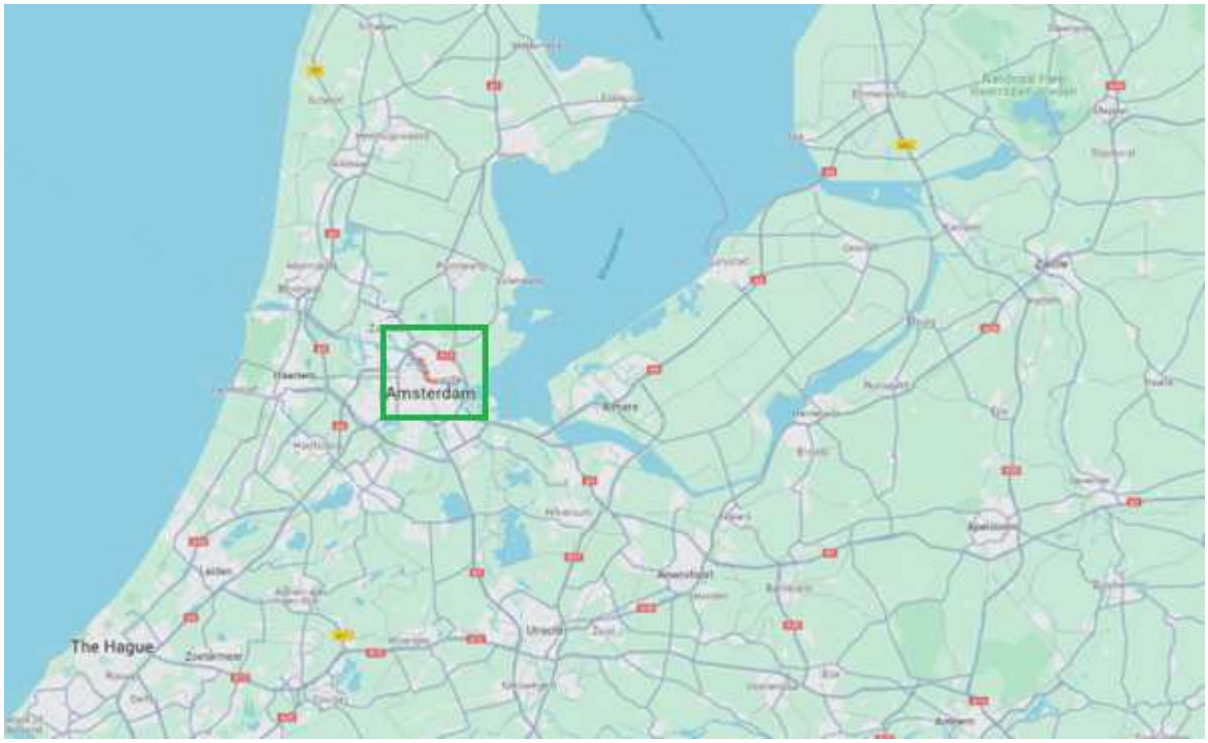

Figure 24 - River IJ location in the Netherlands (Google Maps 11/12/2023)

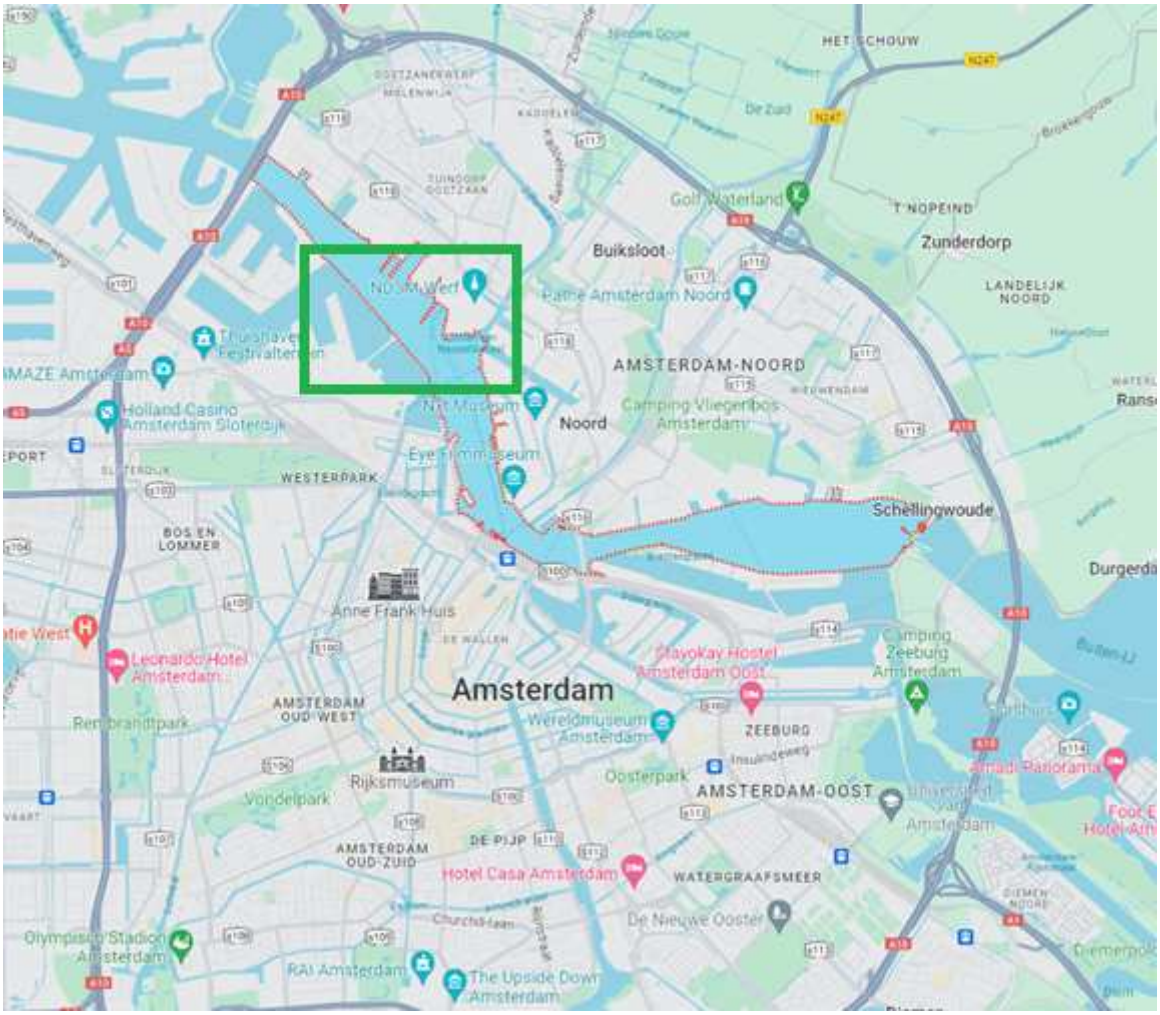

Figure 25 - Microtunnel location (Google Maps 11/12/2023)

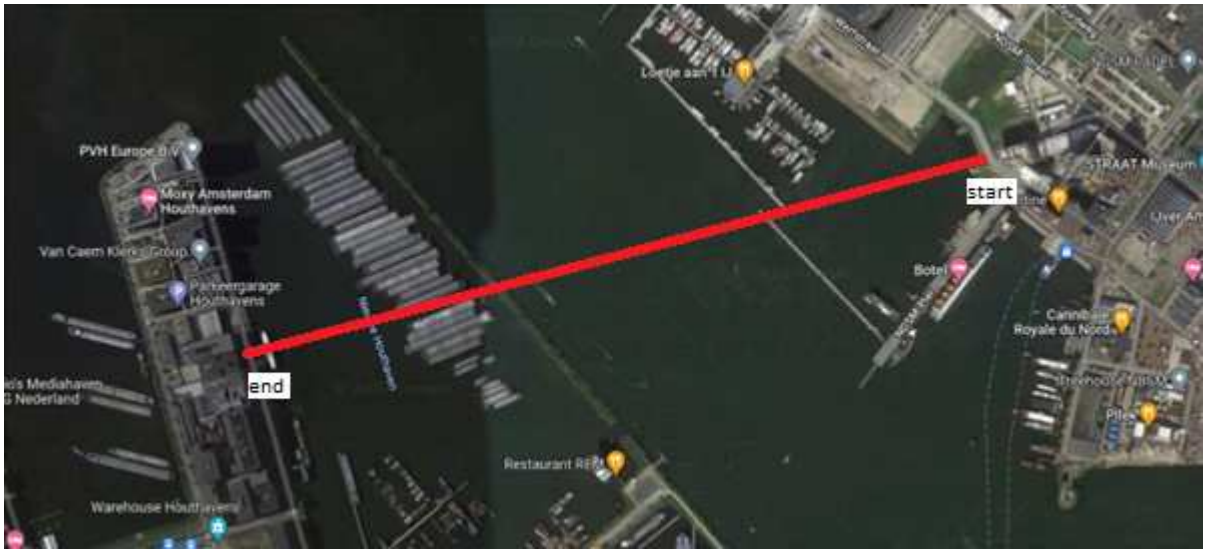

Figure 26 - Satellite image of microtunnel designed alignment – red line (Google Maps 01/03/2022)

3.1.1.2. General Geology

According to Wong, Batjes, & de Jager (2007), the surface sediments present in the Netherlands are almost entirely from the Quaternary geological period. At the north and west of the country, these sediments are composed of Holocene coastal plain deposits and, at the east and south, of sandy Pleistocene layers cut by Holocene rivers (Figure 27).

In Figure 28, a Noord-Holland cross section presenting the Holocene sequence depositions indicates tidal deposits and lagoonal clays in the upper layers of sediment. These environments are commonly filled with small grain size particles as silts and clays which are also expected to have a low strength. In the polder areas, peat is present at the surface even though a great part of this top layer was excavated in the past. This lead to a lower regulated surface water table which resulted in consolidation of the top sediment layers.

Based on this desktop study, the area where the microtunnel under the IJ was bored is expected to present soft and weak sediments as a general condition.

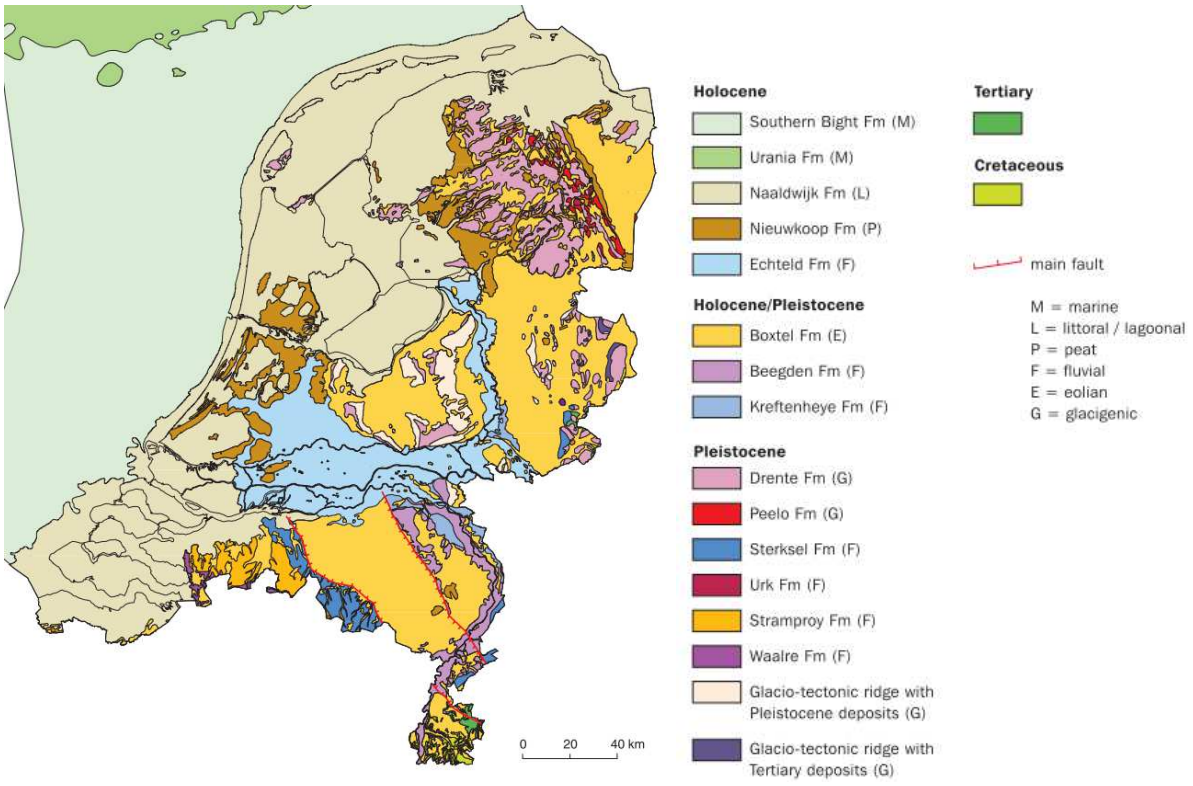

Figure 27 - Geological map of the Netherlands (Wong, Batjes, & de Jager, 2007, p174)

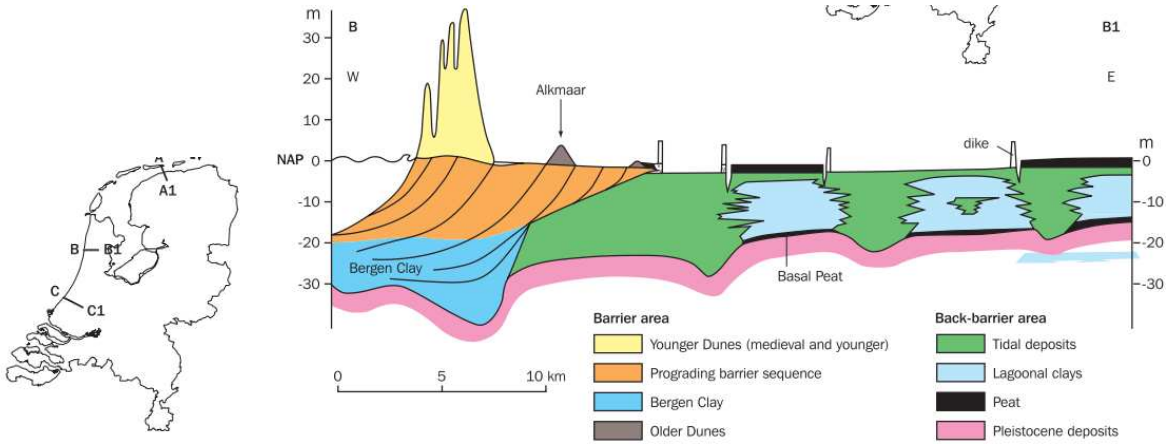

Figure 28 - Cross sections showing the Holocene sequences in the coastal plains of Noord-Holland (B-B1) (after Van der Valk, 1992, and Van der Spek, 1996) . (Wong, Batjes, & de Jager, 2007, p188)

3.1.1.3. Geotechnical Data

Within the available data for this project, the profile shown in Figure 30 was the only soil investigation information provided. It contains 8 boreholes, 35 soundings (CPTs) and the geological profile with description. The visual quality of the image is quite poor and it will not be possible to use the sounding information in detail since no parameter information of any kind was added. Therefore, this will be used as an overall site condition to understand the main soil layers which the microtunnel encountered along the boring.

The data package which was made available for this project will be discussed in detail in Section 3.2.

From the geological profile (Figure 30), it is possible to extract the expected soil conditions at the microtunnel alignment (Table 3). The soil expected in the first 240m is SAND, followed by extremely soft sediments for the next 136m. After that, SAND is the main soil type until the end of the boring with stretches of clay layers in between. Figure 29 for an overview of soil conditions along the alignment..

Table 3 - Expected soil conditions at microtunnel alignment

From (m)	To (m)	Length (m)	Expected soil type
0	243.89	243.89	(5) SAND
243.89	380.075	136.185	(9) Filling after sand extraction pit
380.075	620	239.925	(5) SAND
620	630	10	(5) SAND and (3) Loose SAND with layers of clay
630	723.85	93.85	(5) SAND
723.85	747.98	24.13	(5) SAND and (3) Loose SAND with layers of clay
747.98	760.58	12.6	(3) Loose SAND with layers of clay

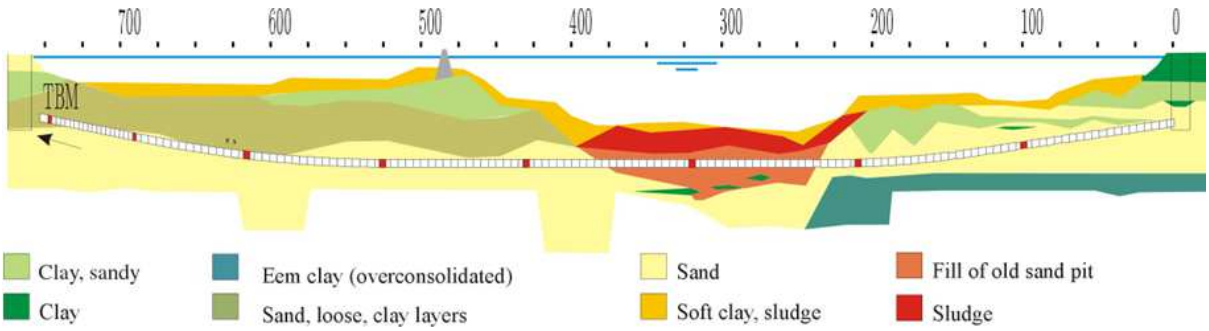

Figure 29 - Overview of soil conditions along the microtunnel alignment (Delft Cluster, 2007)

Legend for Figure 30:

1. Mud, soft CLAY
2. Sandy CLAY
3. Loose SAND with layers of clay
4. CLAY
5. SAND
6. Gravelly SAND
7. Eem CLAY
8. Alluvial sediments (harbour sludge)
9. Filling after sand extraction pit

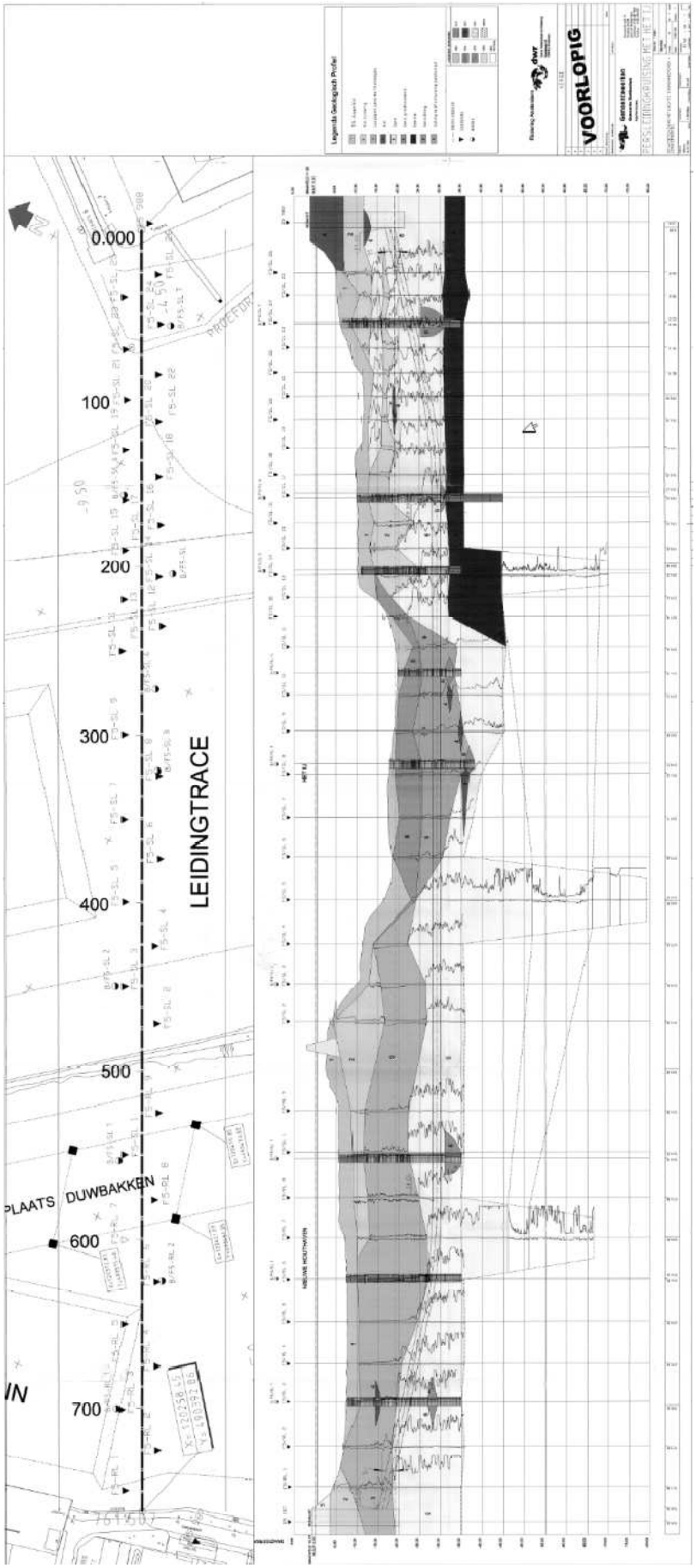

Figure 30 - Microtunnel alignment with geological profile and soil investigation (Delft Cluster, 2007)

3.1.1.4. Microtunnel Alignment

The total drilling length for the boring under the IJ is 785m. It starts in the main shaft in Amsterdam North (ground level 1 m + NAP) at a depth of 19 m – NAP. The borehole trails a straight descend of 135 m at an angle of 5 degrees followed by a curve to horizontal until 250 m, reaching the greatest depth of 30 m - NAP after 200 m. The drilling continues horizontally straight until 500 m and it follows an ascending curve until 650 m and finally rising on a straight ascending until it reaches the reception shaft on Danzigerkade at 17 m – NAP (Figure 29).

3.2. Monitoring

3.2.1. Data acquisition

For the microtunneling project under IJ, monitoring instruments were placed immediately in front of the first intermediate jacking station (viewed in the direction of drilling) in order to monitor forces, pressures, deviation and tilt from the start to the end of the boring (Mastbergen, 2007). Monitoring equipment were also installed at all eight intermediate jacking stations to measure the jacking forces. With one of the project goals being to investigate the joint movement in between the pipes along the boring, instruments were positioned between pipes 32 and 33 (Figure 31), so that displacement and tilt could be measured at approximately 120m behind the TBM. All the instruments had their signals continuously and automatically recorded digitally on data loggers during the entire drilling. Therefore, no measuring cables are required inside the tunnel. The available data from this project are:

- jacking forces in the 8 intermediate jacking stations (IJ bore only) and the main jacks;
- movement of the two instrumented tubes (near intermediate jacking station);
- joint displacements of the joint between the two instrumented pipes;
- strains in the pipe in the longitudinal and transverse direction;
- geotechnical investigation and route of the pipe;
- and relationship between time and drill head progress.

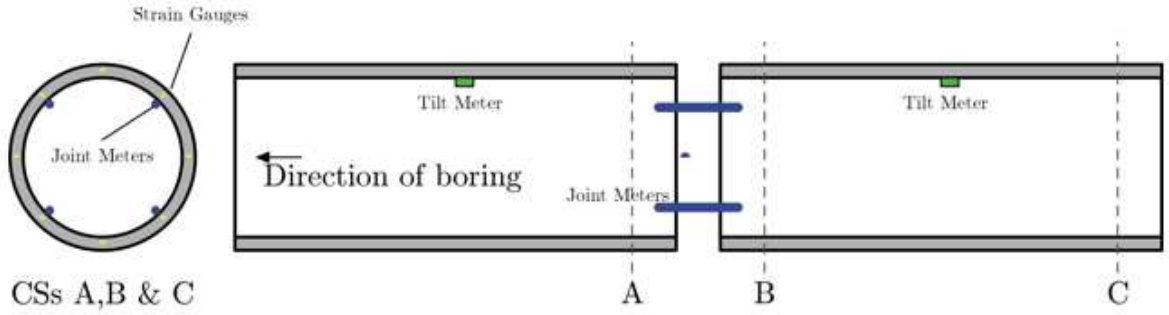

Figure 31 - Monitoring Instruments at pipes 32 and 33 (Delft Cluster, 2007)

The pressure was measured by electric oil pressure transducers that were installed locally in the hydraulic jacks. This way, the jacking forces can be derived directly from the measured pressure. WL | Delft Hydraulics supplied the measuring instruments (type PDCR 930 resp. 410) and associated data loggers type Campbell CR 10 which provided sensor measurement, timekeeping, data reduction, data/program storage and control functions. This way, the hydraulic jacking forces of the main jacks and all 8 intermediate jacking stations were continuously measured throughout the entire boring.

Table 4 indicates for all nine pressure sensors their type, installation location, date and week of placement and start of measurement also location in meters of their position after the TBM.

Table 4 - Location and time of placement of pressure sensors (Delft Cluster, 2007)

Data logger	Pressure sensor	Location	Placement	Start measurement	Week	Location (m)
9	PDCR930	starts main shaft	28 April	2 May	18	0
1	PDCR930	intermediate jacking station 1	5 May	11 May	19	0

Data logger	Pressure sensor	Location	Placement	Start measurement	Week	Location (m)
2	PDCR930	intermediate jacking station 2	5 May	11 May	19	60
		tube no.32 and 33	17 May	17 May	20	125
3	PDCR410	intermediate jacking station 3	12 May	18 May	20	133
4	PDCR410	intermediate jacking station 4	26 May	30 May	22	225
5	PDCR410	intermediate jacking station 5	2 June	22 June	25	320
6	PDCR410	intermediate jacking station 6	8 June	-	-	430
7	PDCR410	intermediate jacking station 7	?	-	-	540
8	PDCR410	intermediate jacking station 8	?	-	-	650
		End		2 July	26	

TU Delft compiled all measurements from three different parties (SMET, GeoDelft & WL | Delft Hydraulics) into a single MySQL database to facilitate any further data analysis. The information that each party had are the following:

- GeoDelft: read out the instrumentation of the measuring pipes 32 and 33 with an interval of 30 seconds and stored it in a data logger. This data logger was read on average once a week. No information on the brands/ model or name of these instruments were provided in the data package. The data included:
    - day, hour, min, sec
    - strain measurements of the moulded strain gauges (28 times) [mm/m]
    - associated temperature measurements (28 times) [ºC]
    - displacement measurements of the joint displacement meters (2 x 3 times) [mm]
    - slope measurements (2 x 2 times) [º]
    - ambient temperature [ºC]
    - voltage of the power supply battery [V]

- WL | Delft Hydraulics: Date, time, pressures in the main jacks and IJS with an interval of 30 seconds.
  When a pressure sensor is not yet connected, in the measurement file, a value of -99 is presented. A value greater than 0 is only measured by the pressure sensor once the IJS are actually under pressure. After all pressure sensors and data loggers were installed, those from the IJS 6 to 8 were not connected. At IJS 5, where measurements were taken, data was ultimately hardly used. Therefore, only data from the TBM, the first 4 IJS and pipes 32 and 33 were assessed.
  The sensors generated binary files which were converted into to ASCII. In the processing, files were created per week with the data of the main jacks and all IJS that were connected at that time and presented per week in Microsoft Excel format. Four columns are used per time measurement, the first two being the original read-in values from the loggers and the other two the processed values. See table below (Table 5).

Date code	Oil pressure	Date and time	Jacking force
38525.95833	4.3	22-7-2005 23:00:00	112.5287

Table 5 - Measurement results example (Delft Cluster, 2007)

The jacking forces are calculated from the measured oil pressure multiplied by the total section of the hydraulic jacks. The main shaft jacks consist of 4 cylinders with a diameter of 280 mm each. Because the cylinders are interconnected, the same oil pressure applies everywhere, so force is always evenly exerted by the jacks. This means that 1 bar oil pressure corresponds to 24,630 kN. The same theory applies for the IJS however they all consist of 17 cylinders, each with a diameter of 140 mm (Figure 32 and Figure 33) therefore, 1 bar oil pressure corresponds to 26,170 kN.

- Smet Tunneling BV: drilling log filled on paper:
  - total drilled length is recorded a number of times during progress, and at these times a record is also made of
  - pressure in the main jack [bar]
  - pressures in intermediate jacking stations 1 to 5 [bar]
  - pressure of the main wheel drive [bar]
  - pressure in the excavation chamber [bar]
  - pressure of the cutting wheel lubrication [bar]
  - volume of the cutting wheel lubrication [m3]
  - volume of drilling fluid incoming [m3]
  - volume of drilling fluid outgoing [m3]
  - tilt measurements of the TBM (2 times) [mm / m]

  The logbook shows that some pages are missing, pages 9 to 12. As a result, no data is available on the basis of the logbook between approximately 153 and 223 m drilled length. Therefore, based on the measured press forces, an estimate of the progress during this period had to be done.

At the TUDelft database, the time base was corrected to the extent possible since GeoDelft reported all times in local wintertime (UTC + 1), while WL | Delft Hydraulics maintained daylight saving time (UTC + 2). Also, time stamps from SMET written by hand are not as accurate as clock readings for the data logger where manual errors/omissions and corrections were present in the hand written sheets. In the database with all available data this has been corrected to the extent possible.

The database also included the drilled length which was determined based on the pressure of the main jacks and the place-time information from the Smet logbook table. The following assumptions were used:

1. If immediately before or immediately after a time at which a drilled length L from the Smet logbook has the pressure in the main jacks (measurement WL) less than 6 bar, it is assumed that no progress has been made in this continuous period and the drilled length in this taken the known length L throughout the entire period.
2. For all other points in time, the drilled length L is interpolated linearly between the preceding and subsequent known place-time combination.

Since this project was not completed due to a flooding of the tunnel at the end of the project, data from the dataloggers has been lost for the last part of the boring.

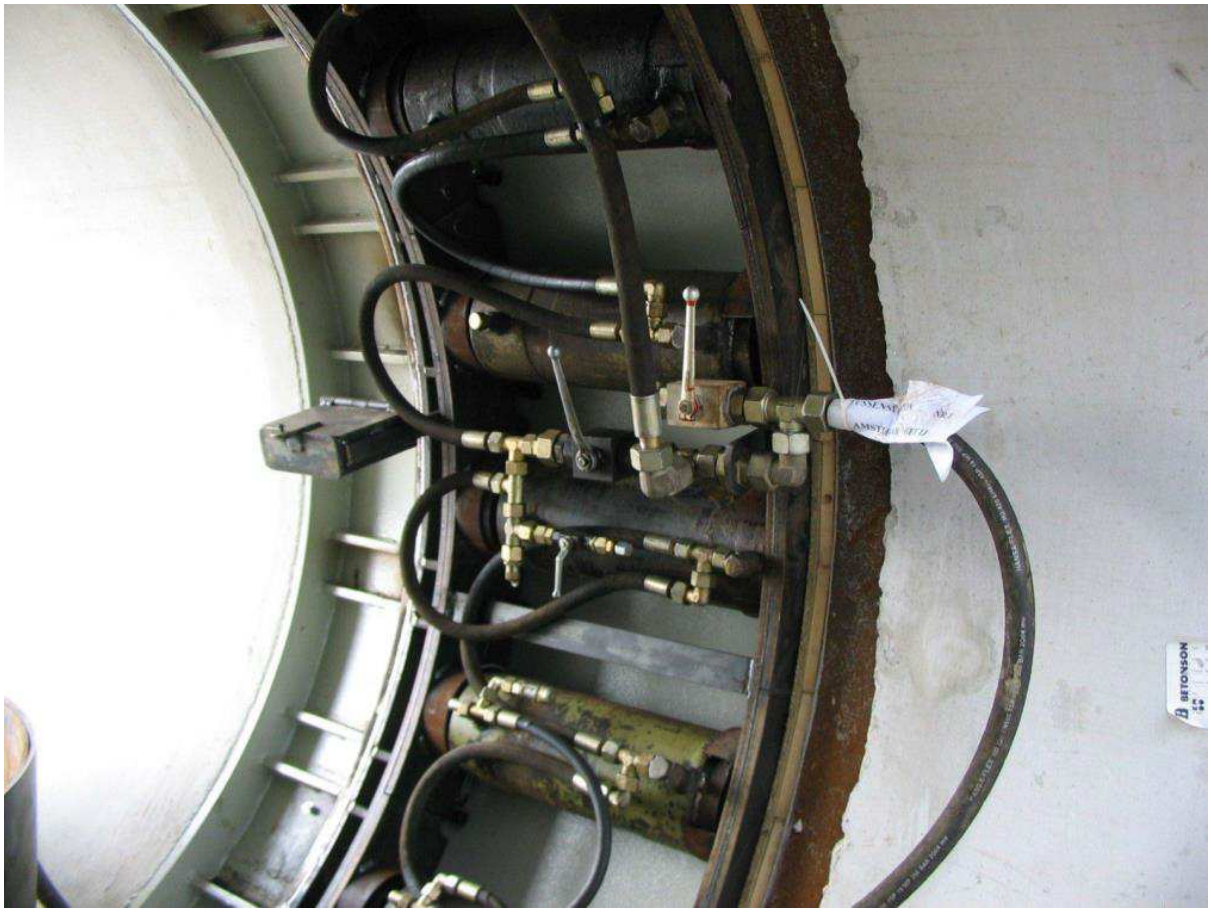

Figure 32 - Intermediate jacking station nr. 1, Amsterdam IJ (Delft Cluster, 2007)

Figure 33 - Intermediate jacking station (Delft Cluster, 2007)

3.2.2. Data processing

After extracting all the parameters available in MySQL database from TU Delft, the following excel table was created for the entire boring length (Figure 34) where each line represents 30 seconds. This was used for further data processing and analysis, as it will be explained next. Its parameters are described in Table 6.

A	B	C	D	E	F	G	H	I	J	K	L	M	N	O	P	Q	R	S	T
Hoofdschacht				TDS 1				TDS 2				TDS 3				TDS 4			
	Oliedruk		Perskrach	Datum / t	Oliedruk	Datum en tijd	Perskrach	Datum / t	Oliedruk	Datum en tijd	Perskrach	Datum / t	Oliedruk	Datum en tijd	Perskrach	Datum / tijd	Oliedruk	Datum en tijd	Perskrach
Datum / tijd	Oil Pressure [bar]	Datum en tijd	Pressing forces [kN]	Datum / tijd	Oil Pressure [bar]	Datum en tijd	Pressing forces [kN]	Datum / tijd	Oil Pressure [bar]	Datum en tijd	Pressing forces [kN]	Datum / tijd	Oil Pressure [bar]	Datum en tijd	Pressing forces [kN]	Datum / tijd	Oil Pressure [bar]	Datum en tijd	Pressing forces [kN]
38509.56	99.1	06-06-2005 13:25:30	2440.842	38509.56	1	06-06-2005 13:25:30	26.16947	38509.56	0.7	06-06-2005 13:25:30	18.31863	38509.56	67.2	06-06-2005 13:25:30	1758.588	38509.55937	0.5	06-06-2005 13:25:30	13.08473
38509.56	99.1	06-06-2005 13:26:00	2440.842	38509.56	1	06-06-2005 13:26:00	26.16947	38509.56	0.7	06-06-2005 13:26:00	18.31863	38509.56	66.9	06-06-2005 13:26:00	1750.737	38509.55972	0.5	06-06-2005 13:26:00	13.08473
38509.56	99.1	06-06-2005 13:26:30	2440.842	38509.56	1	06-06-2005 13:26:30	26.16947	38509.56	0.7	06-06-2005 13:26:30	18.31863	38509.56	66.9	06-06-2005 13:26:30	1750.737	38509.56007	0.5	06-06-2005 13:26:30	13.08473
38509.56	99.1	06-06-2005 13:27:00	2440.842	38509.56	1	06-06-2005 13:27:00	26.16947	38509.56	0.7	06-06-2005 13:27:00	18.31863	38509.56	66.9	06-06-2005 13:27:00	1750.737	38509.56042	0.5	06-06-2005 13:27:00	13.08473
38509.56	99.1	06-06-2005 13:27:30	2440.842	38509.56	1	06-06-2005 13:27:30	26.16947	38509.56	0.7	06-06-2005 13:27:30	18.31863	38509.56	67.2	06-06-2005 13:27:30	1758.588	38509.56076	0.5	06-06-2005 13:27:30	13.08473
38509.56	99.1	06-06-2005 13:28:00	2440.842	38509.56	1	06-06-2005 13:28:00	26.16947	38509.56	0.7	06-06-2005 13:28:00	18.31863	38509.56	66.9	06-06-2005 13:28:00	1750.737	38509.56111	0.5	06-06-2005 13:28:00	13.08473
38509.56	98.8	06-06-2005 13:28:30	2433.453	38509.56	1	06-06-2005 13:28:30	26.16947	38509.56	0.7	06-06-2005 13:28:30	18.31863	38509.56	66.9	06-06-2005 13:28:30	1750.737	38509.56146	0.5	06-06-2005 13:28:30	13.08473
38509.56	99.1	06-06-2005 13:29:00	2440.842	38509.56	1	06-06-2005 13:29:00	26.16947	38509.56	0.7	06-06-2005 13:29:00	18.31863	38509.56	66.9	06-06-2005 13:29:00	1750.737	38509.56181	0.5	06-06-2005 13:29:00	13.08473
38509.56	99.1	06-06-2005 13:29:30	2440.842	38509.56	1	06-06-2005 13:29:30	26.16947	38509.56	0.7	06-06-2005 13:29:30	18.31863	38509.56	67	06-06-2005 13:29:30	1753.354	38509.56215	0.5	06-06-2005 13:29:30	13.08473
38509.56	99.1	06-06-2005 13:30:00	2440.842	38509.56	1	06-06-2005 13:30:00	26.16947	38509.56	0.7	06-06-2005 13:30:00	18.31863	38509.56	66.7	06-06-2005 13:30:00	1745.503	38509.5625	0.5	06-06-2005 13:30:00	13.08473
38509.56	99.1	06-06-2005 13:30:30	2440.842	38509.56	1	06-06-2005 13:30:30	26.16947	38509.56	0.7	06-06-2005 13:30:30	18.31863	38509.56	66.9	06-06-2005 13:30:30	1750.737	38509.56285	0.5	06-06-2005 13:30:30	13.08473

U	V	W	X	Y	Z	AA	AB	AC	AD	AE	AF	AG	AH	AI	AJ	AK	AL	AM	AN	AO
From GeoDelft	From GeoDelft	From GeoDelft	From GeoDelft	From GeoDelft	From GeoDelft	From GeoDelft	From GeoDelft	From GeoDelft	From GeoDelft	From GeoDelft	From GeoDelft	From GeoDelft	From GeoDelft	From GeoDelft	From GeoDelft	From GeoDelft	From GeoDelft	From GeoDelft	From GeoDelft	From GeoDelft
t																				
# Location [m]	Pipe number	pipe Length [m]	Oil Pressure TBM cutting wheel [bar]	Pressure mixing chamber [bar]	Volume IN [m^3]	Volume OUT [m^3]	Deviation horizontal [mm]	Deviation vertical [mm]	Tilt TBM 1 [mm/m]	Tilt TBM 2 [mm/m]	LVDT 1 [mm]	LVDT 2 [mm]	LVDT 3 [mm]	LVDT 4 [mm]	LVDT 5 [mm]	LVDT 6 [mm]	Tilt 1 [degr.]	Tilt 2 [degr.]	Tilt 3 [degr.]	Tilt 4 [degr.]
376.2594	87	5.00	0	0	0	0	132.4919	296.3629	-6.98906	-1.01094	33.503	33.312	36.438	36.021	9.8691	4.9604	-2.8565	1.1938	-3.4119	-1.12
376.2688	87	5.00	0	0	0	0	132.2581	296.3871	-6.98916	-1.01084	33.503	33.312	36.438	36.021	9.8691	4.9604	-2.8555	1.1938	-3.4117	-1.1198
376.2781	87	5.00	0	0	0	0	132.0242	296.4113	-6.98926	-1.01074	33.503	33.3	36.438	36.021	9.8691	4.9604	-2.8559	1.1939	-3.4118	-1.1198
376.2875	87	5.00	0	0	0	0	131.7903	296.4355	-6.98936	-1.01064	33.503	33.3	36.425	36.021	9.8691	4.9604	-2.8554	1.1933	-3.4114	-1.1196
376.2969	87	5.00	0	0	0	0	131.5565	296.4597	-6.98946	-1.01054	33.503	33.3	36.425	36.021	9.8691	4.9604	-2.8551	1.1935	-3.4109	-1.1194
376.3063	87	5.00	0	0	0	0	131.3226	296.4839	-6.98956	-1.01044	33.597	33.501	36.721	36.21	9.8691	4.9604	-2.8547	1.1942	-3.411	-1.1214
376.3157	87	5.00	0	0	0	0	131.0887	296.5081	-6.98966	-1.01034	33.544	33.38	36.559	36.103	9.8691	4.9535	-2.854	1.1939	-3.4105	-1.12
376.3250	87	5.00	0	0	0	0	130.8548	296.5323	-6.98976	-1.01024	33.503	33.3	36.438	36.035	9.8691	4.9535	-2.8534	1.1929	-3.4095	-1.1196
376.3344	87	5.00	0	0	0	0	130.621	296.5565	-6.98986	-1.01014	33.636	33.568	36.815	36.278	9.8691	4.9743	-2.8526	1.1946	-3.4099	-1.122
376.3438	87	5.00	0	0	0	0	130.3871	296.5806	-6.98996	-1.01004	33.609	33.501	36.721	36.236	9.8621	4.9604	-2.8538	1.1942	-3.4103	-1.1214
376.3532	87	5.00	0	0	0	0	130.1532	296.6048	-6.99006	-1.00994	33.556	33.38	36.546	36.103	9.8691	4.9535	-2.8533	1.1938	-3.4099	-1.1201

Figure 34 - Output file from MySQL database

Table 6 - Parameters available in MySQL database

Field name	Unit / example	comment
Hoofdschacht Datum / tijd	Coded time / 38499.1441	Main shaft
Hoofdschacht Oil Pressure	bar	Main shaft
Hoofdschacht Datum en tijd	27-5-2005 03:27:30	Main shaft
Hoofdschacht Pressing forces	kN	Main shaft
TDS1 Datum / tijd	Coded time / 38499.1441	Intermediate Jacking Station 1
TDS1 Oil Pressure	bar	Intermediate Jacking Station 1
TDS1 Datum en tijd	27-5-2005 03:27:30	Intermediate Jacking Station 1
TDS1 Jacking forces	kN	Intermediate Jacking Station 1
TDS2 Datum / tijd	Coded time / 38499.1441	Intermediate Jacking Station 2
TDS2 Oil Pressure	bar	Intermediate Jacking Station 2
TDS2 Datum en tijd	27-5-2005 03:27:30	Intermediate Jacking Station 2
TDS2 Jacking forces	kN	Intermediate Jacking Station 2
TDS3 Datum / tijd	Coded time / 38499.1441	Intermediate Jacking Station 3
TDS3 Oil Pressure	bar	Intermediate Jacking Station 3

TDS3 Datum en tijd	27-5-2005 03:27:30	Intermediate Jacking Station 3
TDS3 Jacking forces	kN	Intermediate Jacking Station 3
TDS4 Datum / tijd	Coded time / 38499.1441	Intermediate Jacking Station 4
TDS4 Oil Pressure	bar	Intermediate Jacking Station 4
TDS4 Datum en tijd	27-5-2005 03:27:30	Intermediate Jacking Station 4
TDS4 Jacking forces	kN	Intermediate Jacking Station 4
Location	m	Relative to the head of TBM
Pipe number	-	
Pipe Length	m	From 2.45m to 5m
Oil Pressure TBM cutting wheel	bar	
Pressure mixing chamber	bar	
Volume IN	m^3	Lubricant volume added
Volume OUT	m^3	Lubricant volume retrieved
Deviation horizontal	mm	Deviation from proposed alignment
Deviation vertical	mm	Deviation from proposed alignment
Tilt TBM 1	mm/m	
Tilt TBM 2	mm/m	
LVDT 1	mm	Displacement gauges installed in between pipes 32 and 33
LVDT 2	mm	Displacement gauges installed in between pipes 32 and 33
LVDT 3	mm	Displacement gauges installed in between pipes 32 and 33
LVDT 4	mm	Displacement gauges installed in between pipes 32 and 33
LVDT 5	mm	Displacement gauges installed in between pipes 32 and 33
LVDT 6	mm	Displacement gauges installed in between pipes 32 and 33
Tilt 1	degree	Tilt gauges installed in between pipes 32 and 33
Tilt 2	degree	Tilt gauges installed in between pipes 32 and 33
Tilt 3	degree	Tilt gauges installed in between pipes 32 and 33
Tilt 4	degree	Tilt gauges installed in between pipes 32 and 33

After having an overview of the entire boring, it was possible to start the detailed data processing part. The first step was to delete the holidays and free weekends from the readings. For calculation purposes, these days do not add any relevant information to the analysis.

Next, it was spotted that the pipe numbering was not correct along the boring since they were not matching with the locations that were logged in the TU Delft database or the SMET logbook. The way to understand this was to compare both database and logbook with the oil pressure of the installation. At some locations a start date and end date of a pipe installation was added however no significant oil pressure change was in place for this to be realistic.

During the installation of a pipe, the oil pressure increases to an average value range of 120 to 200 bar and drops to a theoretical value of 0 bar during standstill, but in practice, the residual value is observed to be 2.8 to 4.3 bar. This is the case of a pipe that was installed entirely in one go. There are cases where the pipes are partially jacked into the soil and then later the installation is completed. In this scenario, they are possible to be distinguished because the residual oil pressure in the main jacks remains usually with a value higher than 30 bar for a longer period of time and only after the complete installation it drops to 2.8 bar.

Therefore, the pipe locations were rearranged according to the following rules:

- Every pipe starts when the oil pressure in the main jacks are at 2.8;
- Every pipe ends when the oil pressure in the main jacks reaches 2.8 (by the end of the boring this becomes around 4.3) or before the residual peak happens.

It was chosen to decrease the oil pressure from 6 bar (as mentioned in Section 3.2.1) to 2.8 bar to identify a new pipe installation since some high values of residual pressure where available in the data and could be used for further investigation.

At some locations, it was possible to notice a big oil pressure change as if a pipe was being installed but there was no record in any log of this being an installation. Thus, these locations where ignored and not treated as an actual installation therefore the pipe number column in the database was left blank.

It was also noticed that the last three pipes available in the logs do not have oil pressure information available. Therefore, pipes 161, 162 and 163 are disregarded from the assessment and the last available pipe is 160 starting at 740.65m. The table ends at location 744.1187m and 02/07/2005 06:59:30 instead of 785m as designed due to a flooding and complete stop of the works.

The last step before having a complete and clean database ready for data analysis was to remove outliers in the data. The outliers could appear for many reasons for instance, the TBM could have hit a boulder and the machine read a much higher value or stronger soils were encountered with a sudden change in soil property. These will only be speculation since there is no way to know the actual reason for these smaller changes.

The outliers were identified by visual inspection based on judgement. Six sections along the boring were modified due to an identified outlier representing 0.44% of the entire length. The replacement of these values were done as a linear interpolation between the measurement before and after the section where the outlier takes place. Figure 35 below exemplifies one outlier that was modified from the dataset, namely the peak in Main jack force from 70.7m to 70.9333m.

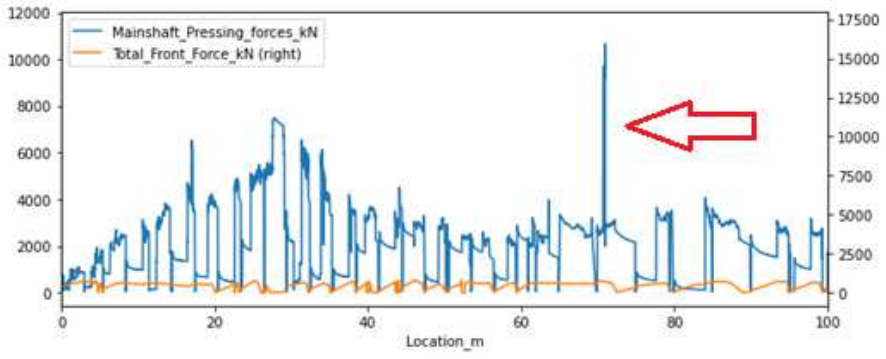

Figure 35 - Outlier in Main Pressing forces at 70.7m

3.3. data analysis

3.3.1. Methodology

The first part of the data analysis was to create plots of the entire boring with the parameters that where available and could have an influence on the friction. This can be seen in the next section 3.3.2.Findings.

With the goal of correlating those parameters, the total length was divided into six sections where changes in soil conditions and in the boring alignment, were the decisive factor for the section selection. Figure 36 presents an overview of the section breaks which are at 135m, 250m, 380m, 500m and 650m. Each will be reviewed in detail in section 3.3.3.General Findings Discussion

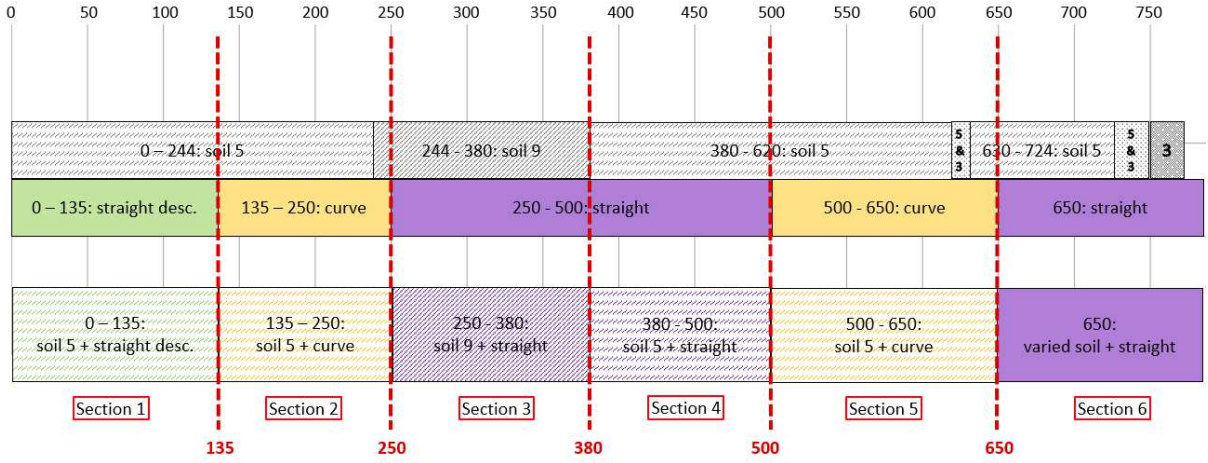

Figure 36 - Divided sections for Data analysis

The parameters available and shown in Table 6 were used to define a number of auxiliary parameters needed for the proposed analysis. The new parameters are:

- *Total_Front_Force_kN* : The *Oil Pressure TBM cutting wheel* and *Pressure mixing chamber in bar were was converted to kPa*. The TBM cross section of 1800mm (2.54m2) was used to calculate the Pressure mixing chamber in kN and an assumption was made to have the equivalent of one jack of 280mm (0.0615m2) behind the cutting wheel so the force could be calculated in kN. This is based on the data available for the main jacking station. Both forces in kN were then summed.
- *Front_Force_IJS_MN*: using the *TDS Jacking forces* this parameter substitutes the *Total_Front_Force_kN* since the forces acting in front and behind each pipe needs to be considered for the friction calculation. The difference between the *Mainshaft_Pressing_forces_kN* and *Total_Front_Force_kN* can be misleading if IJS are active. Note MN is being used.
- *Friction_final*: using Formula (1) the friction is calculated as the difference between the *Mainshaft_Pressing_forces_kN* and *Front_Force_IJS_kN* for the entire boring and it was divided by the outside area of the tunnel using a d=2.16m and variable length depending on location of the calculation. This results in a friction in kPa.
- All the blanks in the data were substituted by zeros for ease of running the calculations. This can have an impact on the data visualization.

The second part was to understand if there was any statistically relevant correlation between the available parameters. A Pearson's correlation analysis and a Spearman's rank correlation were created in python.

The Pearson's correlation analysis results in the Pearson correlation coefficient (PCC) which measures the strength of a linear relationship between two variables where the outcome always has a value between -1 to 1, where -1 means a total negative linear correlation (if parameter X increases, parameter Y decreases), 0 means no correlation (no linear dependency between X and Y), and + 1 means a total positive correlation (if parameter X increases then parameter Y also increases) (Penn State Eberly College of Science, n.d.). When there is no linear relationship then Spearman's rank correlation is an alternative analysis in which measures the strength and direction of a monotonic relationship between two variables. "A monotonic relationship means that does the function is one that either never increases or never decreases as its independent variable increases." (Statstutor, n.d.). This results in the Spearman's correlation coefficient (r_s) in which, similar to PCC, ranges from -1 to 1 where -1 represents a perfect negative monotonic relationship

(parameter X increases, parameter Y decreases), 0 represents no correlation between variables and +1 represents a perfect monotonic relationship (parameter X increases, parameter Y also increases).

Three analyses were created to understand the results from these coefficients, one with all the parameters available against all parameters, for the entire boring length, resulting in a table with 48 rows × 48 columns (named Part 1). The second, with all the parameters available against all parameters but divided into the six sections mentioned in Figure 36 (Part 2) and the third analysis using only the parameters that directly influence the alignment (Tilt_TBM_1_mm/m, Tilt_TBM_2_mm/m, Deviation_horizontal_mm, Deviation_vertical_mm) against the friction for the entire boring length also divided into six sections (Part 3). These analysis are discussed and presented in Section 3.3.4.

The final analysis was performed to estimate the impact that subsequential pipe segment installations have on the friction over time at a specific location. For this to be possible, the forces of IJS1, IJS2, IJS3 and IJS4 were plotted along the entire boring length and identifying the location of sections in between two active IJS. These are the only positions where a local friction can be calculated, after the TBM has passed, since the only available data are at an active IJS. They are available in Table 7 and are subdivided to combine same soil conditions and alignment ensuring that the primary parameter influencing the friction is the installation of pipe segments.

Table 7 - Sections in between two active IJS

Active IJS	Section ID	Location start [m]	Location end [m]	Soil type	Alignment
IJS1 - IJS2	A1	62	135	SAND	Straight descend
	A 2	135	200	SAND	Curve from straight descend to horizontal
	A3	240	244	SAND	Curve from straight descend to horizontal
	A4	244	250	extremely soft sediment	Curve from straight descend to horizontal
	A5	250	350	extremely soft sediment	Straight horizontal
IJS2 - IJS3	B1	155	244	SAND	Curve from straight descend to horizontal
	B2	244	250	extremely soft sediment	Curve from straight descend to horizontal
	B3	250	366	extremely soft sediment	Straight horizontal
	B4	371	380	extremely soft sediment	Straight horizontal
	B5	380	400.9	SAND	Straight horizontal
	B6	430	448	SAND	Straight horizontal
	B7	458	493	SAND	Straight horizontal
	B8	515.5	518.7	SAND	Curve from horizontal to straight ascending
	B9	533	537	SAND	Curve from horizontal to

Active IJS	Section ID	Location start [m]	Location end [m]	Soil type	Alignment
					straight ascending
	B10	542.6	552.1	SAND	Curve from horizontal to straight ascending
IJS3 - IJS4	C1	371	380	extremely soft sediment	Straight horizontal
	C2	380	388.5	SAND	Straight horizontal
	C3	535.3	546.8	SAND	Curve from horizontal to straight ascending

The local friction is calculated subtracting IJS 2 – IJS 1, IJS 3 – IJS 2 and IJS 4 – IJS 3 at the specific locations presented in Table 7. This local friction is subtracted from the variable *Friction_final* so the difference in friction based on the pipe segments that travelled at a specific location could be assessed.

Some consideration had to be made for this calculation. For instance, each IJS was located at a different point along the boring therefore the data had to be shifted to the location where the variable *Friction_final* was calculated since this will be compared with the other local friction. *Friction_final* is calculated starting at the TBM (location 0).The variable *Local_frction_IJS 2 – IJS 1* have the friction calculated starting at IJS1 which is also at the TBM (location 0), therefore they could be directly compared. However, for the variable *Local_frction_IJS 3 – IJS 2*, the start of the friction calculation is at IJS 2 which is located 60m behind the TBM and for *Local_frction_IJS 4 – IJS 3*, the start of the calculation is at IJS 3, 133m behind the TBM. See Figure 37.

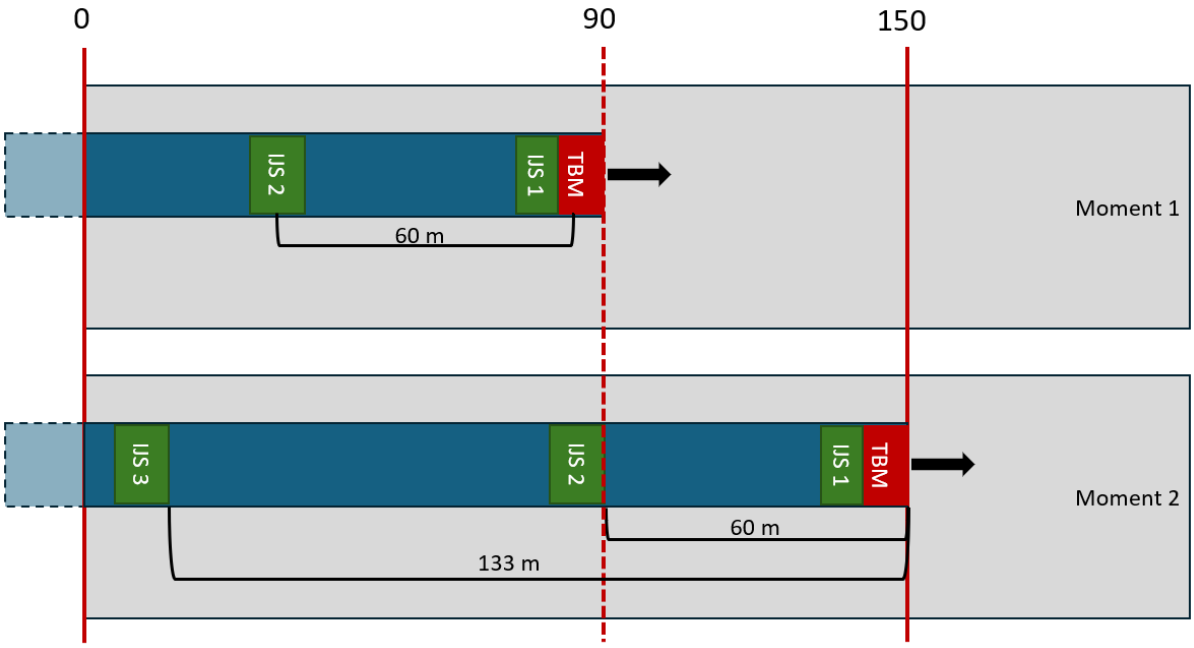

Figure 37 - Difference in Location of the IJS for the local friction calculation

3.3.2. Findings

In this section, the findings are presented in the form of graphs resulting from the data acquisition, processing and analysis.

3.3.2.1. General

The horizontal and vertical deviation, provided from a sensor located at the TBM, were plotted along the entire length of the boring (Figure 38). In the first section, from 0m until roughly 240m the TBM almost does not deviate from the proposed alignment. After that, the vertical deviation increases to approximately 250mm and remains relatively constant until 670m where it decreases reaching -250mm at 700m. The horizontal deviation at 250m increases and maintains almost constant at 500mm until 380m where it drops back to zero and it swiftly comes back up again leaving a V shape indentation in the graph. From 400m to 500m the horizontal deviation remains unstable with two more V shaped patterns, however less steep than the first one. At 510m the deviation increases very much leaving almost a vertical line in the graph followed by the peak of 1360mm. After that, the trend of this deviation is to remain higher with an average of 700mm and reaching 330mm at 700m.

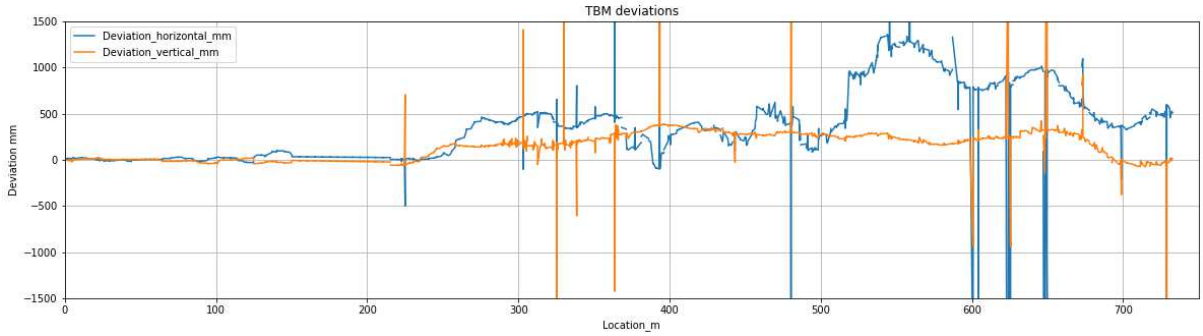

Figure 38 - Horizontal and vertical deviation (mm) along the entire boring length

The tilt at the TBM was also plotted along the entire boring length (Figure 39). Two tilts were measured, one for the head and one for the body of the TBM. (no further explanation was given about the data to be able to make a distinction between Tilt_TBM_1 or Tilt_TBM_2). The tilts measured are the angles that the machine has with respect to a reference plane, horizontal in this case. They represent the steering angle of the TBM (Figure 38). Negative values indicate that the TBM is descending and positive values, ascending. It is observed that in the first 150m the TBM had a constant tilt of approximately -60mm/m. From 150m to 210m, the tilt value starts decreasing and reaches 0mm/m at around 220m. From this location until 500m, the tilt decreases in an almost constant rate to near -10mm/m. From 500m to approximately 620m, the tilt constantly increases followed by a less steep line until the end of the boring reaching a value of approximately 75mm/m.

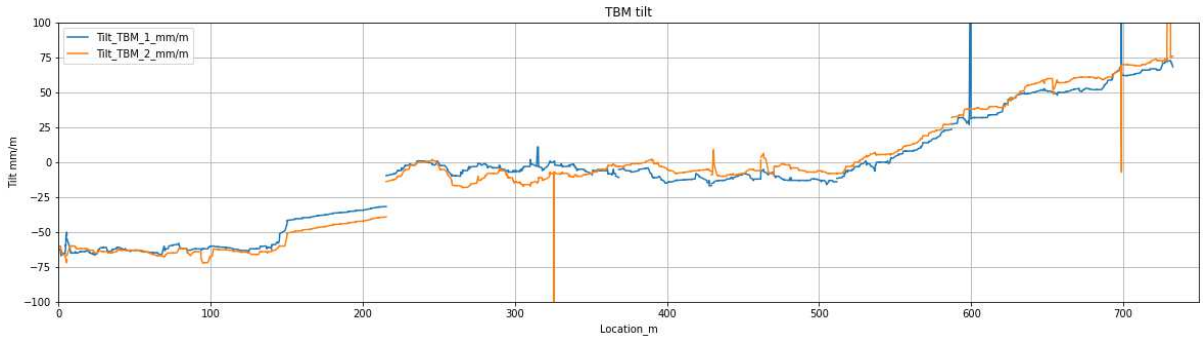

Figure 39 - Tilt from the TBM along the entire boring length

In Figure 40, the frontal forces (FF) and main jacking forces (MJF) along the entire length of the boring are presented. In the first 70m, the MJF are high reaching almost 8MN whereas the FF remains very low. After that, the MJF remains relatively constant and the FF starts to follow the same pattern. At approximately 370m, both forces have an extremely high peak reaching 11MN followed by a valley shaped line at 450m where MJF are around 5MN and FF remains lower at around 3MN.The next peak is at 530m with approximately 9MN. After that, it is possible to notice that the MJF remains constant at that high level until

the end of the boring whereas the FF becomes much lower. It is important to note that every time the MJF goes to zero, it represents a stoppage in the operation, for instance when another pipe is being placed.

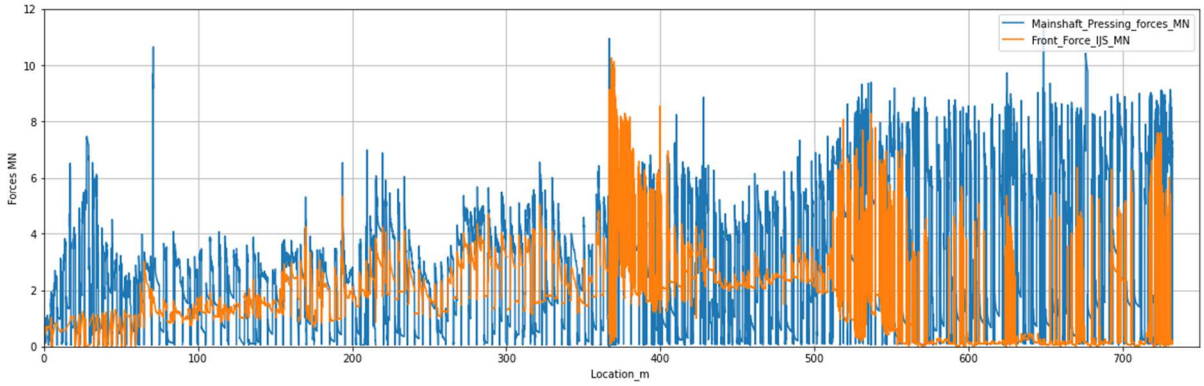

Figure 40 - Main jacking forces and Frontal forces along the entire boring length

The friction at the installation locations can be calculated as the difference between the forces acting in front and behind each pipe and not the difference between the force exerted in front of the TBM and the MJF. Therefore this assessment takes into account the IJS activation to determine these forces. The friction development along the boring has been visualized in Figure 41. Since this graph is related to Figure 40, it is clear to spot the locations where the resistance is higher which are from the start of the boring until approximately location 60m and at location 370m. At location 530m the friction increases even more and remains high until the end of the boring.

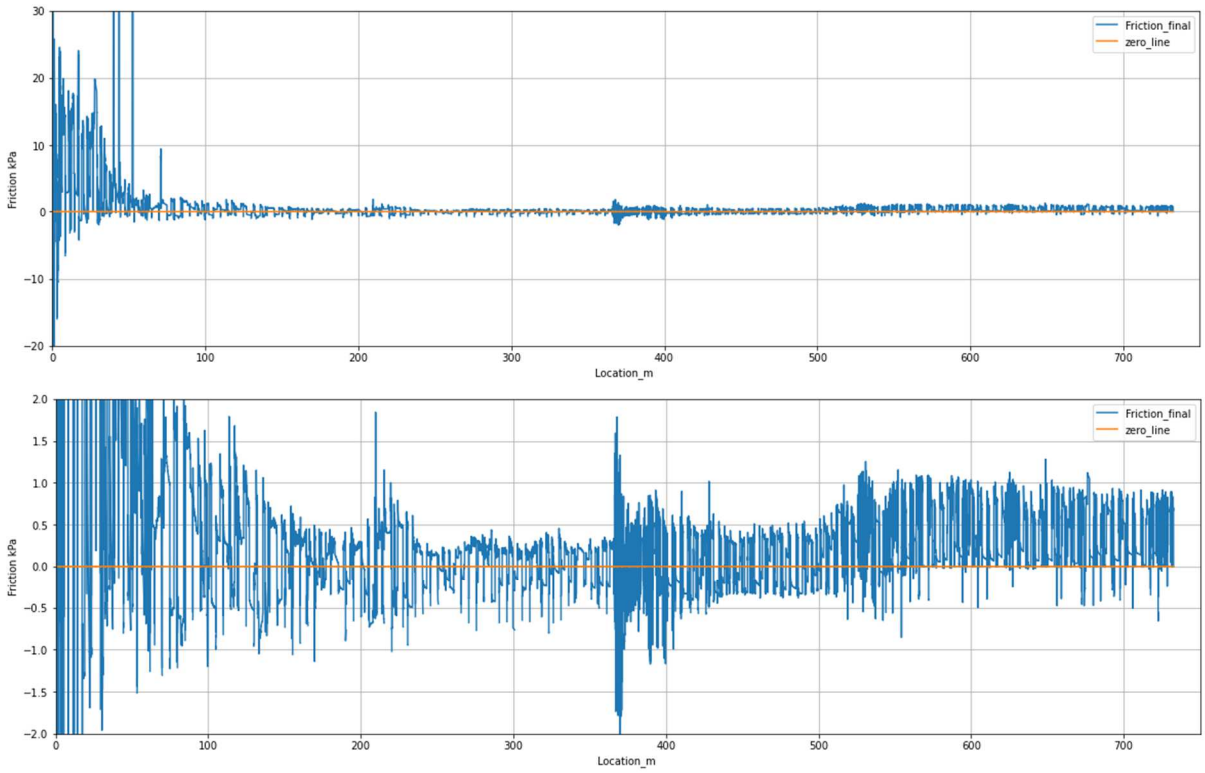

Figure 41 - Friction development along the entire boring length

3.3.2.2. Joint LVDT's

At 127m behind the head of the shield, in between pipes 32 and 33, six linear variable differential transformers (LVDT' s) were installed to measure the joint width in relation to the longitudinal direction in mm (Figure 31). The LVDTs were installed with an initial wooden packer opening and based on the

dataset, this opening width is assumed to be 40mm. Their position and numbering inside the pipe can be visualized in Figure 42.

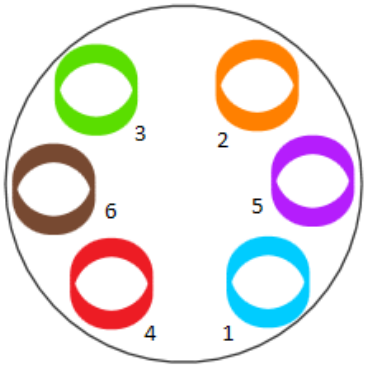

Figure 42 - LVDT's position inside the pipe

The relative displacement results of LVDT 1 to 4 are present in Figure 43 and the results of LVDT 5 and 6 in Figure 44. Negative values indicate joint compression and positive values joint opening. As previously mentioned, the measuring devices are located and start recording 127m behind the TBM until the end of the route.

Analysing Figure 43, from 127m to approximately 220m, joint compression is observed for all LVDT's with the exception of LVDT1 which presents slight joint opening at the start of the reading. From 218m to 230m, LVDT's 1 and 4, at the bottom of the pipe, presents a slight peak of joint opening while LVDT's 2 and 3, at the top, an increase in joint compression. Right after, both opening and compression presents a decrease before LVDT 1 peaks to 11mm at 275m. LVDT 2 follows this peak going from compression to opening and LVDT 3 reaches -7.3mm. At 294m LVDT 1 drops to -3.15mm and LVDT 3 and 4 has a peak in opening reaching 5.85mm. This is followed by another high peak of LVDT 1, reaching 11mm at 317m where LVDT 2 presents a peak of 4.7mm. After that, LVDT 2 and 3 remains in compression and LVDT 1 and 4 in opening with a mild peak at 345m. From 355m to 515m all LVDT's are in compression with the exception of two peaks at 400m and 496m where LVDT 1 and 2 present positive values. At 516.7m, LDVT 3 stopped giving results. At 520m, 573m and 623m, LVDT 4 presents peaks of opening always returning to compression afterwards while at 539m and 598m, LVDT's 1 and 2 present peaks in opening also returning to compression afterwards. At 645m and 694m, LVDT 1 peaks in tension and LVDT 2 follows the same pattern but not reaching opening, only reducing compression.

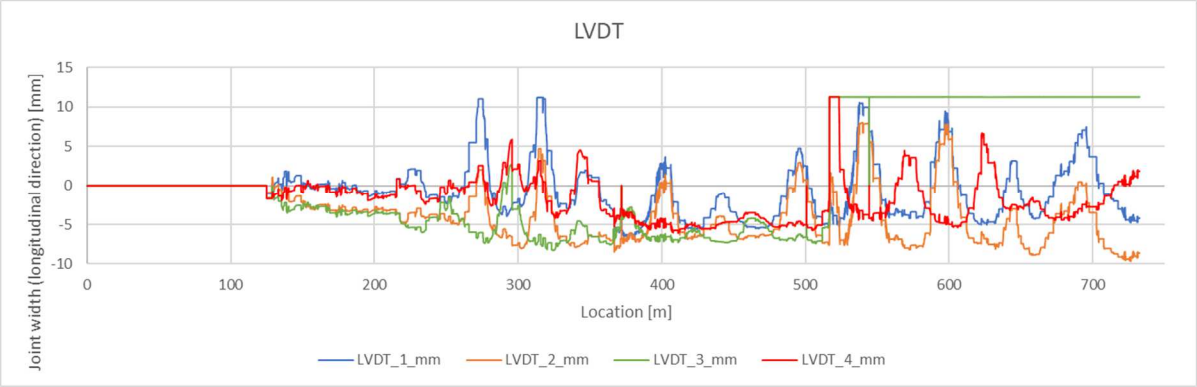

Figure 43 - LVDT relative readings in between pipe 32 and 33 for the entire boring length

Analysing Figure 44, LVDT 5 remains in joint compression until 349m with the exception at 317m where a small peak in joint opening is observed. For the remainder of the route it presents small increases in opening continuing constant for relatively long lengths, as is the case from 400m to 500m. At 535m, it presents a sudden decrease with valley shaped line. The highest recorded value is 8.26mm at 598.25m. In case of LVDT 6, it remains almost zero for the first 100m of readings and it presents two locations where an increase in compression is present, at 250m and 296m. The readings remain constant until

approximately 517m where a peak is observed and opening takes place until 560m then compression is again restored until the end of the route.

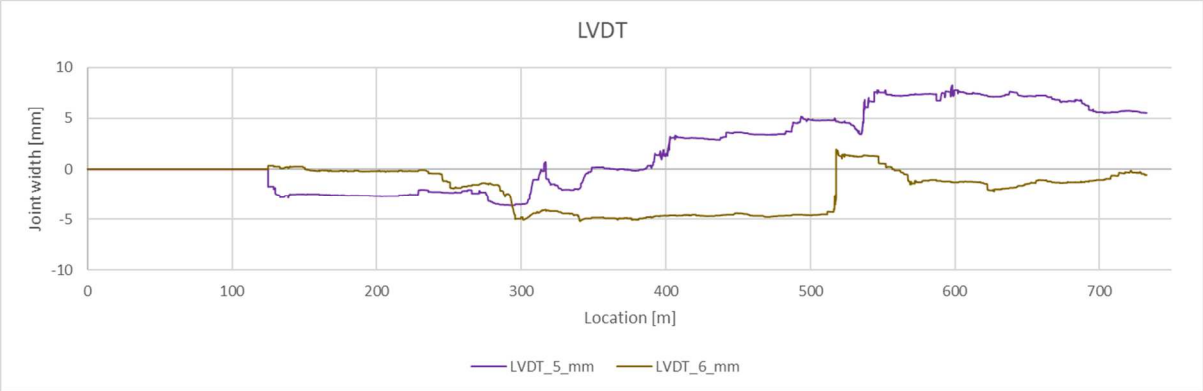

Figure 44 - Radial relative LVDT readings in between pipe 32 and 33 for the entire boring length

With the available data it is not possible to find any meaningful correlation between the LVDT results with the Friction and this was confirmed by the outcome of the statistical analysis which will be presented in the discussion section. Therefore, the join displacement results will not be further discussed in the next sections.

3.3.2.3. Subsequential Pipe Segment Analysis

In order to identify the locations that fall in between two active IJS, the forces of IJS1, IJS2, IJS3 and IJS4 were plotted along the entire boring as shown in Figure 45. This was used to create the sections presented in Table 7. To estimate the impact that subsequential pipe segment installations have on the friction over time at a specific location, the plots presented from Figure 46 to Figure 50, represent this analysis at sections A1 to A5. From Figure 51 to Figure 60, the analysis is presented at sections B1 until B10 and from Figure 61 to Figure 63, at sections C1 to C3. In these plots, a positive value means that at a specific location the friction increased after the subsequent pipe installations and with a negative value the friction has decreased. Table 8 presents a summary of the findings.

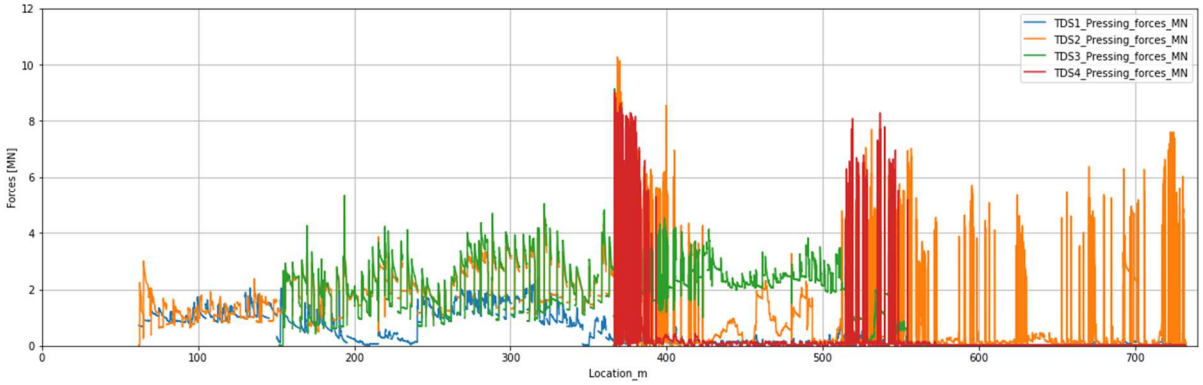

Figure 45 - Forces of IJS1, IJS2, IJS3, IJS4 along the entire boring length

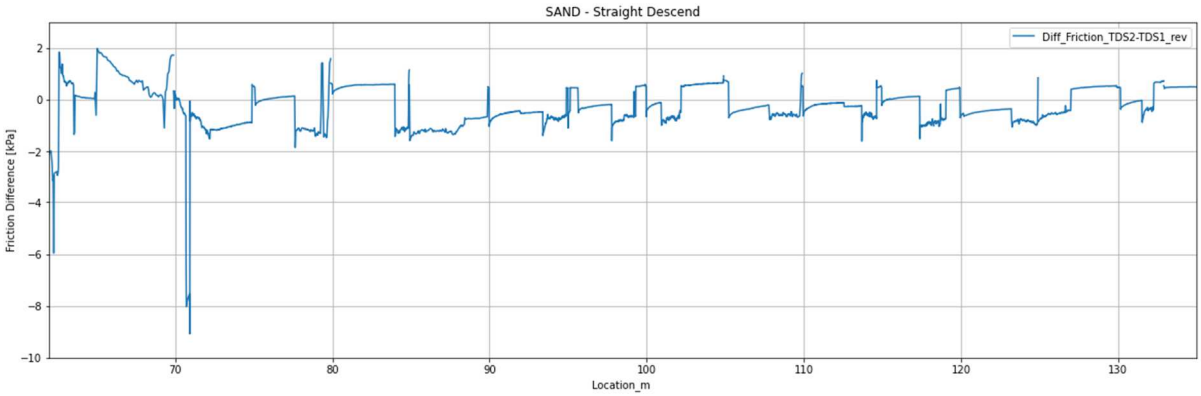

Figure 46 - Difference in friction at Section A1(SAND, Straight Descend)

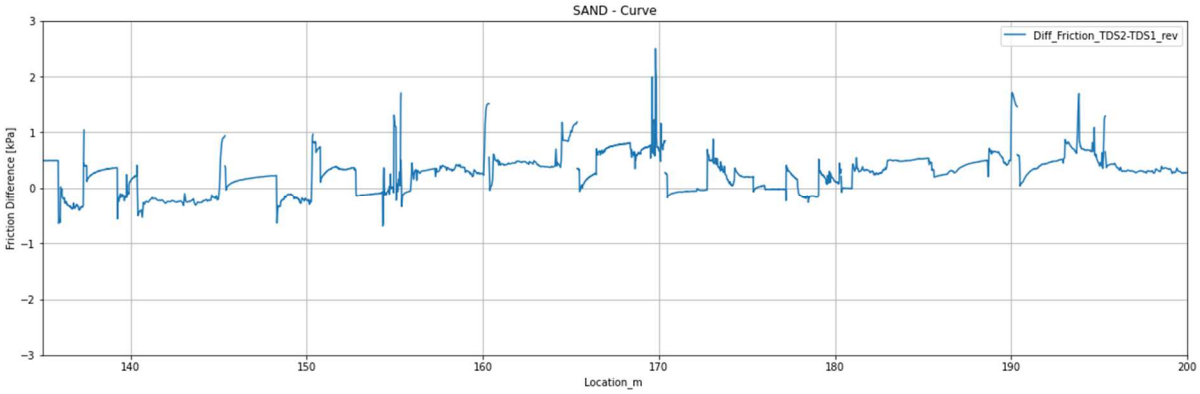

Figure 47 - Difference in friction at Section A2(SAND, Curve)

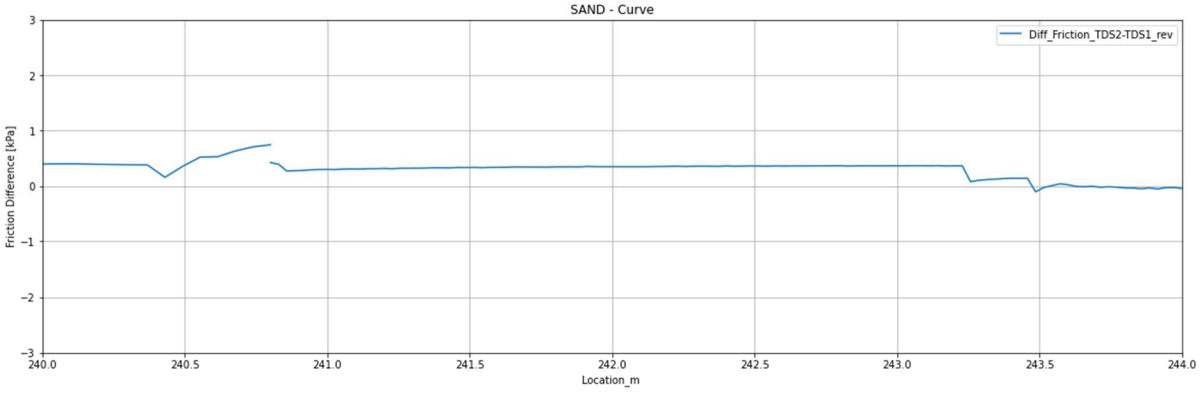

Figure 48 - Difference in friction at Section A3 (SAND, Curve)

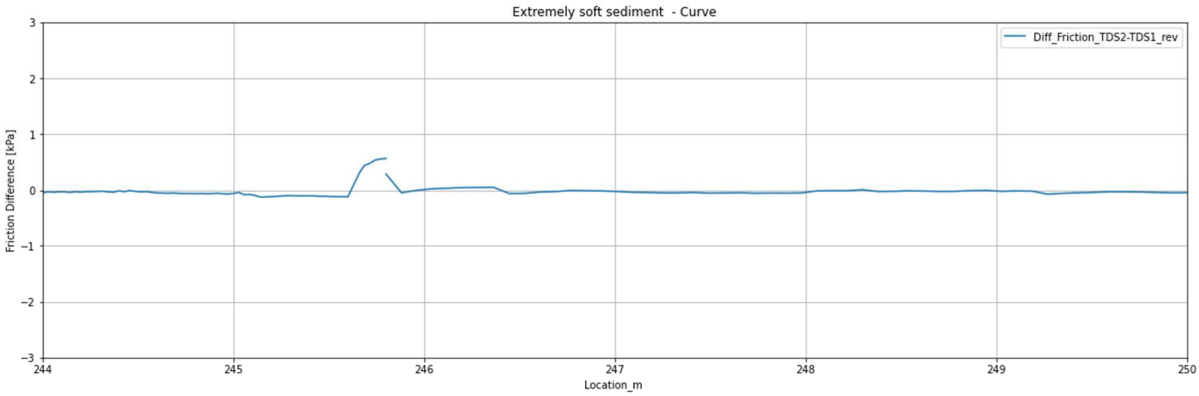

Figure 49 - Difference in friction at Section A4 (Extremely soft sediment, Curve)

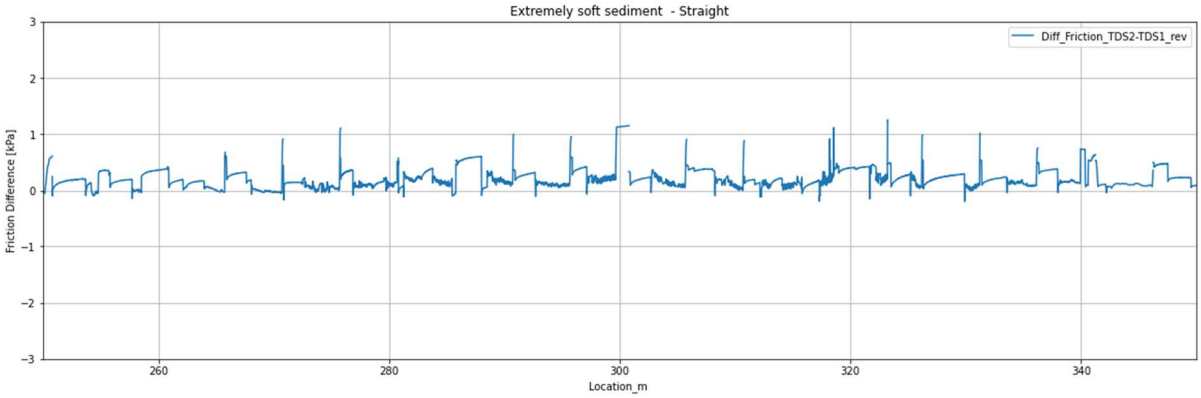

Figure 50 - Difference in friction at Section A5(Extremely soft sediment, Straight)

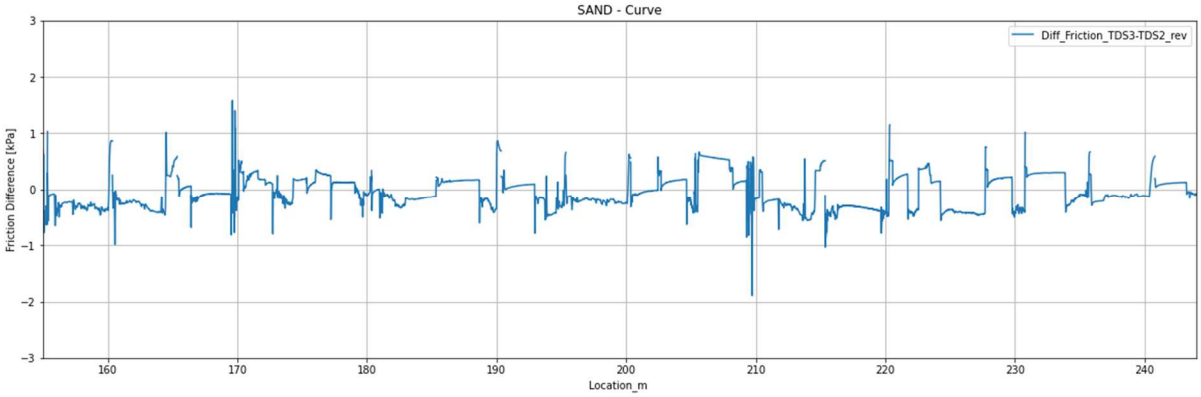

Figure 51 - Difference in friction at Section B1 (SAND, Curve)

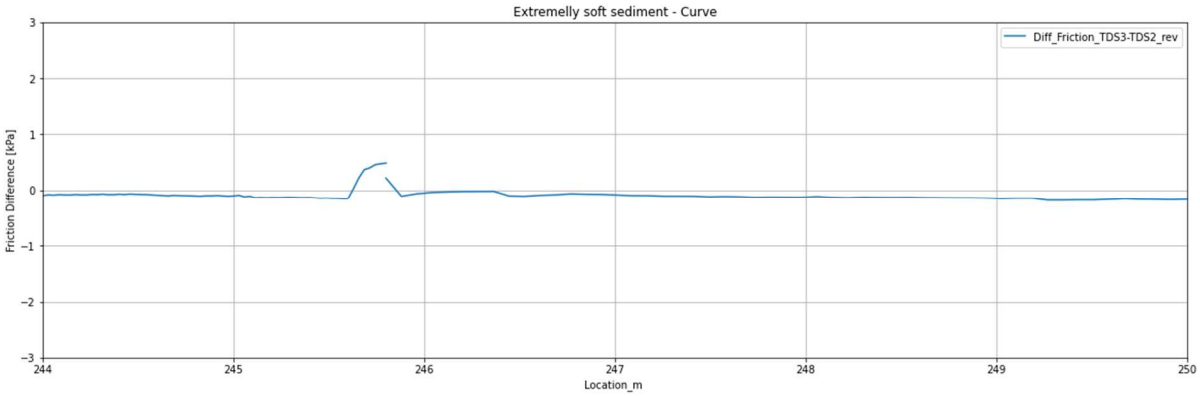

Figure 52 - Difference in friction at Section B2 (Extremely soft sediment, Curve)

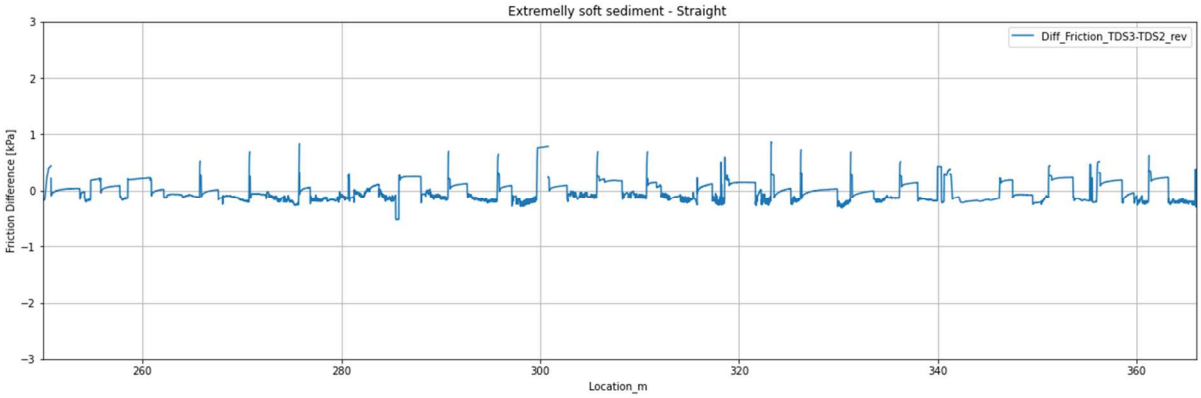

Figure 53 - Difference in friction at Section B3 (Extremely soft sediment, Straight)

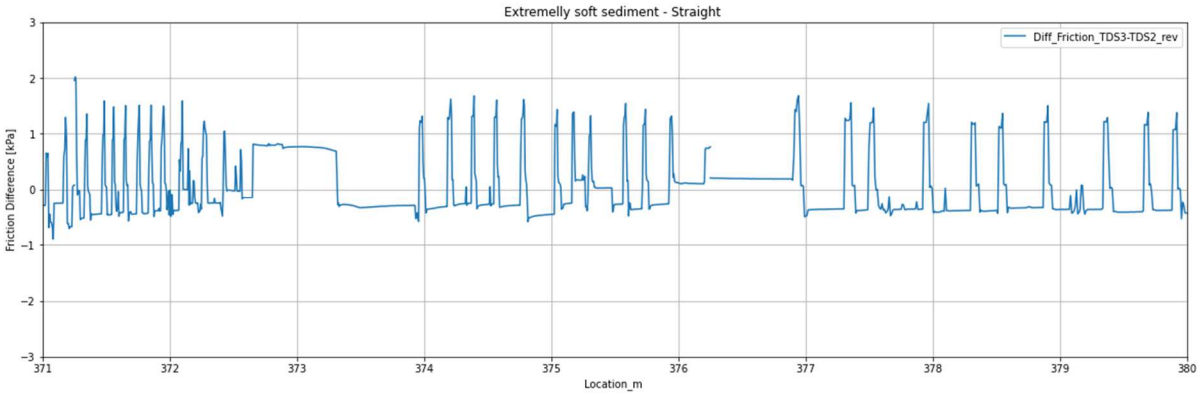

Figure 54 - Difference in friction at Section B4 (Extremely soft sediment, Straight)

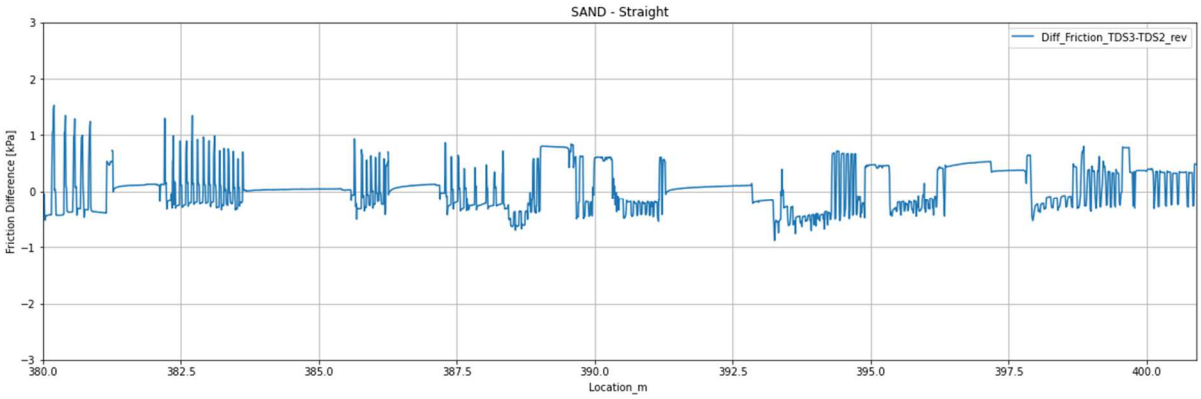

Figure 55 - Difference in friction at Section B5 (SAND, Straight)

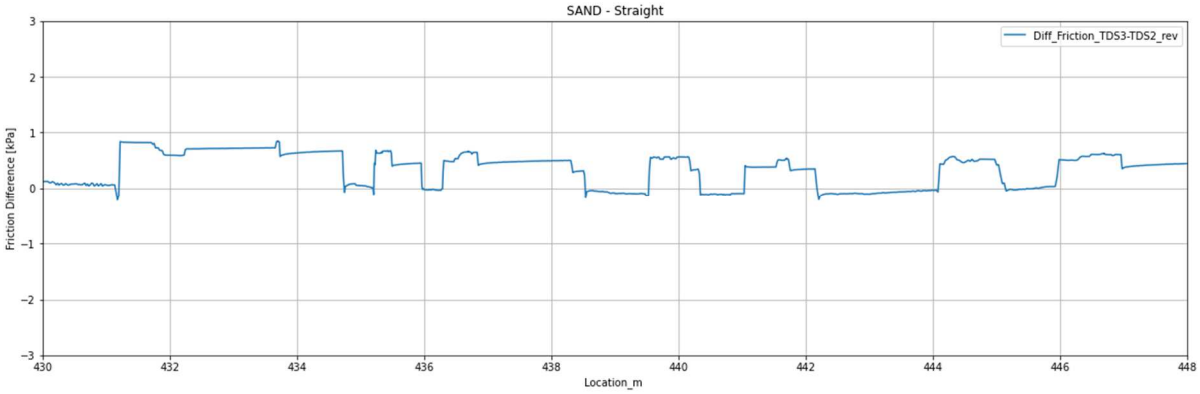

Figure 56 - Difference in friction at Section B6 (SAND, Straight)

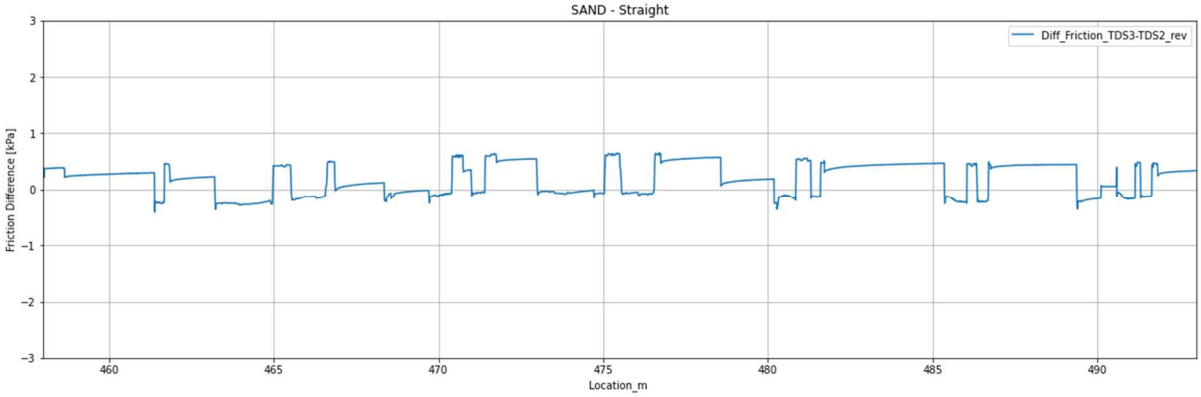

Figure 57 - Difference in friction at Section B7 (SAND, Straight)

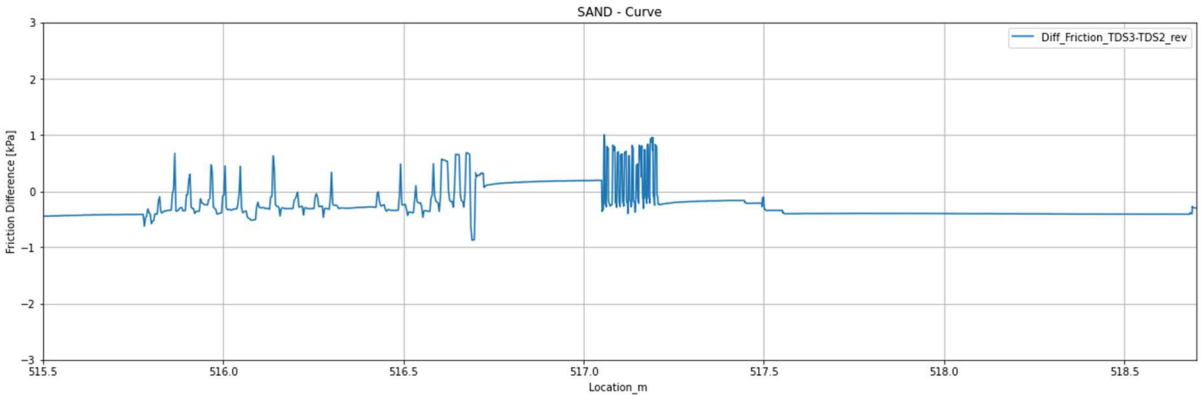

Figure 58 - Difference in friction at Section B8 (SAND, Curve)

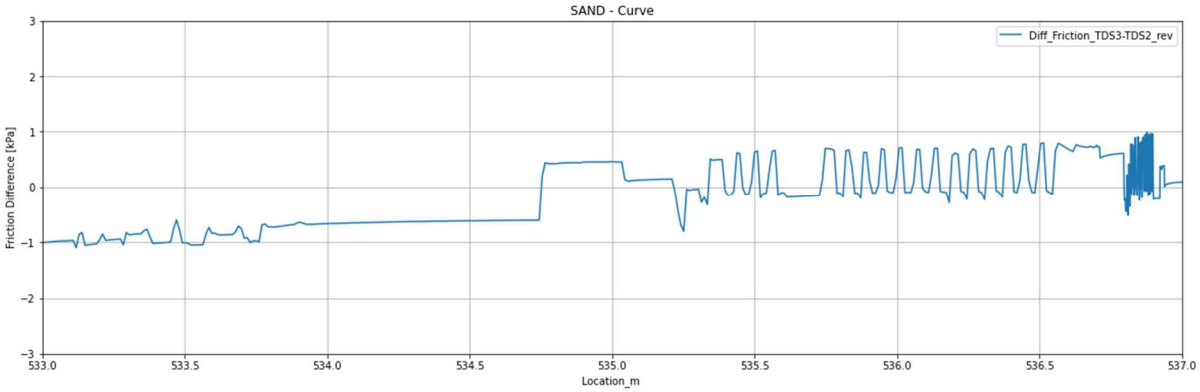

Figure 59 - Difference in friction at Section B9 (SAND, Curve)

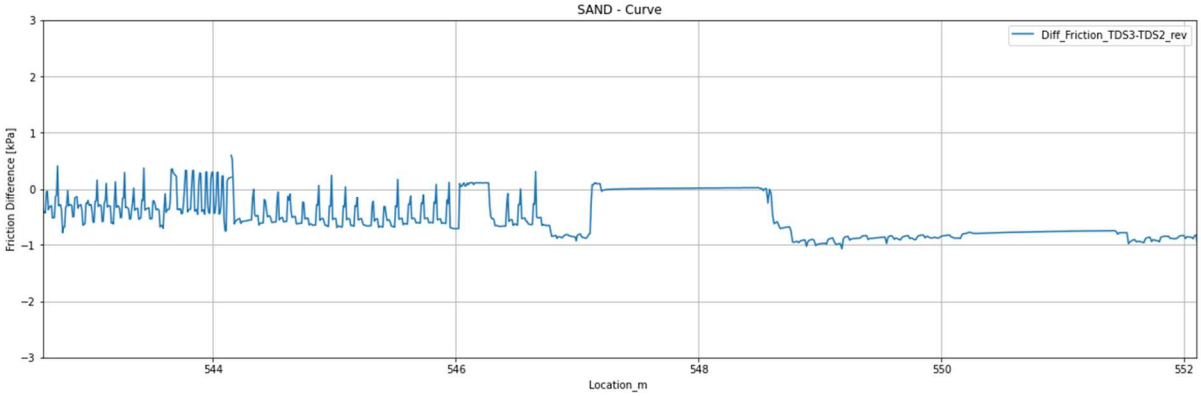

Figure 60 - Difference in friction at Section B10 (SAND, Curve)

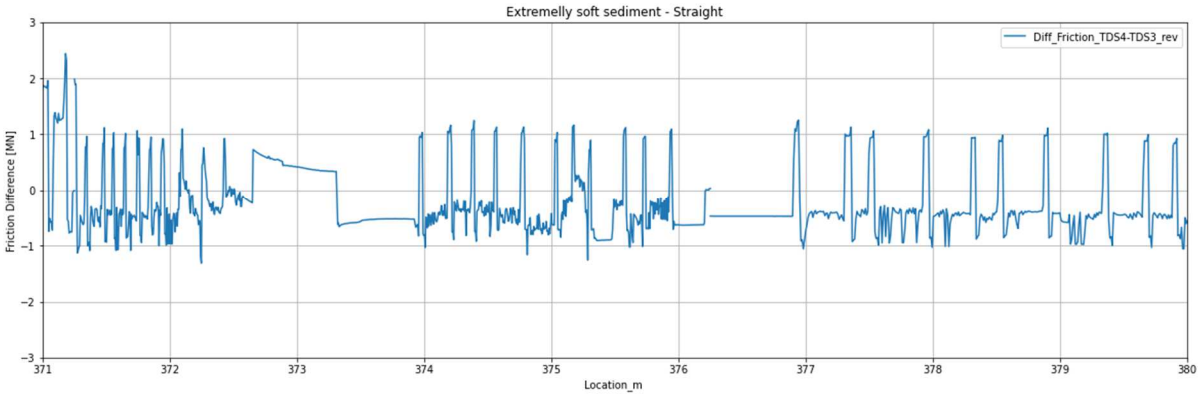

Figure 61 - Difference in friction at Section C1 (Extremely soft sediment, Straight)

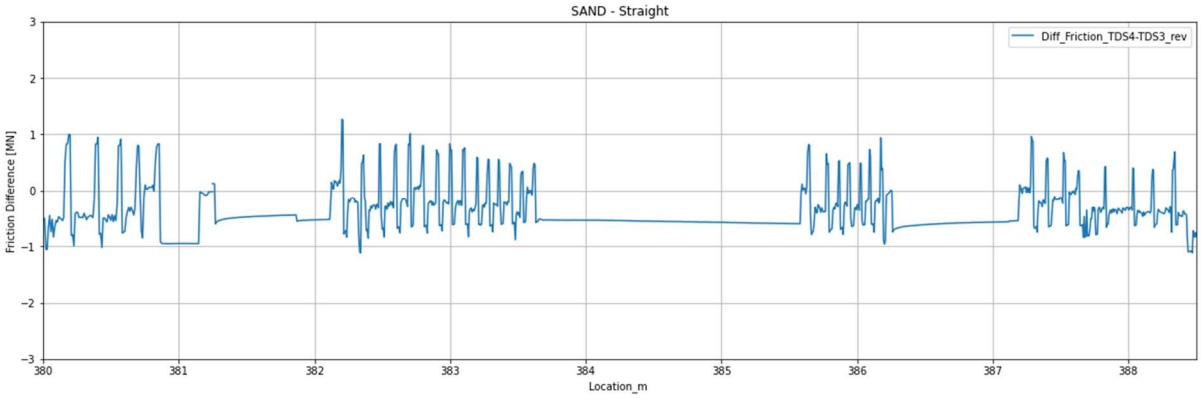

Figure 62 - Difference in friction at Section C2 (SAND, Straight)

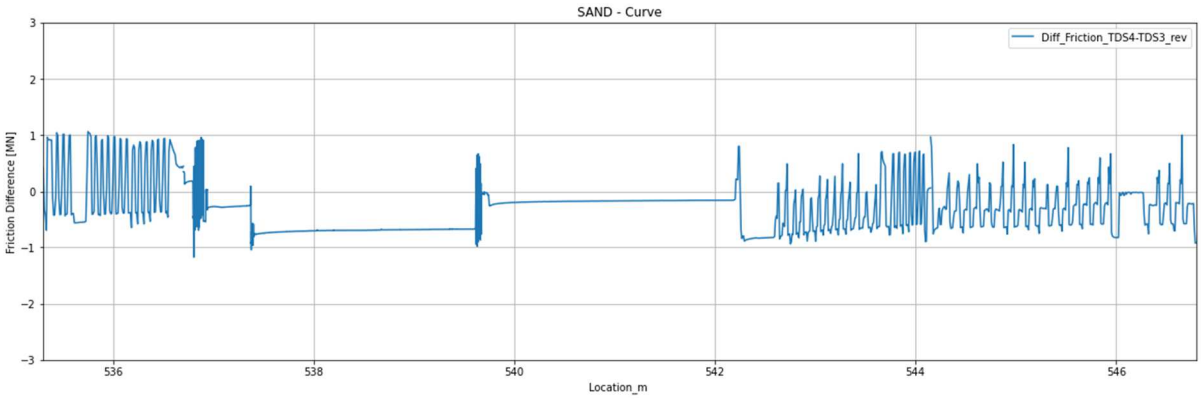

Figure 63 - Difference in friction at Section C3 (SAND, Curve)

Table 8 - Overall difference in friction tendency - Summary of results

Active IJS	Section ID	Location start [m]	Location end [m]	Soil type	Alignment	Results	Overall Difference in friction tendency [kPa]
IJS1 - IJS2	A1	62	135	SAND	Straight descend	Decrease	Decrease in friction of approximately 1kPa to 2kPa
	A2	135	200	SAND	Curve from straight descend to horizontal	Increase	Decrease and increase low amplitude fluctuation of friction values around 0 kPa. The majority of the section presents an increase in friction of approximately 0.8kPa
	A3	240	244	SAND	Curve from straight descend to horizontal	Increase	In the first meter, mainly constant increase in friction until approximately 0.4kPa and in the last meter a decrease to 0kPa.
	A4	244	250	extremely soft sediment	Curve from straight descend to horizontal	neutral	Constant values at 0kPa therefore no difference in friction
	A5	250	350	extremely soft sediment	Straight horizontal	neutral and Increase	For the first 20m of this section, the friction values remain almost constant at 0kPa but afterwards, the values increase ranging from 0kPa to 1kPa
IJS2 - IJS3	B1	155	244	SAND	Curve from straight descend to horizontal	Decrease and Increase	First 55m of this section, the friction values fluctuate with low amplitude around 0kPa but overall the friction mostly decreases. For the remaining of this section, the friction values decreases reaching up to -0.6kPa
	B2	244	250	extremely soft sediment	Curve from straight descend to horizontal	Decrease	Decrease in friction at constant value of approximately less than -0.1kPa
	B3	250	366	extremely soft sediment	Straight horizontal	Decrease	Decrease in friction at a fairly constant value of approximately -0.2kPa
	B4	371	380	extremely soft sediment	Straight horizontal	Decrease	Mainly decrease in friction values to approximately -0.4kPa
	B5	380	400.9	SAND	Straight horizontal	Decrease	Decrease in friction from approximately -0.3kPa to -0.7kPa
	B6	430	448	SAND	Straight horizontal	Decrease and	Decrease and increase in friction values varying from approximately

Active IJS	Section ID	Location start [m]	Location end [m]	Soil type	Alignment	Results	Overall Difference in friction tendency [kPa]
						Increase	-0.1kPa to 0.9kPa
	B7	458	493	SAND	Straight horizontal	Decrease and Increase	Mainly decrease in friction values varying from approximately 0kPa to -0.4kPa
	B8	515.5	518.7	SAND	Curve from horizontal to straight ascending	Decrease and Increase	Decrease and increase in friction values with high amplitude ranging from -0.6kPa to 1kPa
	B9	533	537	SAND	Curve from horizontal to straight ascending	Decrease and Increase	This section presents a high variation in friction difference. It starts with a low amplitude decrease in friction values at approximately -1kPa and ending with high amplitude of 0.8kPa decrease and increase in values until almost 1kPa.
	B10	542.6	552.1	SAND	Curve from horizontal to straight ascending	Decrease	For the first 4m of this section, there are mainly high amplitude, around -0.3kPa, decrease in friction values reaching -0.8kPa. At the last 4m, the friction values decrease and remain constant at approximately -0.9kPa.
IJS3 - IJS4	C1	371	380	extremely soft sediment	Straight horizontal	Decrease	Mostly high amplitude decrease of friction values. It fluctuates around -0.5kPa, reaching a minimum of -1kPa and a maximum of 1.1kPa
	C2	380	388.5	SAND	Straight horizontal	Decrease	Mostly high amplitude decrease of friction values. It fluctuates around -0.5kPa, reaching a minimum of -1kPa and a maximum of 1.2kPa
	C3	535.3	546.8	SAND	Curve from horizontal to straight ascending	Decrease and Increase	Very high variability in friction with high amplitude decrease and increase in values. They reach a maximum of 1kPa and a minimum of -1kPa

3.3.3. General Findings Discussion

In the previous section, the findings on the data were described and illustrated. In this section, they will be interpreted and discussed with the exception of The LVDT' s. Since no correlation was found from Pearson's analysis, it was decided to present the findings but they will not be discussed.

The division of the following sections are based on the soil conditions and boring alignment as mentioned in Figure 36.

3.3.3.1. Section 1 (0m – 135m), SAND, Straight descend

From the starting shaft until 135m, the TBM trails a straight descend where the main soil type is SAND. Almost no deviation from the alignment, relative to the remainder of the route, is observed in the first 60m (Figure 64). The tilt of the TBM is represented by a constant value of approximately -63mm/m (Figure 65), which is consistent with the designed constant descend. The FF remains low and constant for this section whereas the MJF presents a constant rate increase until peak of ~7.5MN at location 30m and decreasing at almost the same rate until 60m (Figure 66). The friction presents a very high pressure from the start of the boring and slowly reduces with the advance of the TBM (Figure 67). This increase is result of the advance through the watertight seal at the starting shaft. Since there is no specific information on the start of the boring, not enough data was provided to correct this starting friction thus to better understand what is the actual soil contribution on the friction at this section. At location 30m the friction starts to have a significant reduction following the MJF decrease, as shown in Figure 66. Due to higher MJF at location 30m, the progress rate increases however the progress rate also increases where the MJF decreases from 30m to 60m (Figure 68). Please note that the progress rates are calculated based on the start and end date/time of each pipe installation thus every horizontal line represents the duration of one pipe being installed without the stoppage in between pipes. Also, the progress rate was not provided as an actual reading therefore this should be taken as an indication and not used to draw any significant conclusions. Nothing can be visualized in the deviation or tilt that can justify this increase in forces therefore this can represent the limits of the TBM being tested at the start of the execution in a very homogenous soil layer.

Also in Figure 66, when the MJF line reaches 0MN it indicates the end of a pipe installation and the start of the subsequent pipe when the forces increase afterwards. Therefore, the horizontal distance between MJF lines indicates the rate of pipe installation (larger distance indicates slower progress and smaller distance indicates faster progress). It is interesting to observe that the pipes are being installed more rapidly within the first 60m when comparing to the following 75m. This can represent the change in soil characteristics and the start of a more challenging soil for the boring.

After 60m, the vertical deviation decreases to -40mm and the horizontal deviation increases to 60mm (Figure 64), which can be stated as minor relative to the remainder of the route. The tilt remains fairly constant and presents only one peak of 73mm at location 97m (Figure 65). The MJF values remains constant at approximately 3.5MN and the FF starts increasing but remains constant at approximately 1.5MN (Figure 66). This can verify the presence of a more challenging soil condition. The friction values also remains fairly constant with maximum reading of approximately 2MN (Figure 67).

The assumption of a new soil characteristics at the second half of this section could be leading the boring into some steering difficulty and this results into small deviations and slower progress. Also, the higher peaks presented in the forces could represent an object being hit, for instance, a boulder.

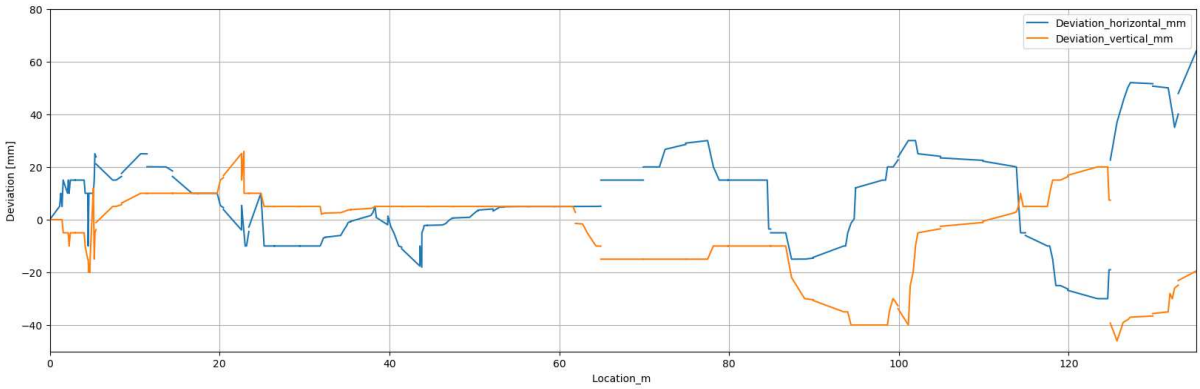

Figure 64 - Horizontal and vertical deviation – Section 1

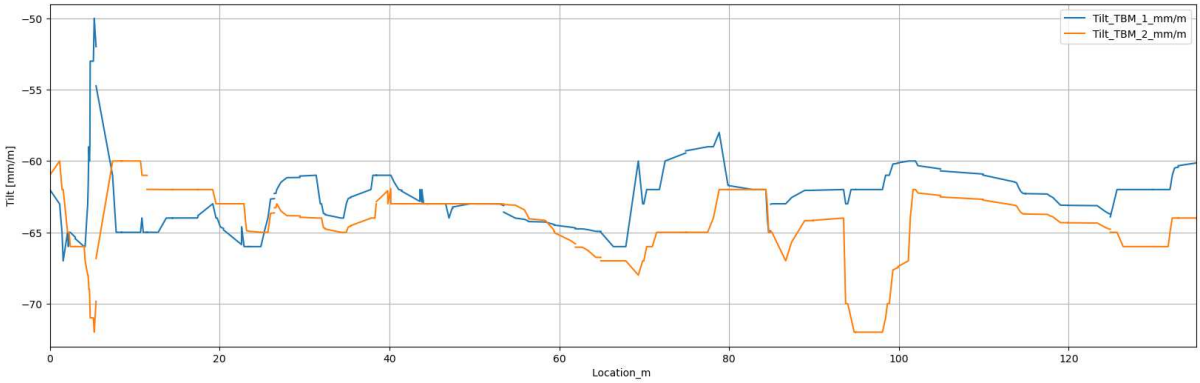

Figure 65 - Tilt from the TBM – Section 1

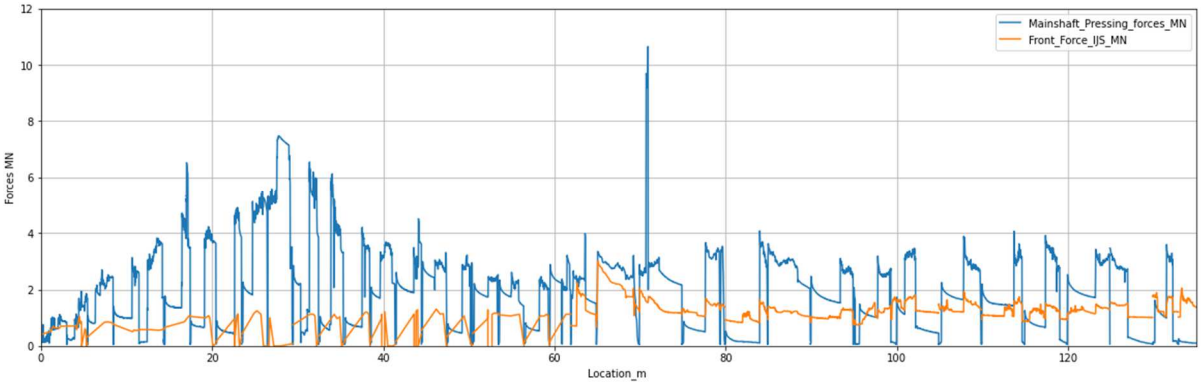

Figure 66 - Main jacking forces and Frontal forces – Section 1

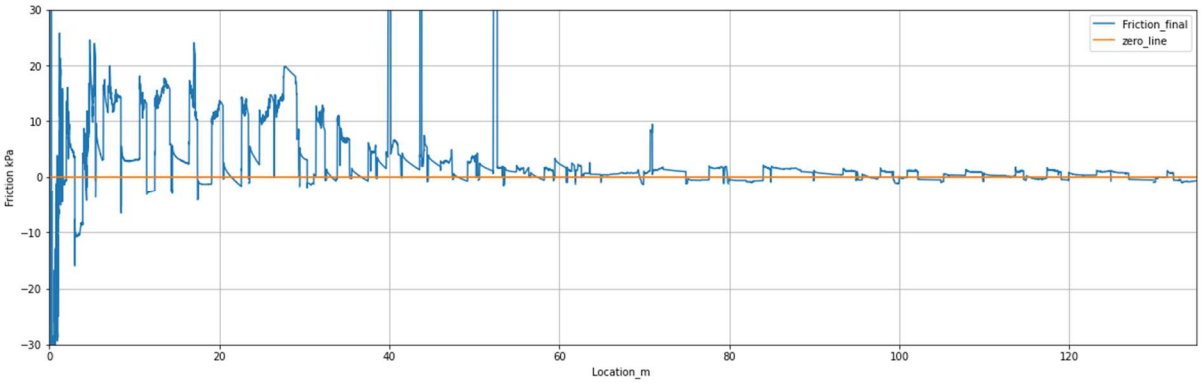

Figure 67 - Friction development – Section 1

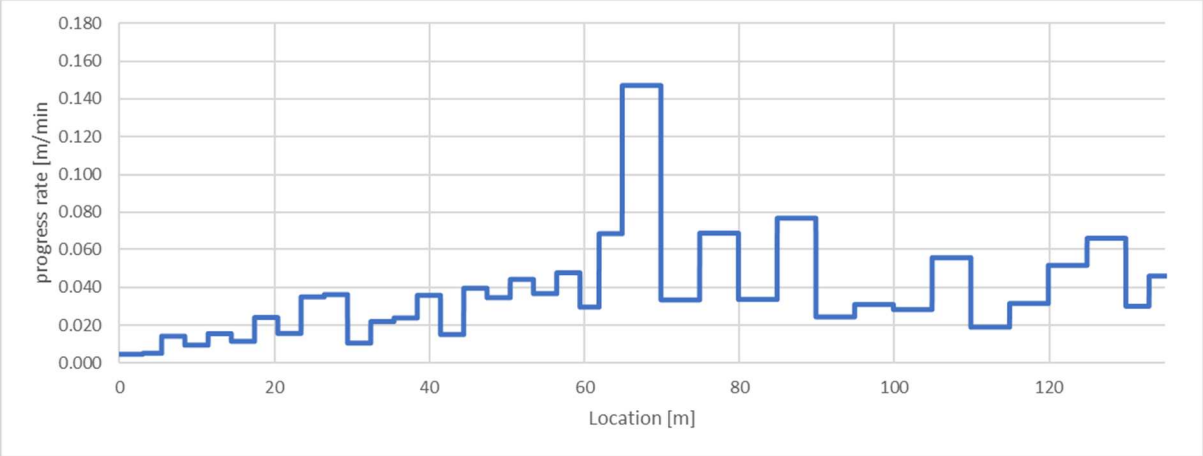

Figure 68 - Progress Rate – Section 1

3.3.3.2. Section 2 (135m – 250), SAND, Downward curve

In this section, the TBM crosses 115m of SAND. From 135m until 150m, a horizontal deviation of 100mm and a vertical deviation of -40mm are present (Figure 69). The tilt presents a rather sharp decrease from -60mm to -40mm and remains decreasing at constant rate (Figure 70). This clearly indicates a curve in which the TBM is changing directions from a straight descend and heading towards a horizontal position and it is possible to notice a longer duration of the installation of the pipe at location 140m. In this section, one would expect an increase in force and friction due to a curve, as mentioned in Milligan and Norris (1993), but this is not observed during installation. Instead, the MJF and FF remain fairly constant along the section until 210m (Figure 71). When reaching this distance, an increase and a small peak in forces are observed and this can be related to the TBM trailing the end part of the curve and adjusting the angle to start a straight alignment. Interesting to note that the increase in force is present a few meters before the TBM reaches a complete horizontal position. The same happens for the friction developments (Figure 72). Right after location 210m, the reading is interrupted leaving a jump in the plots. According to the logbook a new measuring station was installed and it had a malfunction.

At approximately location 235m, the tilt reaches 0mm/m, meaning the TBM is in alignment with the horizontal plane. From there, the boring continues straight in the horizontal direction. At location 243.9m, the TBM faces a change in soil conditions from SAND to extremely soft sediment which was a filling after sand extraction pit. In the last 6m of this section, the horizontal and vertical deviation start to increase up to 150mm and a decrease in MJF, FF and friction are observed (Figure 69).

Analysing the overall friction for this section, it is possible to notice that a constant negative value is predominant (Figure 72). This happens because the MJF readings always goes to zero when a new pipe is being installed while the FF remains active. Therefore, in this case the absolute value should be accounted for and it indicates a constant trend for the entire section with the exception where the TBM curve ends. At this position, it is possible to notice an increase in the friction development before the boring alignment is completely stabilized in the horizontal position and before the change in soil layer. After which the friction development starts decreasing.

In this section it is possible to notice that after a standstill there is an increase in MJF. This is due to the static friction that needs to be overcome, as mentioned in Van Seters et al. (1999) as cited in Verburg (2006).

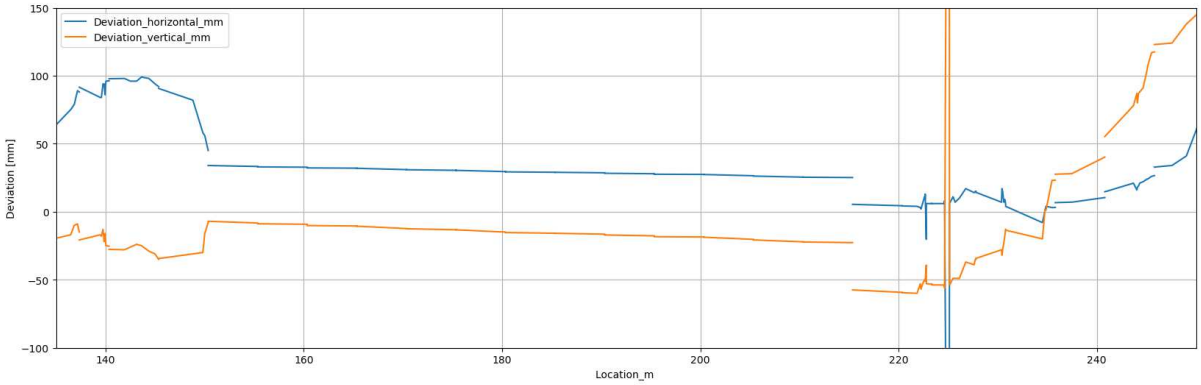

Figure 69 - Horizontal and vertical deviation – Section 2

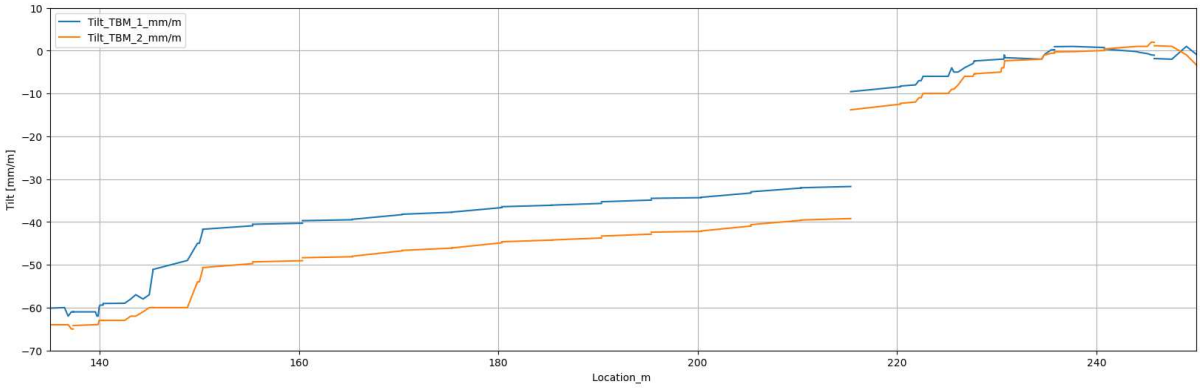

Figure 70 - Tilt from the TBM – Section 2

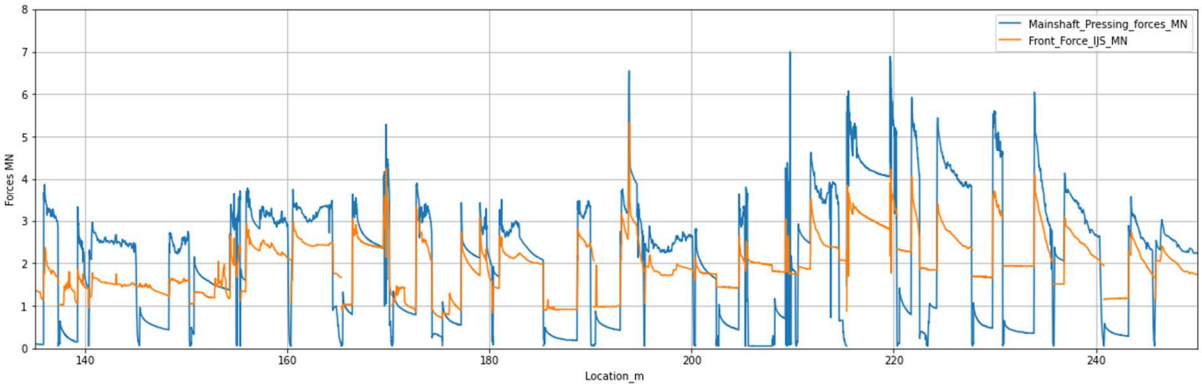

Figure 71 - Main jacking forces and Frontal forces – Section 2

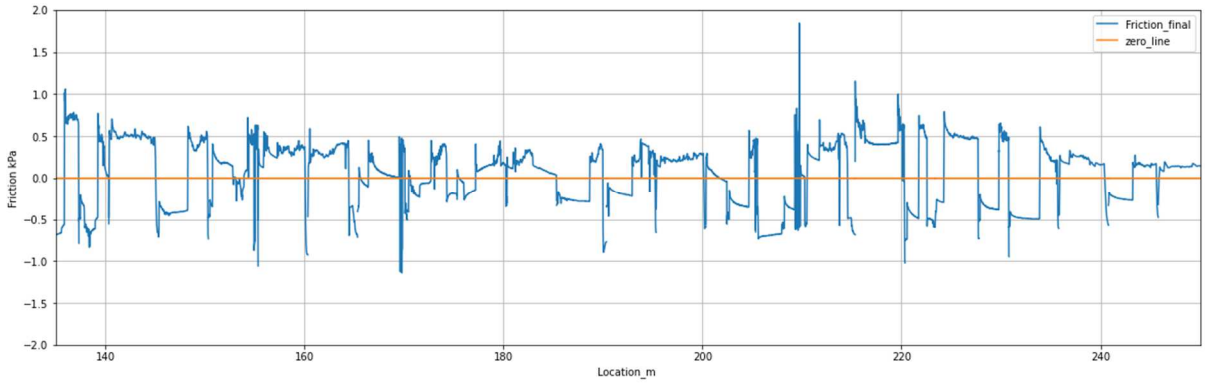

Figure 72 - Friction development – Section 2

3.3.3.3. Section 3 (250m – 380m), Extremely soft sediment, Straight horizontal

As previously discussed, from 250m until 380m the TBM is crossing an extremely soft sediment layer under the river IJ. In the first 10m of this section, until location 260m, there is a slight decrease in MJF and FF (Figure 73) however this decrease is less visible in the friction plot (Figure 74). The tilt decreases to -17mm/m (Figure 75) and the horizontal deviation starts an increase trend while the vertical deviation increases to approximately 200mm and remains fairly constant after this location (Figure 76). Therefore, a deviation from the alignment does not show an increase in forces for this small section.

A wave shape increase trend is then present in the MJF and FF from location 260m until 370m (Figure 73). There is a peak at location 280m followed by a valley at approximately 300m. Afterwards, the highest peak at 325m and the lowest valley at location 350m. The friction follows the same pattern (Figure 74). The same wave shape is also seen at the tilt plot mainly in the blue reading (Figure 75), even though the values are not that high it could have a correlation. The horizontal deviation presents a significant increase to ~450mm just before location 280m which is where the first peak in force is observed (Figure 76). From there, a smaller wave shape curve is also present with the deviations being right before where a peak or a valley in the forces is present. This could be an indication of how the horizontal deviation in the tunnel alignment is impacting the friction at this section, as expected and seen in Milligan and Norris (1993). However, this is the opposite of what was mentioned by Thomson (1993) which states that according to published jacking records, greater force increases are a result of vertical misalignments rather than horizontal ones. This contradiction can be due to difference in boring parameters as soil types, lubricant use, overcut values, etc. Since these records were not mentioned in detail further comparison is not possible.

On the other hand, at location 313m, a V shape indentation in the horizontal and vertical deviation is present which is also seen in the tilt plot as a peak but no difference is seen in the forces which contradicts the previous statement. This indentation could indicate a relatively sharp curve at that location that could be caused by the TBM steering back to the alignment and then away from it relatively sudden.

At location 370m, the forces present a sudden jump and no extreme deviation is seen that could justify this increase. Therefore, the assumption is that a transition zone from extremely soft cohesive soil to the sand layer. This can also be seen in the higher force values after this location when comparing to the soft sediment section.

As already mentioned in section 2, it is possible to notice increase in MJF after a stoppage, no explanation is found for these in the reports provided. However, in this case, from location 170m until 350m, the jacking forces seems to be higher and this can be explained by a soil profile with more cohesive sediments. And according to Milligan and Norris (1993) and (1996), in cohesive soils, an even higher jacking force is

needed due to pore pressure dissipation in more cohesive soil profiles.

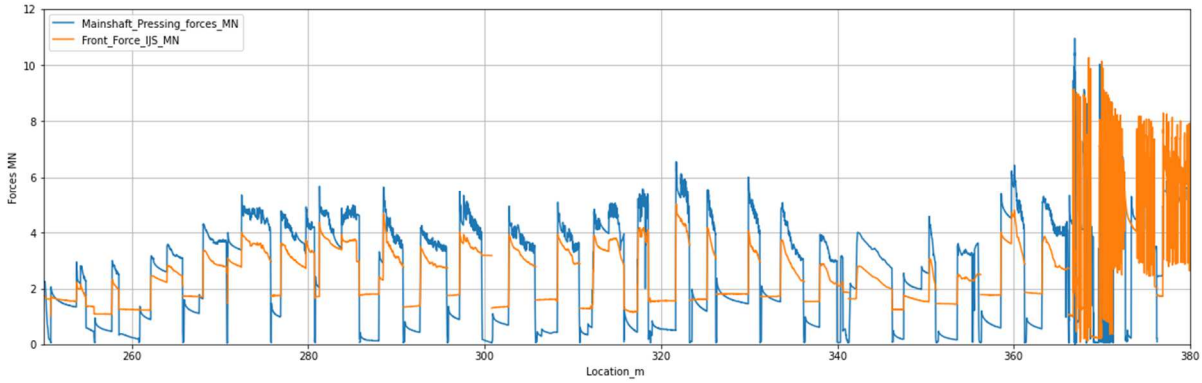

Figure 73 - Main jacking forces and Frontal forces – Section 3

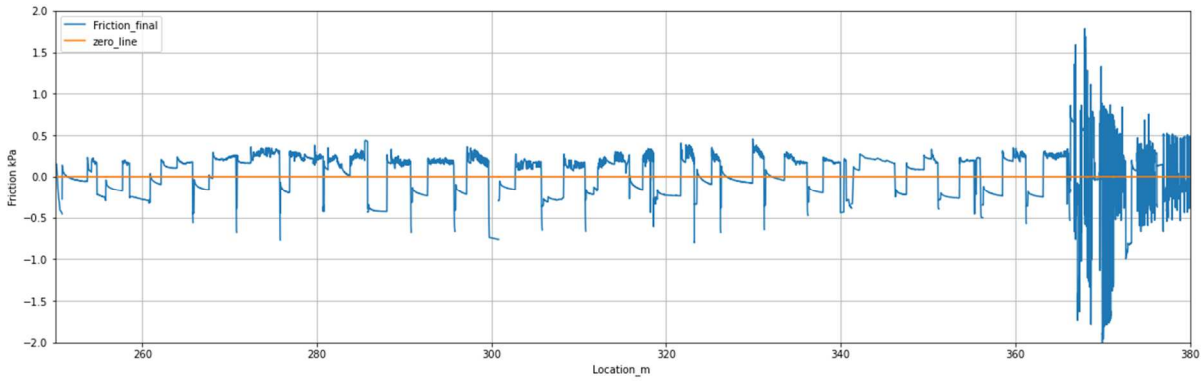

Figure 74 - Friction development – Section 3

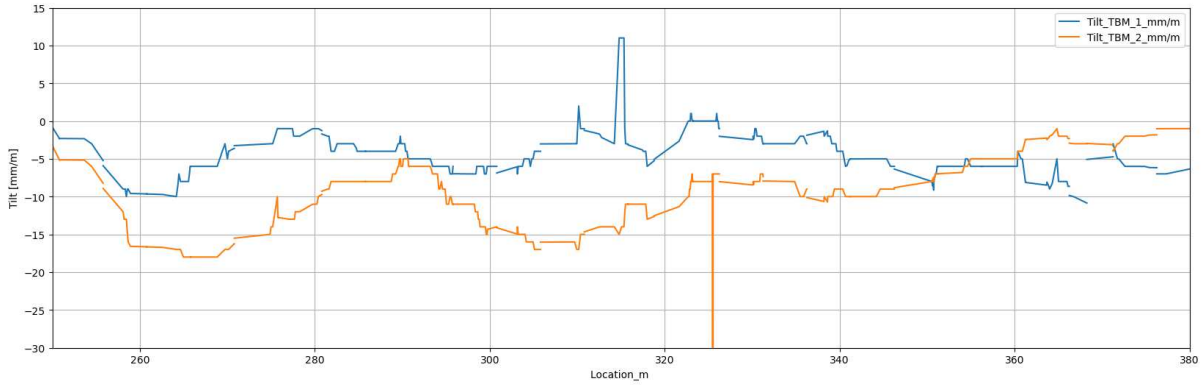

Figure 75 - Tilt from the TBM – Section 3

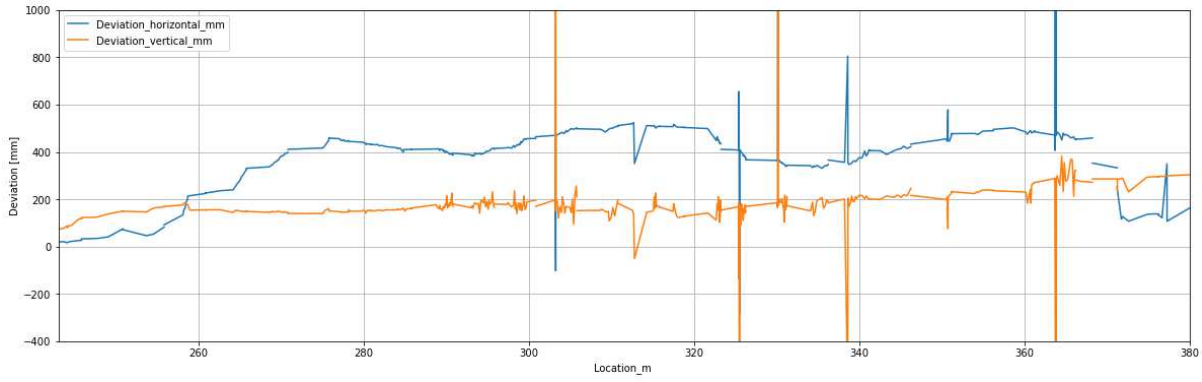

Figure 76 - Horizontal and vertical deviation – Section 3

3.3.3.4. Section 4 (380m – 500m), SAND, Straight horizontal

This section is crossing a sand layer and according to the design, the TBM is boring in a straight horizontal alignment. At the start of this section, an increase in horizontal deviation is present until approximately 250mm followed by a valley shaped decrease with the lowest value of -100mm at 395m and returning to 250mm at 400m (Figure 77). This deviation is clearly seen also in the tilt at the same locations (Figure 78). A significant increase in friction is observed from the start of the valley shaped deviation, at location 387m, until the end at location 410m (Figure 79). This can be an indication that the change in horizontal alignment could be influencing the friction.

At location 410m, the deviation starts to become more constant with no sudden changes and it is where a change in the forces can be seen from a more erratic to a more evenly spaced and constant behaviour (Figure 80). This can be due to the end of the transition soil layer and the start of a more homogeneous sand layer.

A spike in the tilt is present at location 430m (Figure 78) and there is an immediate stop in the boring, this is seen in the MJF sudden drop (Figure 80). The activities were resumed after the tilt was back to the initial level. According to the log book, there was a leakage in the pipe and that was the reason for the deviation and stoppage. At location 443m, a sharp v shape decrease in vertical deviation is present (Figure 77) but no changes are seen in the forces and friction also no explanation in the log book.

At location 457m, there is a sharp increase in horizontal deviation from 310mm to 570mm (Figure 77) leading to another immediate stop in the boring operations. When the execution is resumed, the deviation continues to be high and the tilt is also showing a sharp difference (Figure 78). However, no significant increase in forces is observed (Figure 80). Another spike in deviation is present at location 480m (Figure 77) which could be result of a boulder or other obstacle hit since the execution is again stopped and resumed without any increase in forces. After this until location 500m, the horizontal deviation decreases and the friction remains fairly constant.

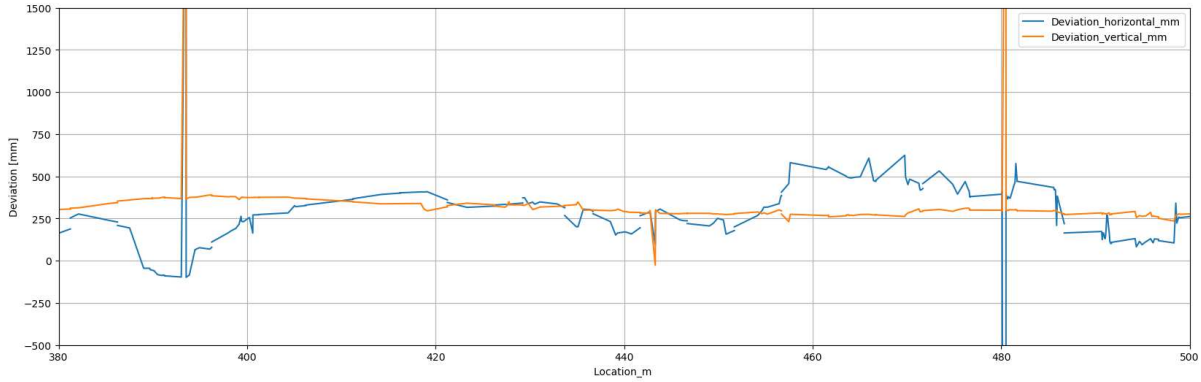

Figure 77 - Horizontal and vertical deviation – Section 4

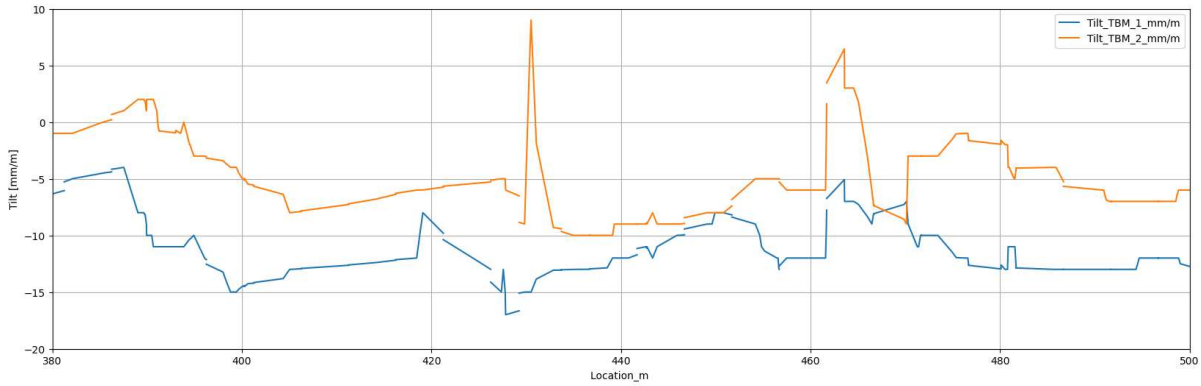

Figure 78 - Tilt from the TBM – Section 4

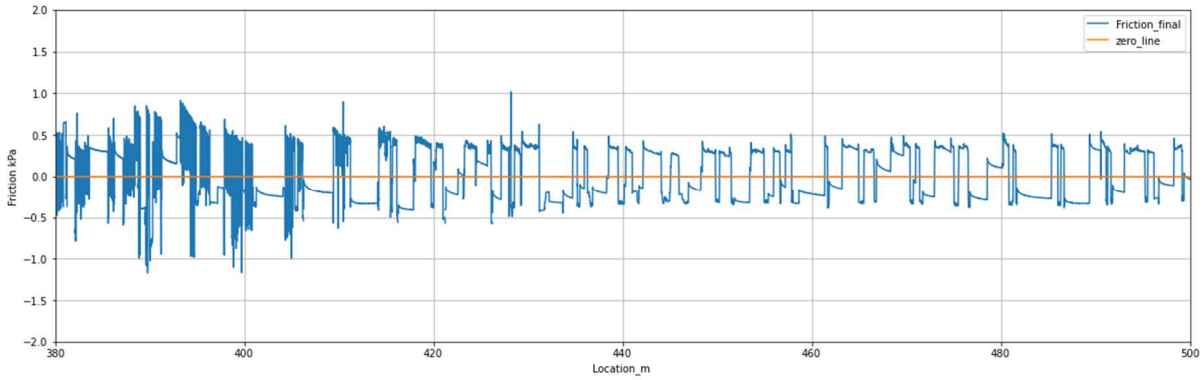

Figure 79 - Friction development – Section 4

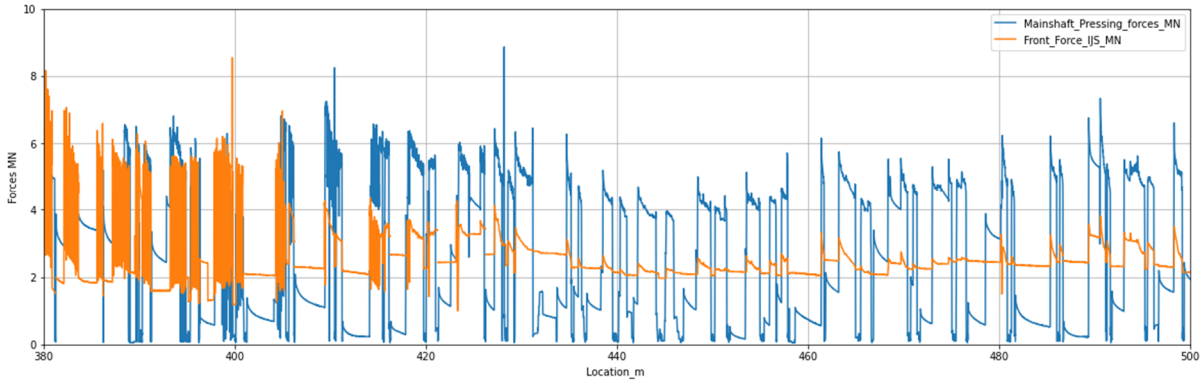

Figure 80 - Main jacking forces and Frontal forces – Section 4

3.3.3.5. Section 5 (500m – 650m), SAND, Upward Curve

This section presents a upward curvature in the design alignment of the boring and the main soil type is sand. The TBM starts tracing the curve at 518m and this can be clearly visualized in the tilt plot where an increase in an almost constant rate is present until approximately 600m (Figure 81).

At location 518m, the horizontal deviation presents a rapid increase to almost 1000mm and it remains constant until 538m when another increase happens to 1350mm (Figure 82). At location 563m the deviation starts to slowly decrease. In this interval, an increase in friction is clearly observed (Figure 83) when comparing to the previous section where a straight alignment was traced.

It is observed that the FF decreases considerably starting at location 563m (Figure 84) leading to a decrease in friction (Figure 83). This can be related with the start of the decrease in horizontal deviation as mentioned above. On the other hand, at location 595m the FF increases leading to an increase in friction and only at location 599m is where a sharp indentation is present in the horizontal and vertical deviation. Therefore in this case the friction was not influenced by a change in alignment but an hypothesis is that the sharp bend introduced in the alignment could have been caused by the increased forces. The FF increased 4.0m before the start of the deviation in alignment and there was no increase afterwards. The same happened with a smaller deviation present at location 604.5m where the FF increased 0.5m before the bend was introduced leading to the same conclusion as before. Until approximately 4.0m after the bend, an increase in FF is still present and after that no increase is observed.

At location 620m, the soil condition changes and presents a stretch of 10m of sand and loose SAND with layers of clay. Here the tilt increases once more (Figure 81) and at 622.5m the horizontal and vertical deviation present a large alteration lasting until 625.7m (Figure 82) probably due to challenges in adjusting the boring to the new soil conditions. And only at location 625m the MJF and specially the FF present an increase (Figure 84). The FF increase could be divided into direct and residual increase due to a large deviation in the alignment. At this section, a direct increase is present after 0.5m of the sharp deviation and a residual increase ranging from 1.0m to 4.5m after the deviation. After that no change in FF is observed.

With the data provided, it is not possible to specify a generalized range of distance after which a bend the FF can still be affected by it. As a result, the friction presents a slight increase as well (Figure 83). At location 631m, the FF decreases considerably (Figure 84) while the deviation remains constant (Figure 82) and no differences are observed in the friction (Figure 83). Therefore, it is not possible to directly relate the increase in friction with the change in alignment since it is also possible to be due to more cohesive sediments present in the soil profile.

When comparing the downward curvature in (Section 1) to the upward curvature in (Section 5) with the same soil condition, it is possible to notice that in this section (5) the MJF is almost 4 times higher than in Section 1. A similar increase is of course also observed in the friction forces. It is important to highlight that Section 5 presents a deviation 10 times higher than the one presented in Section 1.

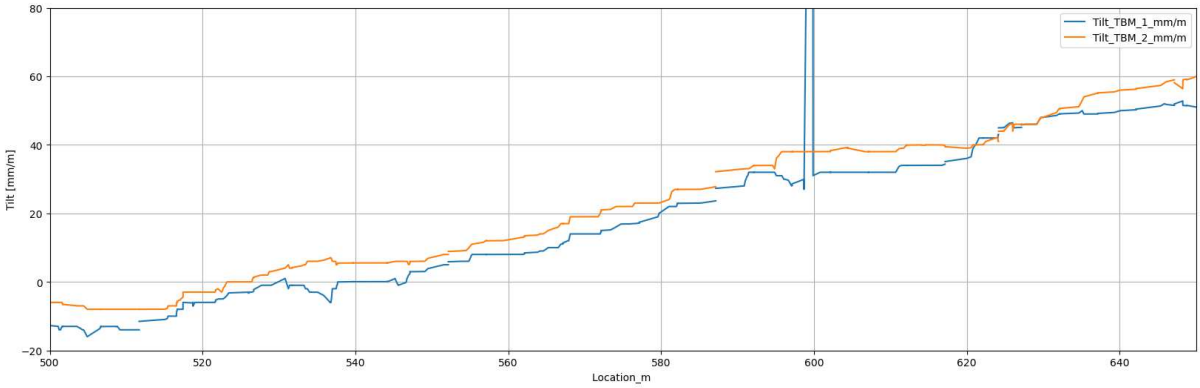

Figure 81 - Tilt from the TBM – Section 5

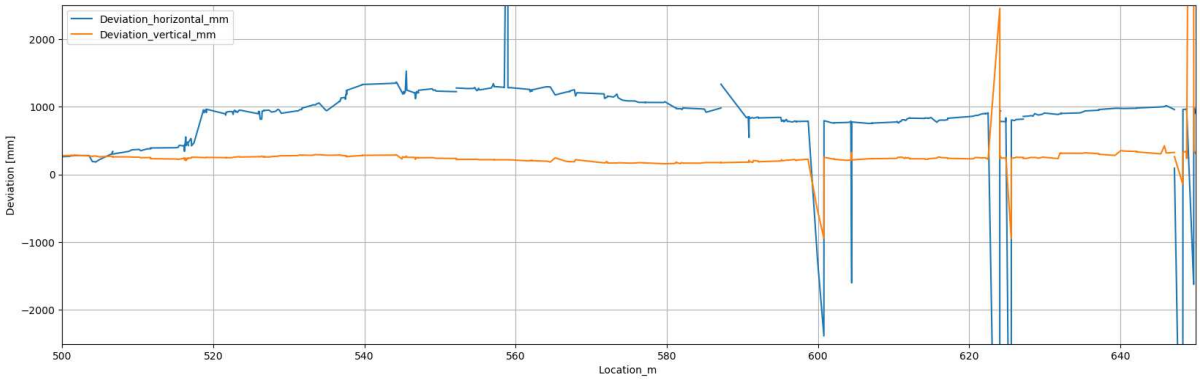

Figure 82 - Horizontal and vertical deviation – Section 5

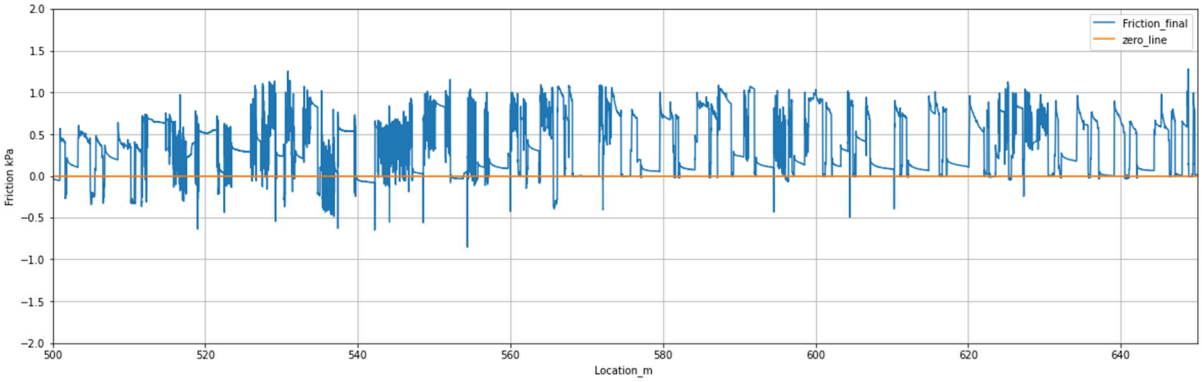

Figure 83 - Friction development – Section 5

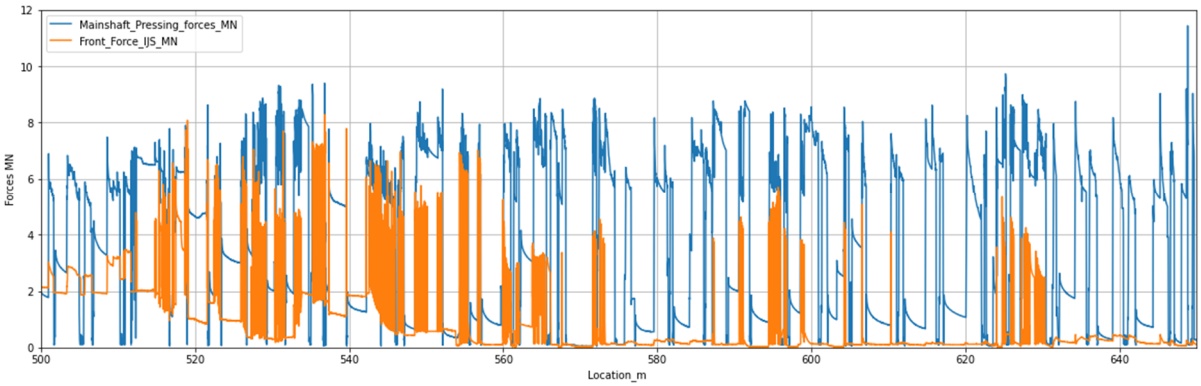

Figure 84 - Main jacking forces and Frontal forces – Section 5

3.3.3.6. Section 6 (650 – end), varied soil, Straight ascend

In the last section, the TBM has a straight horizontal alignment until the end of the boring within SAND until 723m. From there until 745m, there is SAND and loose SAND with layers of clay.

At location 660m, the horizontal deviation starts decreasing (Figure 85) and the tilt presents a v shape indentation (Figure 86). This is followed by an increase in friction value (Figure 87). At location 673m, the deviation plot presents a high and rapid jump in the data (Figure 85) and this is also followed by a high increase in MJF (Figure 88) and in friction (Figure 87). In between these two locations no significant changes in friction or in deviation and tilt were observed.

At locations 680m, 685m and 697m, it is possible to notice a sudden increase in FF (Figure 88) which could have caused the slight change in vertical and horizontal deviation at the few meters that followed (Figure 86). This also impacted the friction at these locations (Figure 87).

Starting at 718m, there is a significant increase in FF, a slight increase and a more erratic behaviour of the friction and no indication of alignment deviation. This can lead to the assumption that this is the beginning of a different soil profile where more cohesive sediments are present.

The readings stop at location 732m due to catastrophic failure as the data recorder was lost several meters further on, so data of last stretch is not available.

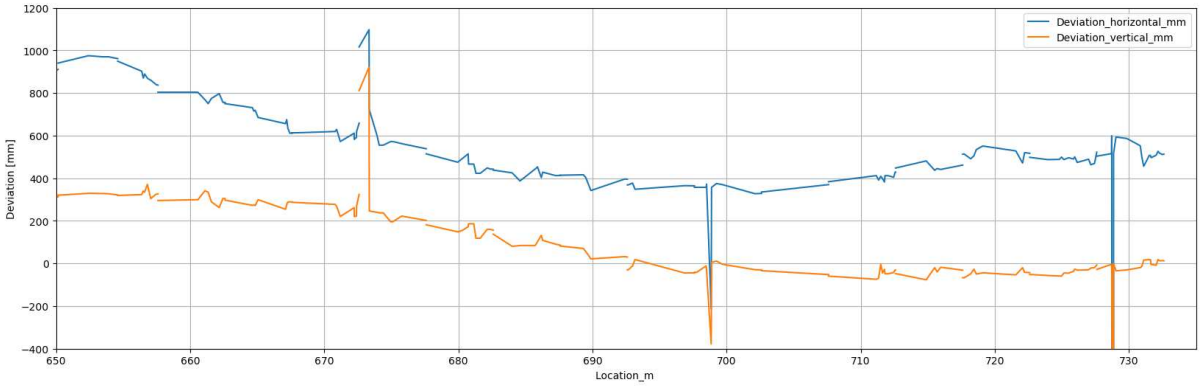

Figure 85 - Horizontal and vertical deviation – Section 6

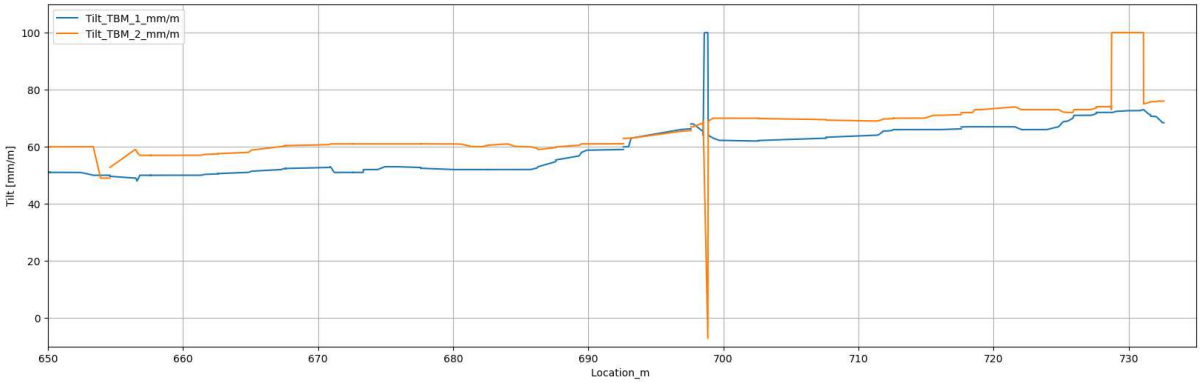

Figure 86 - Tilt from the TBM – Section 6

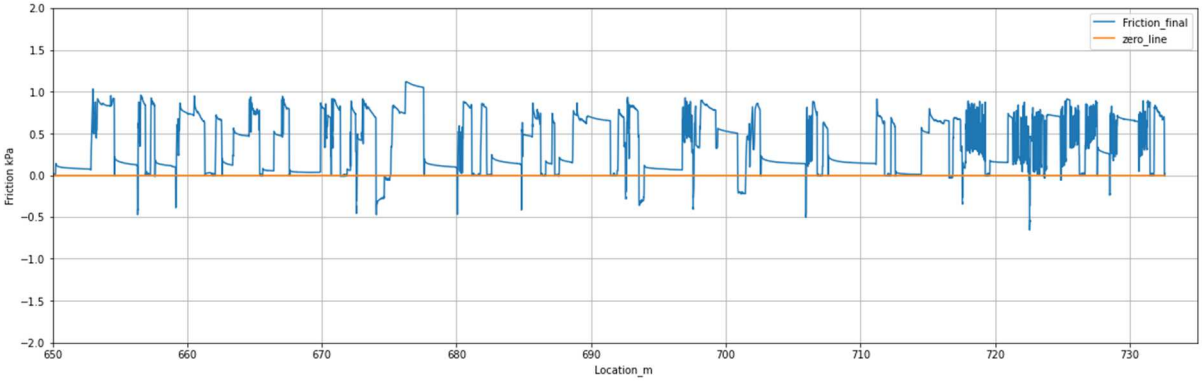

Figure 87 - Friction development – Section 6

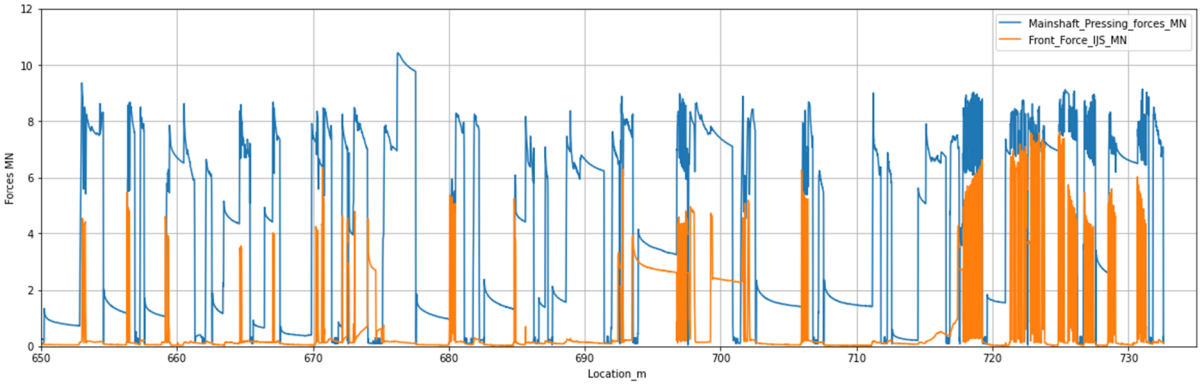

Figure 88 - Main jacking forces and Frontal forces – Section 6

3.3.3.7. Summary

For all the sections, when the MJF line reaches 0 MN, it signifies the completion of one pipe installation and the beginning of the next as forces increase. Consequently, the horizontal distance between MJF lines reflects the rate of pipe installation—a greater distance indicates slower progress, while a shorter distance suggests faster progress.

At the start of the boring, very high MJF are observed which can be related to initial testing of the main jacks in a very homogenous soil layer and extremely high friction is present as result of the advance through the watertight seal at the starting shaft. When assessing the installation rate, possibly due to change in soil conditions to a more challenging sediment, the pipes are being installed more rapidly within the first 60m when comparing to the following 75m.

3.3.4. Correlation Analysis

As mentioned before, Pearson's correlation analysis and Spearman's rank correlation were used to understand if there is any statistically relevant corelation between two variables within the available data set.

The first analysis was divided into two parts, Part 1 between all the parameters available for the entire boring length and Part 2 divided into sections as mentioned in Figure 36. These resulted in an output with 48 rows × 48 columns. The second analysis, called Part 3, focused on the Friction and the parameters that directly influence the alignment.

To compare the results from both Pearson and Spearman correlations the following can be considered:

- Both coefficients are high: suggests a strong linear and monotonic relationship.
- If Pearson is high but Spearman is lower: may indicate a linear but not strongly ranked relationship (the ranking order is not well preserved).
- If Spearman is high but Pearson is lower: suggests a non-linear but consistent ranking relationship.

3.3.4.1 Part 1

For Part 1, conditional formatting was applied for better visualization of the results and they are illustrated in Figure 89 as red (-1), blue (0) and green (+1). The relevant values, chosen to be from +-1 until +-0.5 for Pearson's and +-1 until +-0.6 for Spearman's were further assessed (Statstutor, n.d.).

In summary, all the parameters that were used for the calculation of another internal parameter present a high (close to -1 or +1) Pearson correlation coefficient (PCC). For instance, Main shaft jack force parameters correlate linearly with Friction and the pressure in the mixing chamber and the cutting wheel correlate linearly with the volume of drilling fluid that enters and leaves the boring. This is indicative of good results from this analysis. These type of correlations were removed and the final parameters presenting an almost linear correlation are shown in Table 9.

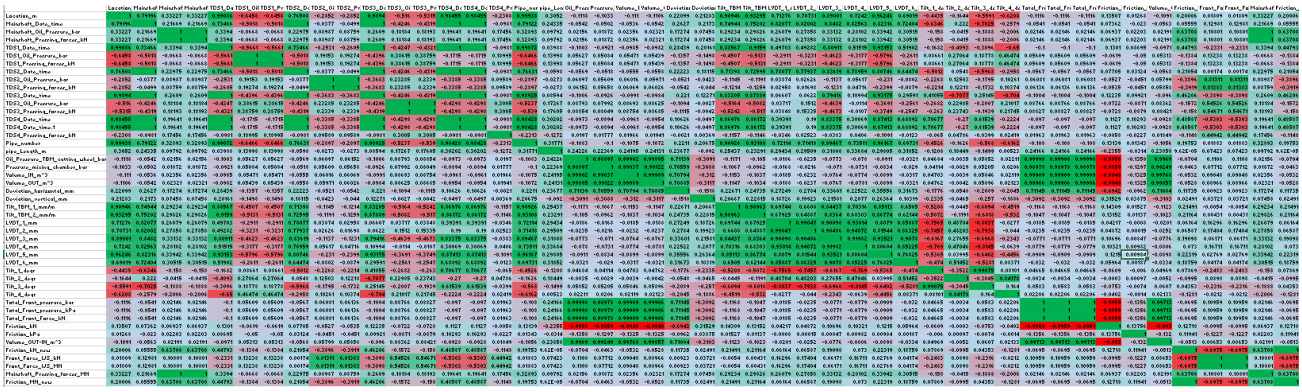

Figure 89 - Illustration of Pearson's correlation analysis for all 48 parameters where red (-1), blue (0) and green (+1).

Table 9 - Relevant results of Pearson correlation coefficient (black) and Spearman's coefficient (blue) for the entire boring length

	Devia-tion_horizontal_mm	Tilt_TBM_1_mm/m	Tilt_TBM_2_mm/m	LVDT_1_mm	LVDT_2_mm	LVDT_3_mm	LVDT_4_mm	LVDT_5_mm	LVDT_6_mm	Front_Force_IJS_MN	Mainshaft_Jack-ing_forces
TDS1_Jacking_forces_kN			-0.51 -0.62					-0.58 -0.62			
TDS2_Jacking_forces_kN										0.81 0.71	
TDS3_Jacking_forces_kN		-0.52 -0.64	-0.52 -0.69							0.55 0.64	
Oil_Pressure_TBM_cutting_wheel_bar	0.71 -0.06										
Pres-sure_mixing_chamber_bar	0.71 -0.09										
Volume_IN_m^3	0.71 0.001										
Volume_OUT_m^3	0.71 -0.06										
Deviation_horizontal_mm		0.23 0.69	0.24 0.70			0.34 0.70		0.36 0.79			
Tilt_TBM_1_mm/m				0.70 0.51	0.66 0.37	0.84 0.76	0.70 0.56	0.85 0.81	0.65 0.56		
Tilt_TBM_2_mm/m				0.70 0.40	0.65 0.30	0.84 0.75	0.69 0.41	0.87 0.86	0.62 0.48		
Friction_kPa										-0.70 -0.30	0.63 0.80

From the analysis it follows that the horizontal deviation presents a high positive Pearson coefficient and a close to zero Spearman's coefficient with the pressure in the mixing chamber, pressure at the cutting wheel, the volume of drilling fluid that enters and volume that leaves the boring. This can indicate that there is a linear correlation between the parameters and they could have been poorly ranked when performing the Spearman analysis. They are all parameters that are used to derive the Total Front force which also presents a positive linear correlation with the horizontal deviation. Therefore from this result, it can be stated that for the overall boring length, when the front pressure changes, the horizontal deviation has a tendency to change linearly in the same direction. The TBM tilt presents a negative correlation with the IJS 1 and IJS 3 forces, meaning that when these forces increase the tilt tends to decrease and vice versa. The LVDT_5 also presents this negative relationship with IJS 1 forces.

Most of the LVDT readings have a strong linear and monotonic correlation with the Tilt of the TBM, which is expected since they all relate to displacement. Also, the horizontal deviation TBM tends to have a non-linear relationship with the tilt of the TBM and to LVDT 3 and 5. All future correlations between LVDTs, tilt and deviation will not be taken into account, when analysing Part 2 and Part 3.

The Front_Force_IJS_MN presents a strong linear and monotonic relationship with IJS 2 force and a not that strong relationship with IJS3 force. Also, the Friction_kPa linearly correlates with the Front_Force_IJS_MN.. These are expected results since the IJS2 and IJS3 forces are used to derive the Front force parameter and this is related to Friction as presented in Formula (1). To derive Front_Force_IJS_MN, the following parameters were used along the route in terms of relative length: Front force [25.7%], IJS1 [4.8%], IJS2 [25.2%], IJS3 [36.5%], IJS4 [7.8%]. Interesting to notice that IJS2 force presented a stronger correlation with the front force while IJS3 force presented a weaker one even though it was active more often along the boring..

Lastly, the Mainshaft_ Jacking_forces presents a relationship with the Friction which is expected since they are parameters which directly influence each other as per Formula (1).

3.3.4.2 Part 2

For Part 2, all the steps mentioned in Part 1 were taken and the results are presented in Table 10 to Table 15 for Section 1 to Section 6, respectively. In Figure 90, the IJS activation is shown and it fits well with the PCC values for different sections, for instance, in Section 1 only IJS1 and IJS2 are active and in Section 2

the IJS1 drops to zero having no meaningful Pearson or Spearman coefficient and so on.

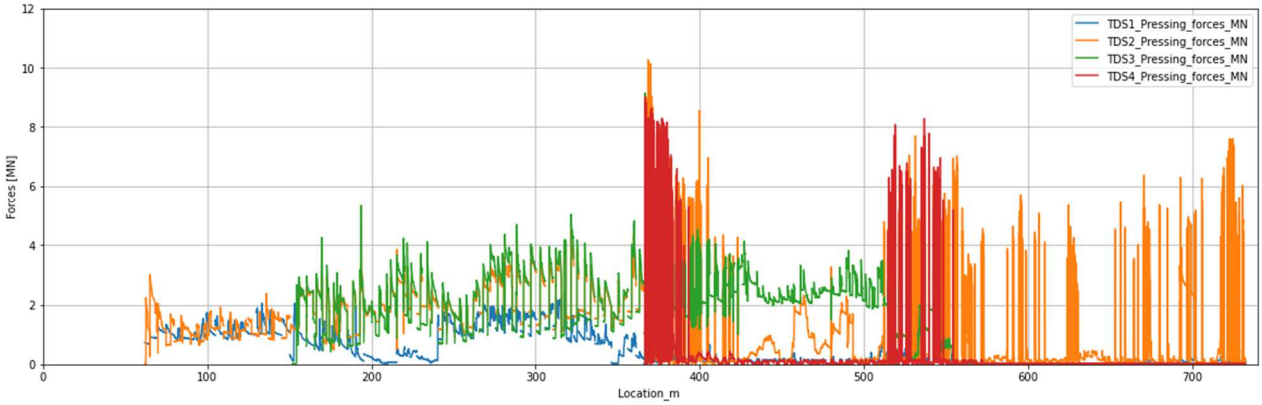

Figure 90 - IJS Forces along the entire boring length

Table 10 - Section 1 (0m – 135m): Relevant results of Pearson correlation coefficient (black) and Spearman's coefficient (blue)

	Tilt_TBM_1_mm/m	Front_Force_IJS_MN
TDS1_ Jacking_forces _kN		0.76 0.81
TDS2_ Jacking_forces _kN	0.53 0.58	0.81 0.81
Friction_kPa		-0.95 0.92

In Section 1, there is a moderate positive linear and monotonic correlation between the Tilt_TBM and the IJS2 Force. Also, a high linear and monotonic relationship is present between Front_Force_IJS and IJS 1 and IJS2 forces. The Front_Force_IJS also correlates with the Friction_kPa, similar to what was presented in Part 1, but with a positive Spearman's coefficient.

Table 11 - Section 2 (135m – 250m): Relevant results of Pearson correlation coefficient (black) and Spearman's coefficient (blue)

	Devia-tion_horizontal_mm	Devia-tion_vertical_mm	LVDT_2_mm	Front_Force_IJS_MN	Mainshaft_ Jack-ing_forces _MN	Fric-tion_kPa
TDS1_ Jacking_forces _kN	0.56 0.62		0.53 0.48			
TDS2_ Jacking_forces _kN				0.95 0.96	0.60 0.32	
TDS3_ Jacking_forces _kN				0.93 0.89	0.77 0.41	
Mainshaft_ Jacking_forces _MN						0.91 0.87

In Section 2, the Deviation_horizontal_mm and LVDT_2_mm have a moderate linear and monotonic positive correlation with the IJS1 Force. As explained, the Front_Force_IJS_MN presents a very strong linear and monotonic positive correlation with the active IJS. The Mainshaft_Jacking_forces_MN present an almost linear correlation with IJS2 and IJS3 also presents a strong linear monotonic correlation with the Friction.

Table 12 - Section 3 (250m – 380m): Relevant results of Pearson correlation coefficient (black) and Spearman's coefficient (blue)

	Deviation_vertical_mm	Tilt_TBM_1_mm/m	Tilt_TBM_2_mm/m	LVDT_1_mm	LVDT_2_mm	LVDT_4_mm	LVDT_5_mm	LVDT_6_mm	Front_Force_IJS_MN	Mainshaft_Jacking_forces_MN	Friction_kPa
TDS1_Jacking_forces_kN	-0.66 -0.68	0.57 0.50	-0.82 -0.71	0.61 0.56			-0.59 -0.35	0.67 0.67			
TDS2_Jacking_forces_kN									0.83 0.80		-0.50 -0.47
TDS3_Jacking_forces_kN					0.30 0.72	0.27 0.74	-0.24 -0.60			0.54 0.52	
TDS4_Jacking_forces_kN									0.54 0.36		
Mainshaft_Jacking_forces_MN											0.66 0.71
Front_Force_IJS_MN											-0.51 -0.54

In Section 3, Tilt_TBM_1_mm/m, LVDT1 and LVDT6 present a positive correlation with IJS1 Force while Deviation_vertical_mm, Tilt_TBM_2_mm/m and LVDT5 present a negative correlation with the IJS1 Force. Since no detailed information is given on the difference between Tilt_TBM_1_mm/m and Tilt_TBM_2_mm/m these results cannot be further assessed. The Mainshaft_Jacking_forces_MN present a moderate positive linear correlation with IJS3 force and with Friction. The Friction has a moderate negative correlation with IJS 2 Force and with Front_Force_IJS_MN.

In Section 4, apart from the already explained correlations between Front_Force_IJS_MN and the active IJS and between Friction and Mainshaft_ Jacking_forces, LVDT5 presents a moderate negative linear correlation with the IJS1 Force.

Table 13 - Section 4 (380m – 500m): Relevant results of Pearson correlation coefficient (black) and Spearman's coefficient (blue)

	Front_Force_IJS_MN	Friction_kPa	LVDT_5_mm
TDS1_ Jacking_forces _kN	0.57 0.23		-0.50 -0.34
TDS2_ Jacking_forces _kN	0.78 0.43		
TDS3_ Jacking_forces _kN	0.84 0.99		
Mainshaft_ Jacking_forces _MN		0.88 0.86	

Table 14 - Section 5 (500m – 650m): Relevant results of Pearson correlation coefficient (black) and Spearman's coefficient (blue)

	Tilt_TBM_1_mm/m	Tilt_TBM_2_mm/m	LVDT_5_mm	Front_Force_IJS_MN	Friction_kPa
TDS1_ Jacking_forces _kN	-0.39 -0.75	-0.40 -0.73	-0.48 -0.61	0.49 0.76	
TDS2_ Jacking_forces _kN	-0.71 -0.40	-0.71 -0.40	-0.72 -0.40	0.75 0.71	
TDS3_ Jacking_forces _kN				0.76 0.84	
TDS4_ Jacking_forces _kN				0.51 0.47	
Deviation_horizontal_mm					
Tilt_TBM_1_mm/m				-0.54 -0.80	
Tilt_TBM_2_mm/m				-0.54 -0.78	
LVDT_5_mm				-0.54 -0.54	
Mainshaft_ Jacking_forces _MN					0.85 0.80

In section 5, the TBM tilts and LVDT5 present a negative linear correlation with the IJS2 Force but a non-linear but consistent negative relationship with IJS1 Force. The Front_Force_IJS_MN has a positive correlation with all active IJS and again Friction is correlated with the Mainshaft_ Jacking_forces, also in Section 6.

Table 15 - Section 6 (650m – 750m): Relevant results of Pearson correlation coefficient (black) and Spearman's coefficient (blue)

	Friction_kPa
Mainshaft_ Jacking_forces _MN	0.88 0.96

Most of the correlations resulted by the Pearson analysis could not be visualized in the charts present in sections 1 to 6 and therefore were not included in the discussion previously. Despite showing interesting insights, the results of the correlation analysis were not investigated further thus it can be viewed as a topic for future researches.

3.3.4.3 Part 3

The second analysis focuses on answering research question 1. Therefore, the parameters that directly influence the alignment (Tilt_TBM_1_mm/m, Tilt_TBM_2_mm/m, Deviation_horizontal_mm, Deviation_vertical_mm) were compared specifically against the friction. This analysis was performed for all six sections (Figure 36) and also for the entire boring length. Table 16 present the results and, statistically, the friction and the alignment parameters have no direct correlation.

Table 16 - Pearson correlation coefficient (black) and Spearman's coefficient (blue) – friction x alignment parameters

	Section 1	Section 2	Section 3	Section 4	Section 5	Section 6	Entire boring length
Tilt_TBM_1_mm/m	0.00 -0.06	0.09 -0.05	-0.08 -0.2	0.16 0.16	0.07 -0.15	0.08 0.18	0.21 -0.01
Tilt_TBM_2_mm/m	0.03 0.04	0.08 -0.05	0.00 0.21	0.07 0.16	0.05 -0.16	0.11 0.17	0.21 0.01
Deviation_horizontal_mm	-0.13 -0.02	-0.10 -0.02	0.10 -0.10	-0.07 -0.14	0.08 -0.23	-0.01 0.01	0.11 0.05
Deviation_vertical_mm	0.08 0.29	-0.04 0.03	-0.00 0.11	0.09 0.15	-0.04 0.18	0.00 -0.07	0.02 -0.14

3.3.4.4 Discussion

From Part 1 analysis, it was observed that all parameters used to derive the Total Front force presents a positive linear correlation with the horizontal deviation. This can be related to the TBM trailing a curve path were these increase in force generates an expected higher deviation specially in soft cohesive soil conditions. Also interesting to note that the IJS1 forces are negatively correlated to the tilt of the TBM and LVDT5. This is something that if investigated further can bring interesting insights. Lastly, the Front_Force_IJS presents a strong linear and monotonic relationship with IJS 2 force and a not that strong relationship with IJS3 force even though the IJS3 was used more frequently along the boring and they are both parameters used to derive the Front_Force_IJS. From Part 2 analysis, in Section 1, there is a moderate positive linear and monotonic correlation between the Tilt_TBM and the IJS2 Force. Since this section is located in SAND, this might be the reason why the relationship is moderate and not strong. Similar to already presented in Part 1, the Front_Force_IJS correlates negative and linear with the Friction_kPa but with a positive Spearman's coefficient which can be indicative of another type of relationship that was not explored in this work.

In Section 2, the deviation parameters present a moderate linear and monotonic positive correlation with the IJS1 Force and the Mainshaft_Jacking_forces_MN present an almost linear correlation with IJS2 and IJS3 which are parameters used to derive the front force and therefore directly related to the main jacking forces. Section 3 is the only section which is located in extremely soft sediments and is the one that presents the most amount of relevant correlations between parameters.

Interesting to note that in Sections 1,4 and 5 the IJS force is correlating only with LVDT 5. One would expect that the opposite pair (LVDT 6) would also be influenced but this is not observed. A common correlation in all sections is the Front_Force_IJS and the active IJS Forces, with the exception of Section 6. Also, from Section 2 to Section 6, the Mainshaft_Jacking_forces_MN is correlating with the Friction Force, which is expected since the Friction is derived from the main jacking force. However, this relationship is not present in Section 1 which can be related to the fact that the starting friction only stabilizes after location 60, approximately.

In summary, all the parameter used to derive another, presents some kind of correlation between each other which indicates a strong result from the analysis.

And finally the results from Part 3 indicates that the friction and the alignment parameters present no direct statistical correlation using the two methods presented.

3.3.5. Difference in friction tendency discussion

The plots presented from Figure 46 to Figure 63 can present very high difference in friction values and in some cases these are not representative of reality. For instance, in section B4 (Figure 54), every time the difference in friction reaches approximately -0.6kPa it represent locations where the IJS2 force goes to zero and when this happens the IJS3 increases as a reaction (Figure 91). This results in a amplification of the difference. This can be observed in many different sections either with a drop in MJF or IJS forces to zero and all these locations are taken into account when creating a summary overview of the difference in friction tendency in Table 8.

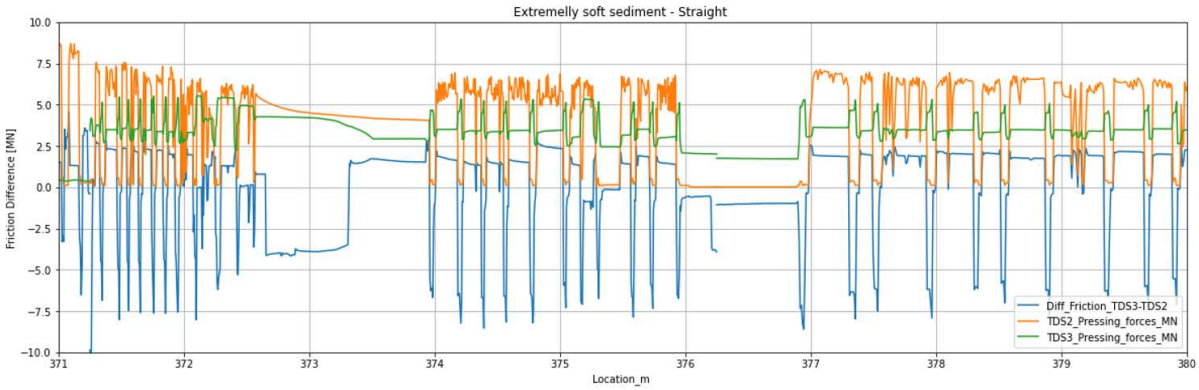

Figure 91 - How difference in friction relates to IJS2 and IJS 3 forces (friction multiplied by the surface area of the tunnel to result in MN for comparison)

As already mentioned in Section 3.3.3.3.3.2, to estimate the impact that subsequential pipe segment installations have on the friction over time at a specific location, plots depicting the difference in friction at a specific section where created, analysed and its results are presented in Table 8.

Figure 92 presents the results of this assessment (Sections A, B and C) and indicates that:

- 350m out of the 587.6m [59%] analysed have a decrease in friction difference after the subsequent pipe installations;
- 155m [26%] have an increase in friction difference after the subsequent pipe installations;
- And 86m [15%] have a neutral relationship meaning that there was no difference in friction observed due to subsequent pipe installations.

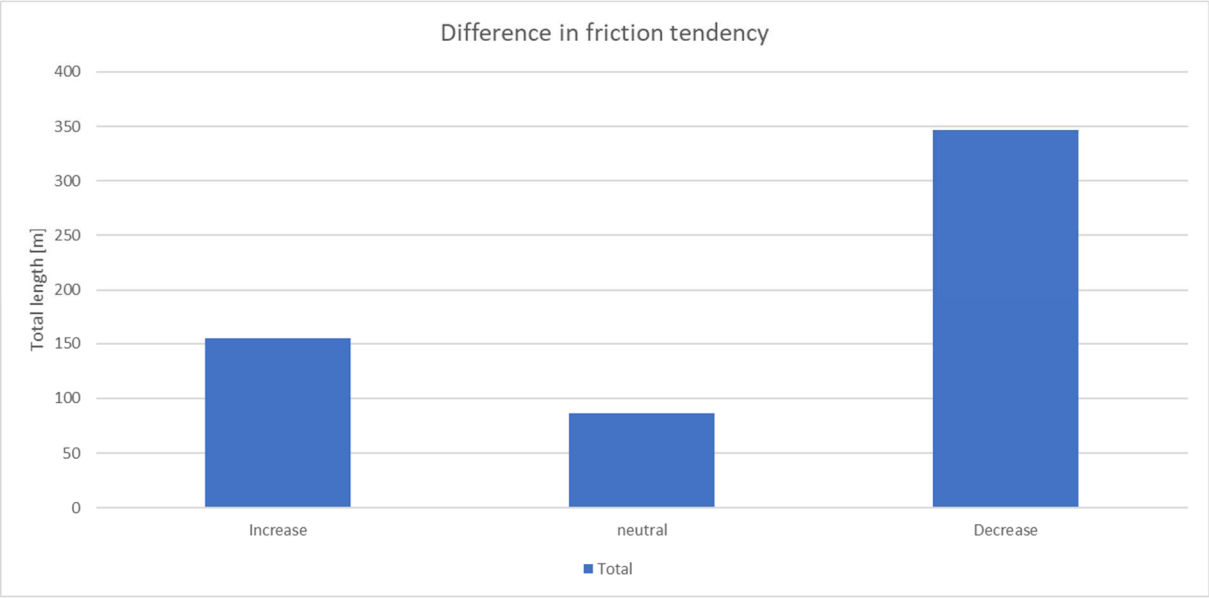

Figure 92 - Difference in friction tendency results

Figure 93 also incorporates the soil type into this assessment where SAND and extremely soft sediments represent approximately 60% and 40% of the total length, respectively. It is observed that both soil types

available (SAND and extremely soft sediment) can lead to an increase, decrease or no change in friction. When SAND is present, in 60% of the alignment, friction forces decrease. In extremely soft sediment, this is true for 40% of the alignment. These percentages are similar to friction forces increase, in 64% and 36% of the alignment in SAND and soft sediment, respectively. No change in friction represents 52% of the alignment in SAND and 48% in soft sediment.

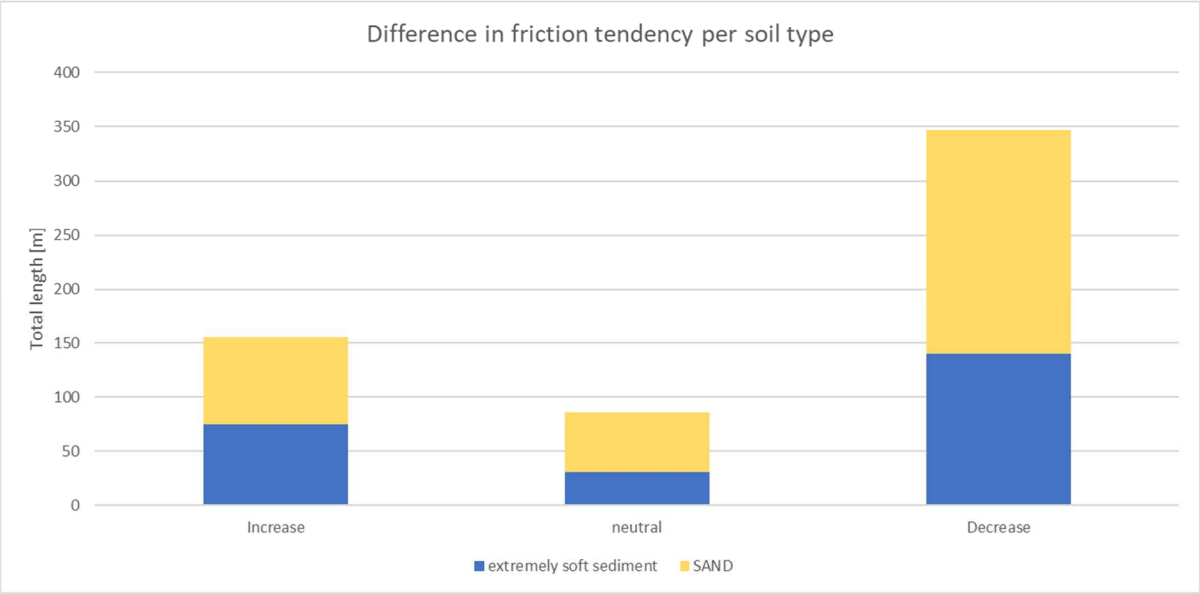

Figure 93 - Difference in friction tendency results per soil type

When the alignment is considered as well, four types are present: Curve from horizontal to straight ascending, Curve from straight descend to horizontal, Straight descend and Straight horizontal. In Figure 94 it is possible to observe that when a curve from horizontal to straight ascending and Straight descend are present, subsequent pipe installations results in a decrease in friction. However, when a curve from straight descend to horizontal is present, the results can indicate an increase, decrease or no change and the differences are not very large. The same holds when a straight horizontal alignment is present, the results also vary between increase, decrease and neutral but the difference are insignificant indicating that the friction mainly decreased after subsequent pipe installations at these locations.

These results are quite interesting because even in locations where curves are present and where the friction is expected to increase, as seen by Norris and Milligan (1992), after many subsequent pipe installations the friction is decreasing, in this case study.

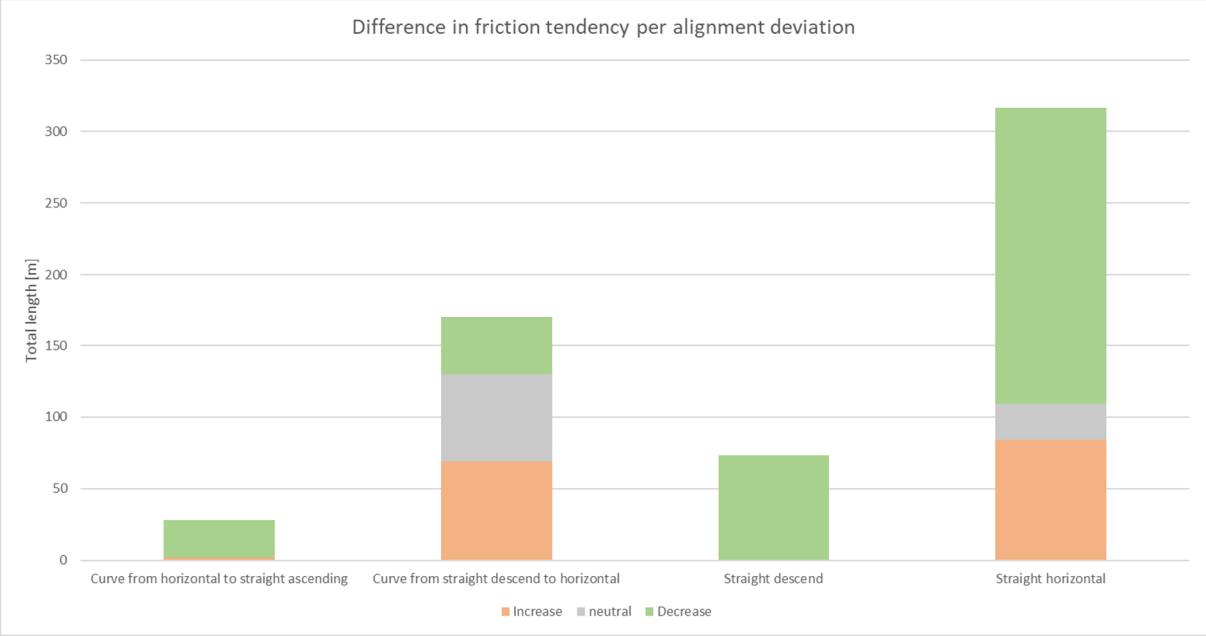

Figure 94 - Difference in friction tendency per alignment deviation

When subdividing Figure 94 - Difference in friction tendency per alignment deviation into soil types, it results in Figure 95. It is interesting to note that the most variation in friction, either increases or decreases, tend to occur when travelling in SAND, with the exception of straight horizontal sections in extremely soft sediments. The TBM works as a blind shield if trenching in soft section of the infilled sand pit, so different behaviour is expected there.

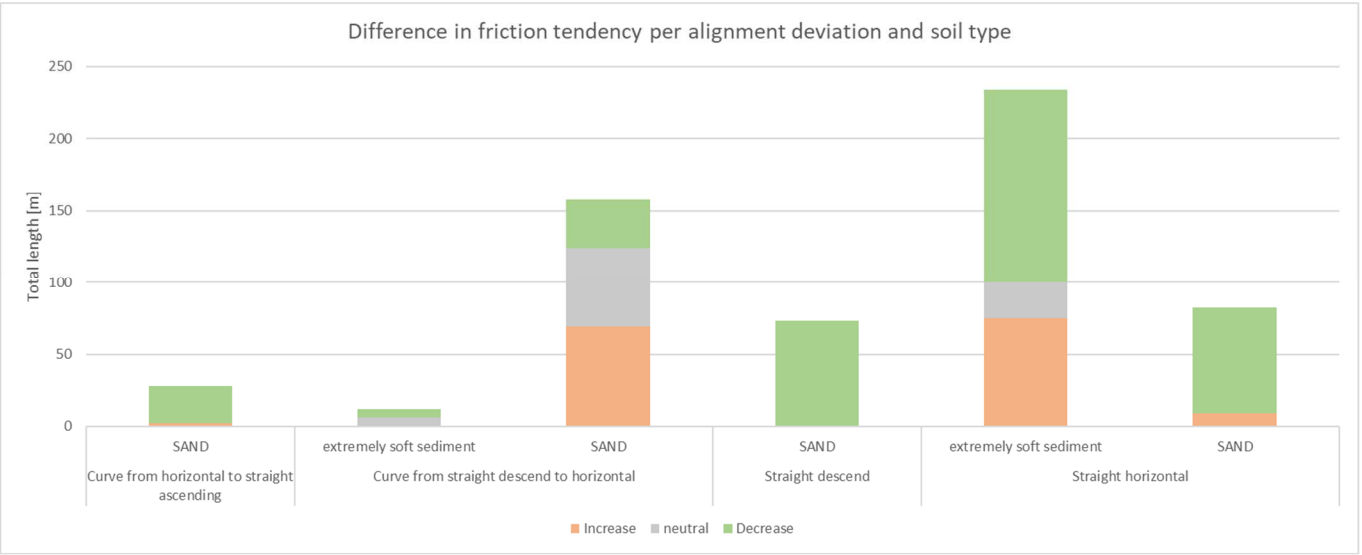

Figure 95 - Difference in friction tendency per alignment deviation and soil type

The result of this analysis clearly shows a tendency for a decrease in friction after subsequent pipe installation throughout the project execution. This can be valuable information so the constant friction coefficient *f,* which is a design parameter mentioned in Section 2.d.ii, can be optimized. Potentially a non-constant value should be considered taking into account the installation parameters observed since there is correlation between the amount of installed pipes and friction.

4. Conclusion

For a microtunneling project, at the design phase, some parameters are considered the main variables to ensure a successful installation. They are:

- Main Jacking forces,
- Resistance at the face of the TBM;
- Friction.

These three parameters drive each design decision as project feasibility since the resistance at the head of the TBM and the friction cannot exceed the Main Jacking Forces (Formula (1)).

The friction can be derived using the tunnel surface area and a friction coefficient (Formula (9)). The friction coefficient is dependent on the effective stress on the contact surface between the soil and the pipe surface and the internal friction angle of the soil (Formula (11)). It is usual practice to use one friction coefficient value for the entire boring length which is based on experience (See Section2.4.3). Comparing the friction coefficient value described in the NEN 3650 when overcut and lubrication is used for concrete pipes (f =7.5 kPa) and the friction development over the entire length at the boring under the river IJ (< 2kPa, with the exception of the start when drilling through the water tight seal the friction is > 20kPa) then this author considers this approach one that overestimates the friction coefficient value given the heterogeneity of the soils that are usually encountered along a boring, and its interaction with the pipe surface. Ye et al. (2019) proposes a thorough calculation to predict the friction coefficient which can reduce risks and costs, especially during the execution phase.

The initial intention of this thesis was to calculate the friction developed during the execution of the microtunneling under the river IJ and compare it with the design parameters using both methods mentioned above. This was not possible due to lack of soil data available. Therefore this comparison can be done at a future project where more soil information is available and the benefit of using a non-constant friction coefficient can be further discussed.

With the available data, it was possible to analyse and understand if there is a clear correlation between the steering action of the TBM and the friction experienced by the pipes along the boring under the river IJ in Amsterdam.

For the data analysis, the entire boring was divided into six sections based in soil conditions and boring alignment changes. For all sections, after a standstill an increase in friction is observed as mentioned in Van Seters et al. (1999) as cited in Verburg (2006). When focusing on the relationship between friction and deviations the following could be observed:

- *Section 1 (0m – 135m), SAND, Straight descend:* No visual correlation between the friction development and deviation parameters could be observed.
- Section 2 (135m – 250), SAND, *Downward curve*: A curve is present at the start of this section where the TBM travels from a straight descend and heads towards a horizontal position. One would expect an increase in force and friction due to a curve, as mentioned in Milligan and Norris (1993), but this is not observed during installation. Therefore no correlation is present in this section.
- *Section 3 (250m – 380m), Extremely soft sediment, Straight horizontal*: An increase in horizontal deviation is observed just before locations where a peak or a valley in MJF is present thus impacting the friction development at those positions. This is expected and seen by Milligan and Norris (1993).
- *Section 4 (380m – 500m), SAND, Straight horizontal*: at the start of this section, a significant increase in friction development is observed and most possibly due to a valley shaped change in horizontal deviation also tilt.
- *Section 5 (500m – 650m), SAND, Upward Curve*: at the start of this section, an increase in friction development is observed possibly due to a rapid increase in horizontal deviation. However, at location 595m, the FF increased leading to an increase in friction and only 4m after a sharp indentation is present in the horizontal and vertical deviation. Therefore, the friction was not influenced by a change in alignment but an hypothesis is that the sharp bend introduced in the alignment could have been caused by the increased forces.
- *Section 6 (650 – end), varied soil, Straight ascend*: correlation between the friction development and deviation parameters could be observed at the start of the section.

At locations where correlation between alignment and forces are apparently present, it is observed that always the horizontal deviation is the influencing parameter. This is also confirmed by the Pearson's correlation analysis in which all the parameters used to derive the Total Front Force presents a positive linear statistical correlation with the horizontal deviation. This result contradicts what is mentioned in Thomson (1993) which is that greater force increases are a result of vertical misalignments rather than horizontal ones. The difference in outcomes indicates the need of further research to better understand the correlation between friction and vertical and horizontal deviation.

In summary, Sections 1 and 2 show no visual correlation between TBM orientation and recorded friction whereas Sections 3, 4, 5 and 6 presents a positive visual correlation. On the other hand, the results from the statistical analysis present differently as no correlation is seen between parameters that directly influence the tunnel alignment and the friction. Since the achieved outcomes is not always consistent based on soil type and tunnel alignment and, does not consistently align with the literature, a back analysis of more installation data from microtunneling projects at different site conditions will give a valuable insight in the relation between friction and TBM orientation history.

The final analysis was performed in a sample with total length of 587.6m to estimate the impact that subsequent pipe segment installations have on the friction over time at a specific location. The results show that at 59% of these locations, the friction decreased after the subsequent pipe installations and at 26% of the total length, the friction increased. When adding the soil type in this assessment, SAND and extremely soft sediments represent approximately 60% and 40% of the total length, respectively, and no relevant distinction in soil type percentage is observed at locations where friction decreases or increases after the subsequent pipe installations.

When the alignment is incorporated into the assessment, it is observed that when a curve from horizontal to straight ascending and straight descend are present, a decrease in friction results from subsequent pipe installations. At a curve from straight descend to horizontal and at straight horizontal alignments, there are locations where the friction decreases, but also increases or remain the same as before subsequent pipe installations. Having observed that the fiction decreases at locations where curves are present is contradictive to what was mentioned and seen by Norris and Milligan (1992) where the friction is expected to increase.

The results of this analysis clearly show a tendency for a decrease in friction after subsequential pipe installation throughout the project execution. Even though the sample size used is relatively small, this can already be valuable information for the friction coefficient *f* calculation as mentioned above. Since no relevant literature work is present to this date which focus on this topic, it could be of benefit to further investigate data from other projects to understand if this tendency can be extrapolated.

In summary, the friction development along the microtunneling project presents a smaller and non-constant value which differs greatly from the one used for calculations at the design phase. Also, it was observed that the friction is impacted by the orientation history of the TBM. The horizontal deviation presents a positive correlation with friction and is confirmed as one of the influencing parameters. Lastly, it was detected a decrease in friction tendency after subsequential pipe installation. Future research could use an extended database to create a prediction model to calculate the friction at the design phase. This database can be developed with the back analysis of more installation data from microtunneling projects, focusing on the above-mentioned topics. Such understanding would enable more accurate predictions in future projects, reducing both risks and costs.

5. References

[1] Broere, W., & van der Woude, S. (2012). Trenchless Technology, lecture notes CIE5741.

[2] Delft Cluster. (2007, February). Monitoring IJ boring Amsterdam: DC 01 16 11 – Analyse metingen perskrachten en wandwrijving (Concept report). Delft Cluster.

[3] International Tunnelling and Underground Space Association. (n.d.-a). Shield TBM. Tunnel. Retrieved November 30, 2024, from https://tunnel.ita-aites.org/en/how-to-go-underground/construction-methods/mechanized-tunnelling/shield-tbm

[4] International Tunnelling and Underground Space Association. (n.d.-b). Shield TBM. Tunnel. Retrieved October 25, 2022, from https://tunnel.ita-aites.org/en/how-to-go-underground/construction-methods/mechanized-tunnelling/slurry-shield

[5] International Tunnelling and Underground Space Association. (n.d.-c). Selection of TBM criteria (PDF). Tunnel. Retrieved November 30, 2024, from https://tunnel.ita-aites.org/media/k2/attachments/public/Selection_of_TBM_criteria_paper.pdf[6] Marshall, M. A. (1998). Pipe-jacked tunnelling: jacking loads and ground movements.

[7] Mastbergen, D. R. (2007). Monitoring IJ borehole Amsterdam: Analysis of measurements of pressure forces and wall friction (Report No. DC 01 16 11).

[8] Milligan, G. (2000). Lubrication and soil conditioning in tunnelling, pipe jacking and microtunnelling: A state-of-the-art review. Geotechnical Consulting Group, London, UK.

[9] Milligan, G., & Norris, P. (1993). The performance of concrete jacking pipes during installation. Report NOUEL 1986/93 University of Oxford, 5.

[10] Milligan, G., & Norris, P. (1996). Site-based research in pipe jacking—objectives, procedures and a case history. Tunnelling and Underground Space Technology, 11, 3-24.

[11] Milligan, G., & Norris, P. (1999). Pipe–soil interaction during pipe jacking. Proceedings of the Institution of Civil Engineers-Geotechnical Engineering, 137(1), 27-44.

[12] Ni, J. C., & Cheng, W. C. (2012). Steering characteristics of microtunnelling in various deposits. Tunnelling and underground space technology, 28, 321-330.

[13] Norris, P., & Milligan, G. (1992). Frictional resistance of jacked concrete pipes at full scale. International congress on trenchless technology,

[14] Norris, P., & Milligan, G. (1994). Pipe jacking Research Results and Recommendations. London Pipe Jacking Association

[15] Pellet-Beaucour, A. L., & Kastner, R. (2002). Experimental and analytical study of friction forces during microtunneling operations. Tunnelling and Underground Space Technology, 17(1), 83-97.

[16] Penn State Eberly College of Science. (n.d.). 4.3 - Residuals vs. predictor plots. STAT 462: Applied regression analysis. Retrieved December 2, 2024, from https://online.stat.psu.edu/stat462/node/96/

[17] Phillips, B. (2023). Soil-lubricant-structure interface mechanics for microtunnelling [PhD thesis]. University of Oxford.

[18] Reilly, C. C., & Orr, T. L. L. (2017). Physical modelling of the effect of lubricants in pipe jacking. Tunnelling and Underground Space Technology, 63, 44-53.

[19] Statstutor. (n.d.). Spearman's rank correlation. Retrieved February 7, 2025, from https://www.statstutor.ac.uk/resources/uploaded/spearmans.pdf

[20] Thomson, J. (1993). Pipejacking and microtunnelling. Springer.

[21] Van Seters, A. J., Bezuijen, A., Talmon, A., Caan, C. P., & Heijmans, R. W. M. G. (1999). BTL-onderzoek 1995-1999; Compilatierapport Micro-Macro Tunneling.

[22] Verburg, N. (2006). An analysis of friction by microtunnelling. Final report TU Delft, 12.

[23] Wong, Th.E., Batjes, D.A.J., & de Jager, J. (Eds.). (2007). Geology of the Netherlands. Royal Netherlands Academy of Arts and Sciences.

[24] Ye, Y., Peng, L., Zhou, Y., Yang, W., Shi, C., & Lin, Y. (2019). Prediction of friction resistance for slurry pipe jacking. Applied Sciences, 10(1), 207.